# The Geochemical Impact of Wildfire and Mining on the Fourmile Creek Watershed, Colorado

Sarah Beganskas

Submitted to the Department of Geology of Amherst College in partial fulfillment of the requirements for the degree of Bachelor of Arts with honors.

Faculty Advisor: Anna Martini

May 3, 2012

# Table of Contents

# List of Figures

# List of Tables

# ACKNOWLEDGMENTS

First and foremost, I thank my advisor, Anna Martini. This project would not have been possible without her guidance and support throughout the year.

My Keck field advisors, David Dethier and Will Ouimet, were vital in helping me to develop this project in the field and beyond, and I cannot thank them enough for their support. Thanks also to my fellow Keck students, Alex, James, and Neil, for their assistance with field measurements. I thank the entire Keck group for an unforgettable summer in Colorado.

I sincerely thank Sheila Murphy at the USGS in Boulder for her collaboration in the field, use of lab equipment, and ongoing communication. Maria Kopicki was vital in helping me to prepare and run my samples, and I sincerely appreciate her time and advice. I would also like to thank David Jones for the use of his lab equipment and his patience in helping me to do so. Thanks to Bill Slocombe for preparing my thin sections and Peter Crowley for helping me analyze them on the SEM. I thank Mike Vollinger and Mike Rhoades at University of Massachusetts Amherst for their help in preparing and running my samples in the XRF lab despite many technical difficulties, and I thank Marc Anderson and Bob Newton at Smith College for their assistance in using their equipment. Many thanks to Andy Anderson for his instrumental help with my GIS analysis.

This project was made possible through generous funding from the Keck Consortium and Amherst College, and I am immensely grateful for this support.

Lastly, I would like to thank my friends and family. Mom, Dad, and Michelle, thank you for always being there for me and supporting my every endeavor. Christine, thank you for being my typographical consultant for this project. All my friends at Amherst, thank you for everything these past four years.

# ABSTRACT

Wildfire and abandoned mines both have profound geochemical effects on a watershed. However, the combined impact of the two disturbances is not well-studied. In September 2010, a severe wildfire burned 26 $km^2$ of the Fourmile Creek catchment in the Colorado Front Range. Located in the Colorado Mineral Belt, the area was historically mined for gold and is still affected by mine drainage and the erosion of tailings. This study, which takes place soon after the first storm event following the fire, examines how the combined disturbances of wildfire and mining affect water and sediment chemistry in this catchment.

Streamwater concentrations of most major and trace solutes increase in burned and mined watersheds relative to unburned and unmined watersheds. Mining intensity correlates positively with $SO_4^{2-}$ and negatively with $HCO_3^-$ in tributaries, while fire intensity correlates positively with $SO_4^{2-}$, $NO_3^-$, and major cations, but notably not with $HCO_3^-$. Acidity from mine drainage and local carbonate deposits reduce the effect of wildfire on streamwater alkalinity. Sulfate concentrations are on average 6.2 times higher in burned than in unburned tributaries, and this exceptional increase is likely due to additional $SO_4^{2-}$ input from mining. Downstream changes in water chemistry along Fourmile Creek reflect substantial influence from burned and mined tributary input, with especially large increases in conductivity, $SO_4^{2-}$, and $Ca^{2+}$ through the disturbed area. Stream sediment from burned watersheds has increased percentages of most major oxides, and less $SiO_2$ and nutrients. Mining is not associated with substantial changes in major oxides or nutrients in stream sediment but supplies increased mercury. In the short-term, the Fourmile Fire, exacerbated by historical mining, dominates the chemistry of Fourmile Creek and its tributaries.

# 1. INTRODUCTION

Wildfire and mining are two disturbances that severely impact stream catchments. Mine drainage chemically affects thousands of kilometers of streams in the United States (Blowes et al. 2005), and over 1,900 km of streams are affected in Colorado alone, many of which are located in high-elevation catchments of the Rocky Mountains (Sullivan and Drever 2001). The effects of mining spread as far as 25 km downstream from the source mine (Lin et al. 2007) and persist for decades after mining has ceased (Sullivan and Drever 2001; Tripole et al. 2006). Wildfires play a large role in driving geomorphic, hydrologic, and chemical processes in a watershed. Post-fire catchments have higher than normal runoff and erosion rates and increased streamwater solute concentrations (Swanson 1981; Bayley and Schindler 1991). Precipitation events that occur after wildfire are more likely to generate devastating floods and debris flows (Ruddy et al. 2010). Mountain catchments provide a significant portion of the world's freshwater supply, as they typically have excellent water quality when undisturbed (Smith et al. 2011). It is thus important to understand how disturbances such as wildfire and mining affect watershed chemistry in both the short- and long-term.

## 1.1. Geomorphic and Hydrologic Impact of Wildfire

Forests undisturbed by wildfire typically have high soil infiltration rates, a lack of overland flow, and low erosion rates (Benavides-Solorio and MacDonald 2001). Wildfire produces profound changes in all of these respects (*Figure 1.1*), reducing infiltration, increasing runoff and erosion rates, and, as a result, increasing stream discharge and sediment yield (Swanson 1981).

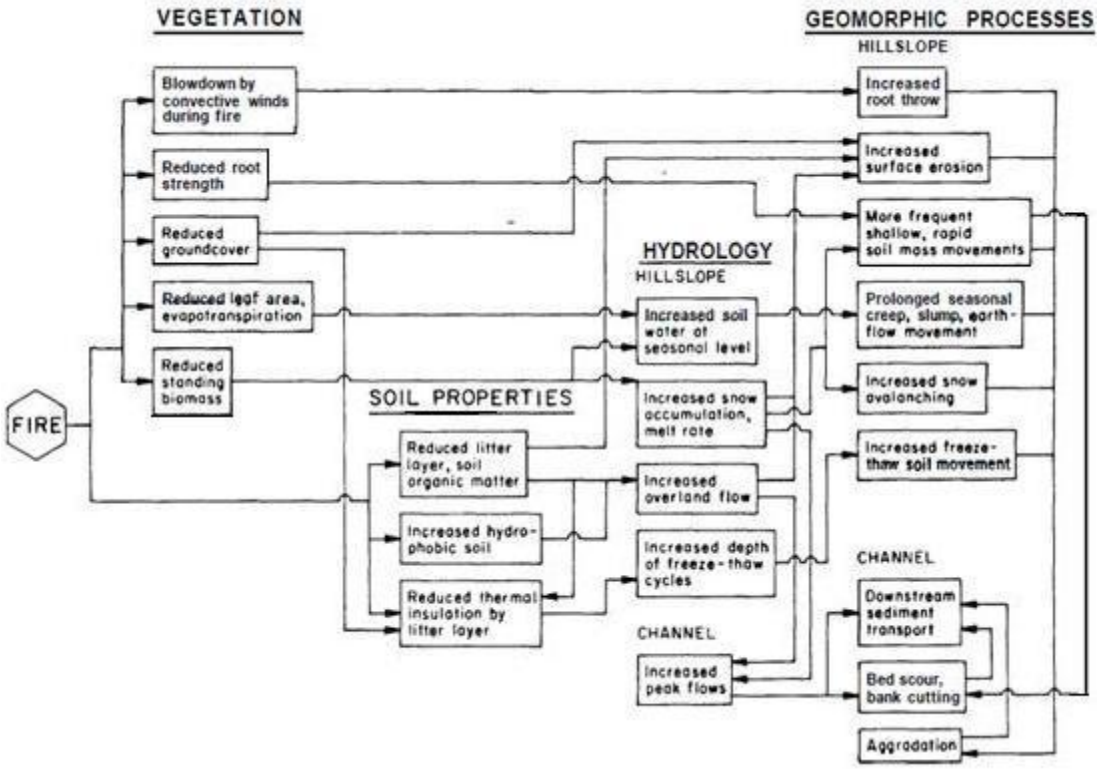


**Figure 1.1. Geomorphic and Hydrologic Impacts of Wildfire.**
A flow chart depicting various impacts of wildfire (Swanson 1981).

Wildfire immediately increases sediment transport via dry ravel, the downslope movement of individual particles by rolling or sliding due to gravity (Gabet 2003; Ice et al. 2004). As they burn, wildfires dry the soil, combust organic matter that binds soil, consume litter and vegetation, and generate strong convective winds. All of these encourage dry ravel, especially in areas with steep slopes (Swanson 1981; Gabet 2003; Ice et al. 2004). A study in Oregon found a large increase in sediment coming down steep burned slopes relative to steep unburned slopes in the 24 hours after a wildfire. As there was no precipitation during that time, downslope transport must have been primarily dry ravel (Ice et al. 2004).

Vegetation is a key factor constraining hillslope runoff and erosion. Root networks bind soil, reducing potential downslope movement and stabilizing floodplain deposits. Organic litter protects soil from surface erosion, and fallen trees and other plants act as sediment storage sites (Swanson 1981). Vegetation also reduces potential runoff through interception and evapotranspiration of rainwater (Bayley and Schindler 1991; Kunze and Stednick 2006). Thus, destruction or alteration of vegetation via wildfire affects the processes transporting sediment and water downslope, destabilizing sediment and causing it to be eroded more easily as well as facilitating increased runoff (Swanson 1981).

A commonly observed feature of burned landscapes is a water repellent layer at or near the soil surface (Swanson 1981; DeBano 2000; Moody and Martin 2001). At high soil surface temperatures during wildfires, organic compounds are volatilized. Soil is a good insulator, and due to the steep temperature gradient, these compounds condense onto cooler soil particles (Swanson 1981; DeBano 2000; Ice et al. 2004; Kunze and Stednick 2006). A negatively-charged layer forms that repels water and

reduces soil infiltration. Coarse soils are more prone to water repellency (Ice et al. 2004), and more severe wildfires are likely to produce intense, persistent water repellency (Benavides-Solorio and MacDonald 2001). Burned vegetation and litter cover expose soil to raindrop impact and splash that seals soil pores at the surface with fine-grained material such as ash, further reducing infiltration (Swanson 1981; Benavides-Solorio and MacDonald 2001; Ice et al. 2004; Smith et al. 2011). Campbell and others (1977) observed a 63% decrease in soil infiltration rates after a wildfire in Arizona as a result of water repellency and soil sealing.

Reduced soil infiltration and burned vegetation increase the amount of water available for runoff. Bayley and Schindler (1991) compared stream discharge in burned and unburned watersheds and found that a greater percentage of precipitation falling in burned basins was accounted for in stream discharge. As a result, post-fire precipitation events with small return intervals generate large volumes of runoff (Moody and Martin 2001) that can be one to two orders of magnitude greater than normal (Inbar et al. 1998; Kunze and Stednick 2006). In response to increased runoff, total and peak streamflow also increase (Swanson 1981). After the Buffalo Creek Fire in the Colorado Front Range, peak flow increased from less than 2 $m^3/s$ pre-fire to over 60 $m^3/s$ post-fire (Benavides-Solorio and MacDonald 2001). Patterns of post-fire precipitation control the magnitude of increases in runoff and streamflow (Moody et al. 2008b).

Increased runoff and reduced vegetation lead to greater erosive potential, and in response, stream sediment yield also increases. Values of suspended stream sediment post-fire can be three orders of magnitude greater than unburned values, and the magnitude of this change reflects many variables, including precipitation

patterns, burn extent and severity, and vegetation cover (Benavides-Solorio and MacDonald 2001; Moody and Martin 2001; Reneau et al. 2007; Smith et al. 2011). After a wildfire in the Colorado Front Range, Moody and Martin (2001) observed increases in sediment yield ranging from 150 to 240 times greater than pre-fire values. Similarly, Reneau and others (2007) found that post-fire sedimentation rates increased by a factor of 140 over pre-fire rates and erosion rates increased by over two orders of magnitude.

Precipitation is the most important factor in determining the magnitude of erosional response to wildfire. Moody and others (2008a) measured post-fire erosional efficiency in two terrains and found that the mass of eroded, transported, and deposited sediment depended on the occurrence of rainstorms and floods, with most transport occurring during flash floods. Tomkins and others (2007) examined the effects of two wildfires in the same catchment in Australia, one in 1968 and one in 2001. Sediment yield increased markedly in 1968, a year with intense rainfall; in contrast, a year with below-average precipitation followed the 2001 fire, and sediment yield increased only modestly.

As time passes after a fire, the magnitude of response to precipitation events decreases. Moody and Martin (2001) found peak discharges three and four years after wildfire to be an order of magnitude lower than those immediately post-burn, and Campbell and others (1977) observed a decline in stream discharge every year after a wildfire as vegetation recovered. Erosion rates typically return to background levels within 3–9 years after a wildfire, depending on how quickly revegetation occurs (Benavides-Solorio and MacDonald 2001; Moody and Martin 2001).

Wildfire substantially contributes to an area's long-term sediment yield (Swanson 1981). In the steep, chaparral terrain of California, wildfire is a dominant geomorphic process. Assuming that sediment yield from a wildfire increases to ~30 times the baseline rate, that recovery takes 8–10 years, and that the fire recurrence interval is 25 years, wildfire-related erosion contributes ~70% of a catchment's total sediment yield (*Figure 1.2*). A similar model for a forested area in Oregon with a longer recurrence interval of hundreds of years still reveals that wildfire contributes ~25% of total sediment yield (Swanson 1981). These models are simple and do not take variability in fire recurrence interval or recovery time into account, but they give a sense of the magnitude of wildfire's potential contribution to an area's long-term erosion and sedimentation.

## 1.2. Chemical Impact of Wildfire

Wildfires produce profound yet varied changes in streamwater and soil chemistry. Ash input has an immediate but short-term chemical impact (Earl and Blinn 2003), while sustained chemical effects of wildfire are a result of vegetation loss and changes in hydrologic processes that control streamflow, peak discharge, soil erosion, channel stability, and runoff (Rhoades et al. 2011). Concentrations of most chemical constituents—major cations and anions, nutrients, and trace elements—increase after wildfire, but the magnitude of impact on stream chemistry depends on many factors, particularly post-fire discharge and precipitation (Rhoades et al. 2011; Smith et al. 2011).

While all studies report increased streamwater concentrations of major cations ($Ca^{2+}$, $Mg^{2+}$, $K^{+}$, and $Na^{+}$) after wildfire, these increases vary widely in magnitude.

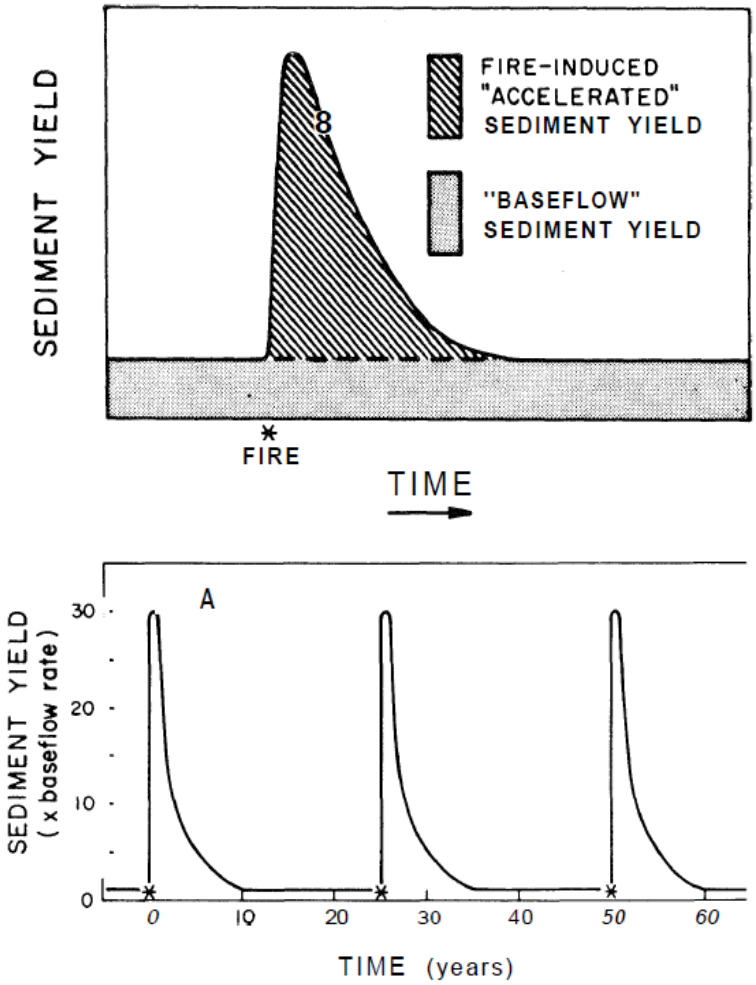


**Figure 1.2. Wildfire and Stream Sediment Yield.**
*Top*: A single fire event can increase sediment yield over baseline levels by several orders of magnitude.
*Bottom*: Depending on the recurrence interval, the combined effects of a sequence of fires on sediment yield can make up a large fraction of the total long-term sediment yield of a system.
(Swanson 1981)

This suggests that site-specific factors, such as fire intensity, type of vegetation and soil, underlying bedrock, and precipitation, determine the magnitude of change. Bayley and Schindler (1991) found that major cations remained elevated for several years after wildfire (*Figure 1.3a*). Chorover and others (1994) observed increased concentrations of major cations in soils post-fire; although their relative abundances were initially unaffected, divalent cations ($Ca^{2+}$, $Mg^{2+}$) were still elevated three years later, while monovalent cations ($K^{+}$, $Na^{+}$) had returned to pre-burn values.

Wildfire substantially increases streamwater $SO_4^{2-}$ and, less consistently, $Cl^{-}$ (Mast and Clow 2008; Betts and Jones 2009). Oxidation of sulfur in burning organic matter increases the supply of $SO_4^{2-}$ available for transport to streams, and leaching of burned plant litter and ash deposits also contributes $SO_4^{2-}$ and $Cl^{-}$ (Mast and Clow 2008; Smith et al. 2011). Khanna and Raison (1986) observed that $SO_4^{2-}$ and $Cl^{-}$ concentrations in soils below ash beds were 9- and 3-fold greater, respectively, than those in soils unaffected by fire.

Increased $SO_4^{2-}$ after wildfire is associated with increased divalent cation concentrations. Bayley and Schindler (1991) reported a post-fire increase in $SO_4^{2-}$ greater than 350% that was sustained for several years; $Ca^{2+}$ and $Mg^{2+}$ followed a similar pattern. Concentrations of $Cl^{-}$ also increased by over 300%, but dropped below pre-fire values relatively quickly, following a different pattern. This demonstrates that increased $SO_4^{2-}$ export in particular is related to base divalent cation export. Chorover and others (1994) also reported that a post-fire $SO_4^{2-}$ pulse was associated with increased divalent cation concentrations.

Fine-grained, widespread ash deposits are easily transported via overland flow into streams, where they substantially impact water chemistry (Smith et al. 2011).

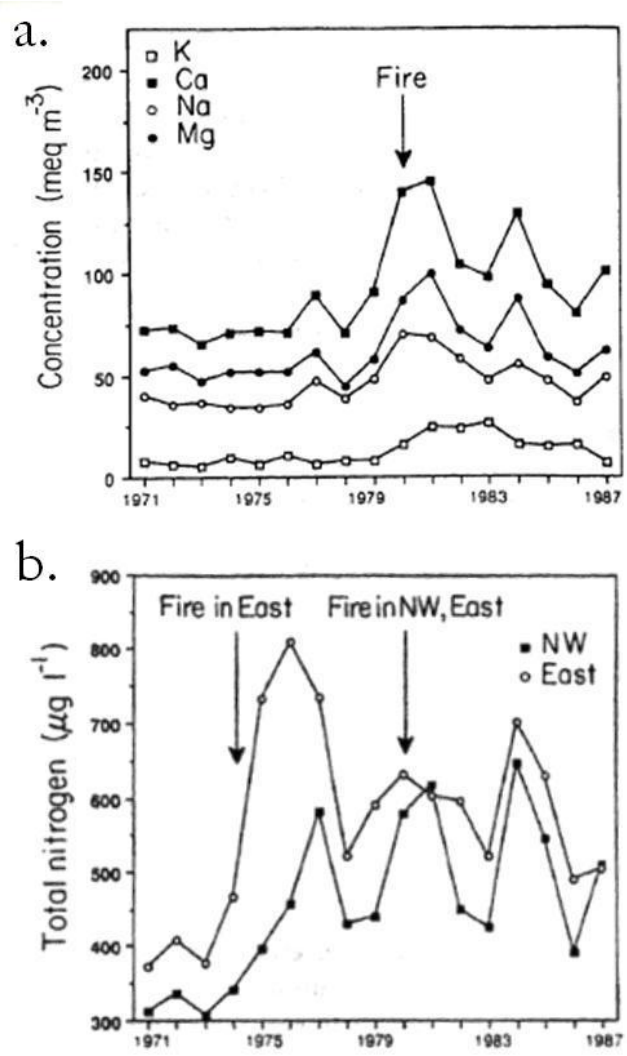


**Figure 1.3. Cations and Nitrogen in Post-Fire Streams.**

a. Yearly concentrations of $Ca^{2+}$, $Mg^{2+}$, $K^{+}$, and $Na^{+}$ in a forested catchment in Ontario affected by wildfire.

b. Yearly total N concentration in two streams, labeled NW and East.

(Bayley and Schindler 1991)

Earl and Blinn (2003) artificially input ash to an otherwise undisturbed stream and found that concentrations of major ions, nutrients, alkalinity, turbidity, and conductivity increased rapidly as a result. The presence of ash also increases erosion on hillslopes via positive feedback: entrained ash in overland flow increases the fluid density of the flow, giving it higher erosive capacity (Smith et al. 2011). Ash is a significant percent of suspended material draining a watershed in the first year after a wildfire (Reneau et al. 2007; Smith et al. 2011).

The chemical composition of ash varies depending on the soil type, vegetation type, climate, and extent of combustion (Earl and Blinn 2003; Smith et al. 2011). Ash deposits typically have high concentrations of nutrients, especially carbon (Smith et al. 2011), and may contain trace elements, including $Cu^{+}$, $Fe^{2+}$, $Mn^{2+}$, and $Zn^{2+}$, from burned vegetation and breakdown of organic matter (Certini 2005; Gonzalez Parra 2006). While wildfire's impact on streamwater trace element concentrations is not well-studied, some have reported various post-fire increases in $Al^{3+}$, $As^{3+}$, $Ba^{2+}$, $Cr^{3+}$, $Fe^{2+}$, $Mn^{2+}$, $Pb^{2+}$, and $Zn^{2+}$ (Smith et al. 2011). Ash is also rich in alkaline earth cations that are quickly altered to carbonates, increasing alkalinity and pH in streams draining burned watersheds (Chorover et al. 1994). Some suggest that fire suppression causes acidification of lakes and streams by removing natural periodic increases in alkalinity from wildfires (Bayley and Schindler 1991).

Atmospheric deposition of ash can affect water chemistry in adjacent, unburned watersheds (Smith et al. 2011). Rhoades and others (2011) observed increased concentrations of several ions in an unburned watershed due to ashfall, and many have found increased nutrient concentrations as a result of aerial ash deposition (Spencer and Hauer 1991; Earl and Blinn 2003; Spencer et al. 2003).

Wildfire impacts the productivity of forests by changing nutrient reserves and disrupting nutrient cycling (Minshall et al. 1989; Baird et al. 1999). Due to the magnitude of nutrients potentially affected, wildfires are a significant factor in terrestrial nutrient cycling and influence global nutrient cycling (Lavoie et al. 2005). During wildfire, nutrients stored in organic matter, litter, and vegetation can be lost to the atmosphere as gases (Baird et al. 1999; Ice et al. 2004; Lavoie et al. 2005). Carbon and nitrogen are particularly susceptible to loss because of their relatively low volatilization temperatures (Baird et al. 1999; Johnson et al. 2007), and emissions from wildfires produce 1410–3139 Tg C/year (Hessl 2011). Sulfur, potassium, and phosphorous have higher volatilization temperatures and less commonly burn off during wildfire (Jonhson et al. 2007). Those nutrients that are not volatilized are left behind in ash deposits and are susceptible to leaching and transport by increased post-fire runoff (Minshall et al. 1989; Ice et al. 2004).

Reduced plant nutrient uptake, increased nutrient mineralization, and a large supply of nutrient-enriched ash are coupled with increased stream levels of nutrients, particularly N and P (Minshall et al. 1989; Ice et al. 2004; Smith et al. 2011). Bayley and Schindler (1991) saw stream exports of N and P increase dramatically after a fire (*Figure 1.3b*), and Mast and Clow (2008) reported $NO_3^-$ concentrations ten times higher in burned relative to unburned catchments. Betts and Jones (2009), however, observed no post-fire change in streamwater P.

Variation in streamwater nutrient levels after a wildfire depends on many factors. Precipitation facilitates increased runoff that transports nutrients to streams (Johnson et al. 2007), and Bladon and others (2008) found post-fire increases of streamwater N to correlate with incoming precipitation and snow melt. Nutrient

response can also depend on vegetation type; Dyrness and others (1989) studied post-fire soil and stream chemistry and found that N increased in black spruce forests but decreased in aspen, birch, and white spruce forests.

Wildfires also play a role in mercury cycling. Mercury accumulates in soil organic matter via atmospheric deposition from natural and anthropogenic sources; wildfires, in turn, revolatilize this accumulated mercury (Biswas et al. 2008; Smith et al. 2011). Once in the atmosphere, gaseous $Hg^0$ is oxidized to reactive mercury, $Hg^{2+}$, and deposited elsewhere. Once deposited, $Hg^{2+}$ can be reduced to methylmercury, which is toxic and bioaccumulates (Biswas et al. 2008; Smith et al. 2011).

Soil reaches high enough temperatures during wildfire to remobilize mercury from organic matter. Depending on soil type and fire severity, temperatures required for soil organic matter combustion and mercury release have been found to extend ~4 cm deep in the soil, and mercury stored deeper than this is a longer-term reservoir (Biswas et al. 2008). The amount of mercury released during wildfire is limited by the amount of mercury present in the soil prior to burning, which is dependent on many factors, including the tree species present (Biswas et al. 2007).

Prescribed fires burn ~$10^6$ hectares of forest in the United States each year, reducing the risk of severe wildfire. Many of these have little to no long-term effect on soils, nutrient cycling, or hydrologic systems (Richter et al. 1982). Prescribed fires are less intense than natural wildfires, and while studies of prescribed fires are useful, caution is necessary, as conditions observed under prescribed fire regimes are not typical of natural wildfire conditions (Baird et al. 1999). Richter and others (1982) observed that a prescribed fire had little to no impact on soil and streamwater chemistry, in stark contrast to most studies of natural wildfire.

## 1.3. Distribution of Wildfire

Over time, patterns of wildfire distribution and recurrence have greatly varied, and this variation has been attributed to changes in climate. Increased wildfire activity over the past few decades has led many to speculate that current global warming is affecting current wildfire regimes (Westerling et al. 2006). The number and extent of wildfires in a given region depend on many factors, including fuel availability, fuel flammability, vegetation type, temperature, precipitation, wind, humidity, and lightning strikes. Climate directly or indirectly affects all of these factors, and therefore affects wildfire season intensity from year to year as well as on longer time scales (Westerling 2008). Many project an increase in wildfire frequency in many parts of the world as a result of climate change (Bergeron and Flannigan 1995; Lavoie et al. 2005; Hessl 2011). Based on research of past wildfires, the overwhelming conclusion is that increased wildfire intensity coincides with periods of severe drought (Sibold and Veblen 2006; Swetnam and Anderson 2008; Westerling 2008; Hessl 2011). Current global warming is expected to result in higher temperatures and more frequent, intense drought (Westerling 2008).

Wildfires in the Western United States are seasonal, peaking in the summer when temperatures are warmest and conditions are driest. Over 90% of wildfires and 98% of burned area annually occur between May and October (Westerling 2008). The frequency of large wildfires, total area burned, and length of wildfire season in the Western United States have increased since the mid 1980s (*Figure 1.4a*), which is attributed to warmer temperatures and earlier snow melt (Westerling et al. 2006; Westerling 2008; Hessl 2011).

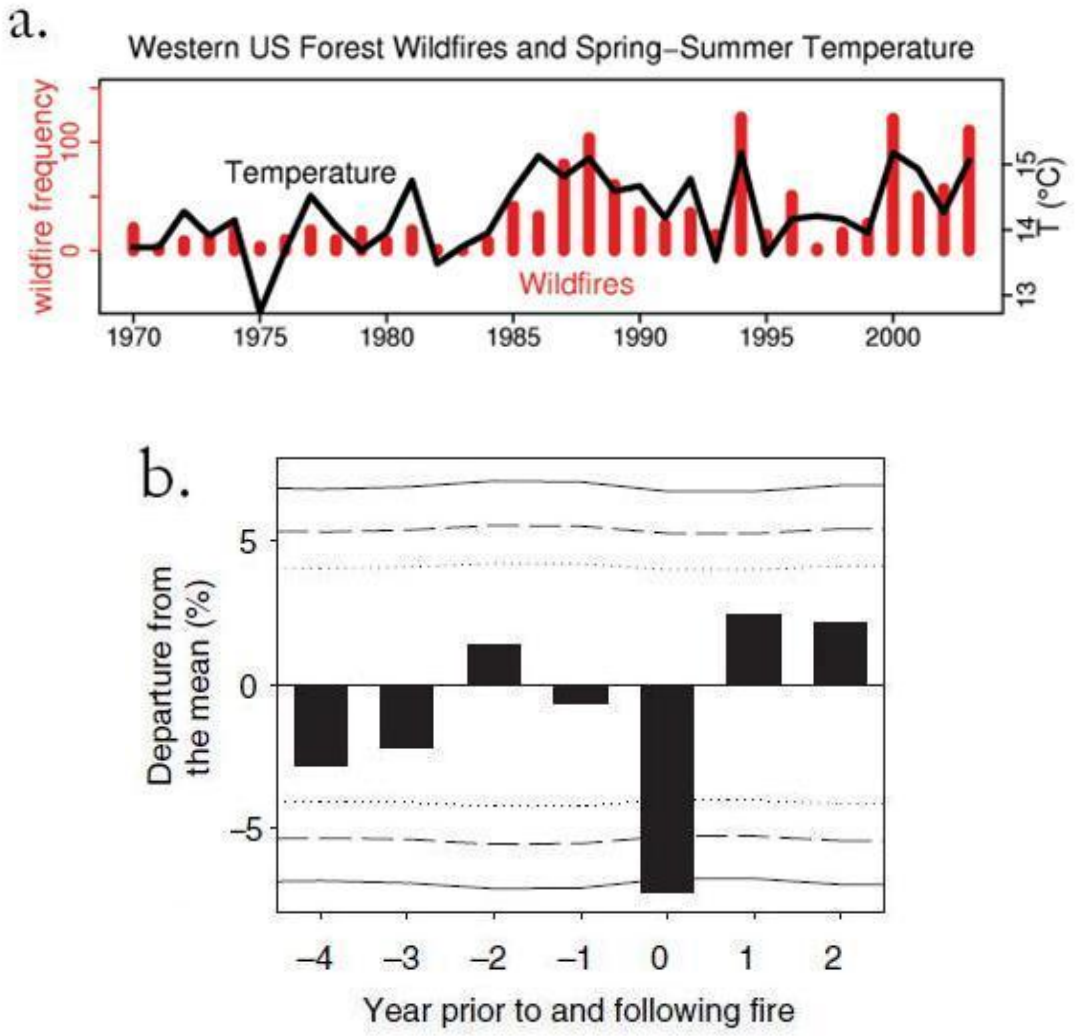


**Figure 1.4. Wildfires and Climate.**

a. An increase in wildfire frequency in the Western United States correlates with increasing average spring/summer temperatures (Westerling et al. 2006).

b. The average departure from mean moisture availability in years prior to and following wildfire in the Colorado Front Range (Sibold and Veblen 2006).

In general, the effects of precipitation on fire frequency depend on an area's balance between fuel availability and fuel flammability (Westerling 2008; Hessl 2011). Hot, dry areas with scarce fuels have more fires in wetter years, when increased moisture allows more vegetation to grow and dry out quickly in the heat. On the other hand, areas with high moisture availability have more fires during dry periods, when fuels are more flammable (Westerling 2008; Hessl 2011). In the subalpine zone of the Colorado Front Range, decreased precipitation facilitates fire activity (*Figure 1.4b*) (Sibold and Veblen 2006).

There are many uncertainties in precisely how wildfire regimes respond to certain changes in climate, and in turn, how exactly regional climate will change in the near future (Bergeron and Flannigan 1995). Human activities also drive wildfire activity (Hessl 2011). It is thus difficult to make generalizations about future wildfire patterns. However, it is likely that wildfire activity will increase in the Western United States, and having a complete understanding of the chemical, geomorphic, and hydrologic effects of wildfire will become increasingly important.

## 1.4. Chemical Impact of Mining

Alpine watersheds are particularly sensitive to the negative impacts of discharge from abandoned mine sites (Sullivan and Drever 2001). Mine tailings at these sites consist of residual material that is left over after extracting metals from their ores (Blowes et al. 2005). Most commonly, these ores contain metal sulfides (Lin et al. 2007), and mining exposes these minerals, which had been isolated from the atmosphere in reduced form, to oxygen in the atmosphere (Blowes et al. 2005; Tripole et al. 2006). Oxidation of these reduced sulfides provides energy to

chemolithic bacteria, which catalyzes further oxidation and dissolution of minerals (Tripole et al. 2006).

Pyrite is the primary contributor to acid mine drainage production (Bradley 2008). Oxidation of one mole of pyrite produces 4 moles of $H^+$, and the products of oxidation, including $H^+$, $SO_4^{2-}$, $Fe^{2+}$, and other metals, are released into water flowing through the waste (Blowes et al. 2005). Iron released into water becomes oxidized, which increases ferric iron precipitation in streams and depletes the oxygen available to stream ecosystems (Bradley 2008). The general chemical mechanism of acid mine drainage is well understood, although precise assessment and prediction of its impacts are difficult because many other factors—climatic, hydrologic, geomorphic, geologic, and biologic—affect the rates of sulfide-derived acid production and transport of oxidation products (Lin et al. 2007).

Production of sulfuric acid through oxidation of sulfide minerals increases streamwater acidity, and the susceptibility of streamwater to acidification depends on the system buffering capacity (Blowes et al. 2005; Tripole et al. 2006). Calcareous sediments provide streams with dissolved carbonate and bicarbonate, which act as pH buffers (Bradley 2008). In the absence of such buffering, streamwater pH decreases and metals become more soluble (Hall et al. 1980). As a result, acidic waters in mined areas have increased leaching of metals, including $Cu^+$, $Fe^{2+}$, $Ni^{2+}$, and $Pb^{2+}$ (Bradley 2008).

Sullivan and Drever (2001) studied the chemistry of a high-elevation stream in the Colorado Rocky Mountains within a watershed that contains many abandoned silver mines and tailings piles. Although the mines had been inactive for nearly a century, they still impacted stream chemistry. Upstream from mine input, waters had

low metal concentrations and neutral pH. After input from mine drainage, alkalinity and pH decreased, while the concentrations of many metals (including $Al^{3+}$, $Ca^{2+}$, $Cu^{+}$, $Fe^{2+}$, $Mg^{2+}$, $Mn^{2+}$, and $Zn^{2+}$) and other ions (including $H^{+}$, $SO_4^{2-}$, and $F^{-}$) increased by at least tenfold. Mine drainage also contributed $Cd^{+}$, $Ni^{2+}$, and $Pb^{2+}$, while $SiO_2$, $Na^{+}$, $K^{+}$, and $NO_3^{-}$ were unaffected.

McConnell (1995) collected streamwater upstream and downstream of mine tailings from abandoned copper, gold, silver, and zinc mines. Concentrations of 38 different solutes, especially $As^{3+}$, $Co^{2+}$, $Cu^{+}$, $Pb^{2+}$, $SO_4^{2-}$, and $Zn^{2+}$, increased after mine input, and pH sharply decreased (*Figure 1.5*).

In general, seasonal variation impacts water chemistry. McConnell (1995) found that in areas remote from mining and other disturbances, concentrations of many elements are higher late in summer when conditions are drier and there is less water to dilute solute concentrations. Accordingly, seasonal changes in the hydrologic cycle influence the effect of mining, as changes in precipitation, surface runoff, and evaporation rates affect streamwater discharge and the dilution of mine drainage (Bradley 2008). Summer droughts result in increased acidity and metal concentrations, while spring melting dilutes the impact of mine drainage on streamwater (Sullivan and Drever 2001). Lin and others (2007) found that acidity generated from sulfide oxidation in mine waste rocks was readily available for transport to streams. The main factor in determining how much was transported to streams was the volume of water flowing through, and therefore, spring flooding caused massive discharge of acid to streams.

Mining also affects stream sediment chemistry. Decreased acidity of mine drainage water through dilution or buffering reduces the solubility of metals, which

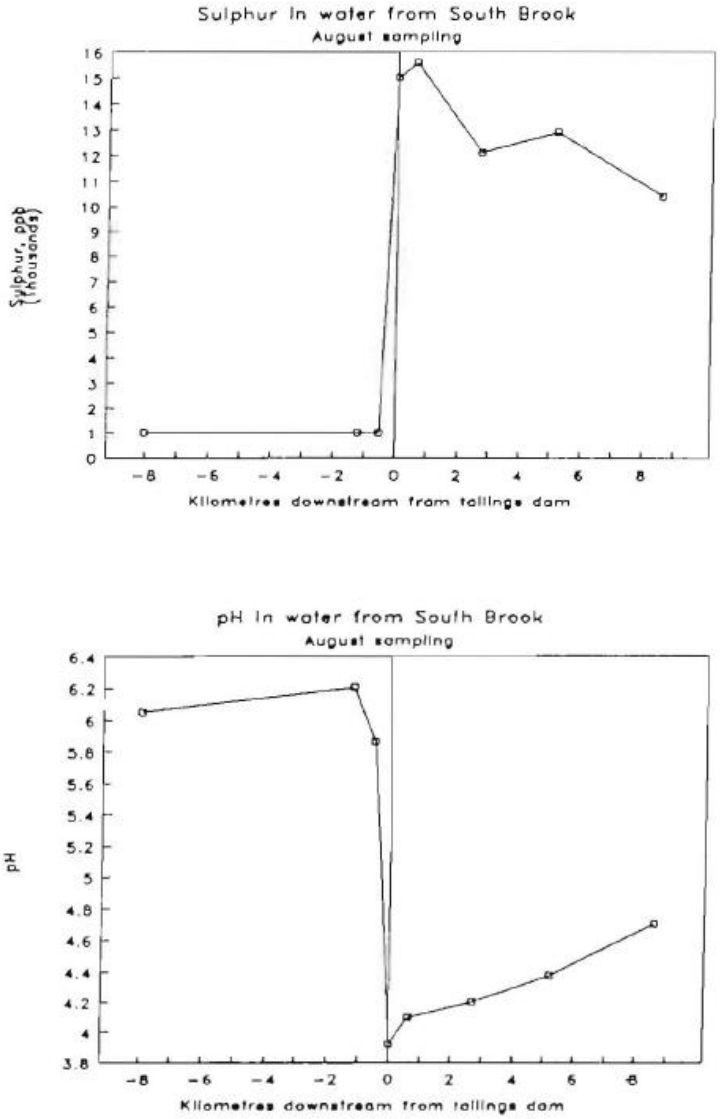


**Figure 1.5. Effects of Mining on Streamwater.**
Sulfur concentrations (*top*) and pH values (*bottom*) in streamwater upstream and downstream of mine drainage input for a stream in Newfoundland (McConnell 1995).

causes them to precipitate out of solution and be deposited on the streambed (Bradley 2008). Often, precipitates include ferric iron, giving the deposits an orange-brown color. Other heavy metals, such as $As^{3+}$, $Cu^{+}$, $Hg^{2+}$, and $Zn^{2+}$, are commonly found in streambeds affected by mine drainage (Alpers et al. 2005; Bradley 2008). Kim and others (2007) found higher-than-average sediment concentrations of $Cd^{+}$, $Fe^{2+}$, $Pb^{2+}$, and $Zn^{2+}$ in a historically mined watershed whose streamwater chemistry was no longer affected by mine drainage. This suggests that the effects of mining on sediment last longer than its effects on streamwater.

## 1.5. Site Description

Located in the Colorado Front Range, Fourmile Creek is a major tributary of Boulder Creek, a source of water for the city of Boulder (*Figure 1.6*) (Murphy et al. 2000). The Colorado Front Range is a mountainous uplift that trends northward. On the east, it is smoothly bounded by plains, while its western border is irregular and bounds other mountain ranges. The Continental Divide is close to its western boundary, and most streams in the Colorado Front Range, including Boulder Creek, flow due east (Lovering and Goddard 1950). Fourmile Creek flows east until Gold Run flows into it from the northwest, at which point it turns southeast to meet Boulder Creek (Graham et al. 2011). Fourmile Creek has approximately two dozen small tributaries that do not always carry water; most flow toward the northeast or southeast (*Figure 1.7*).

Fourmile Creek is located in the upper basin of the Boulder Creek watershed, which is characterized by sparse human population, forested land cover, and steep slopes (Murphy et al. 2000). Slopes in the watershed are as steep as 45 degrees, and

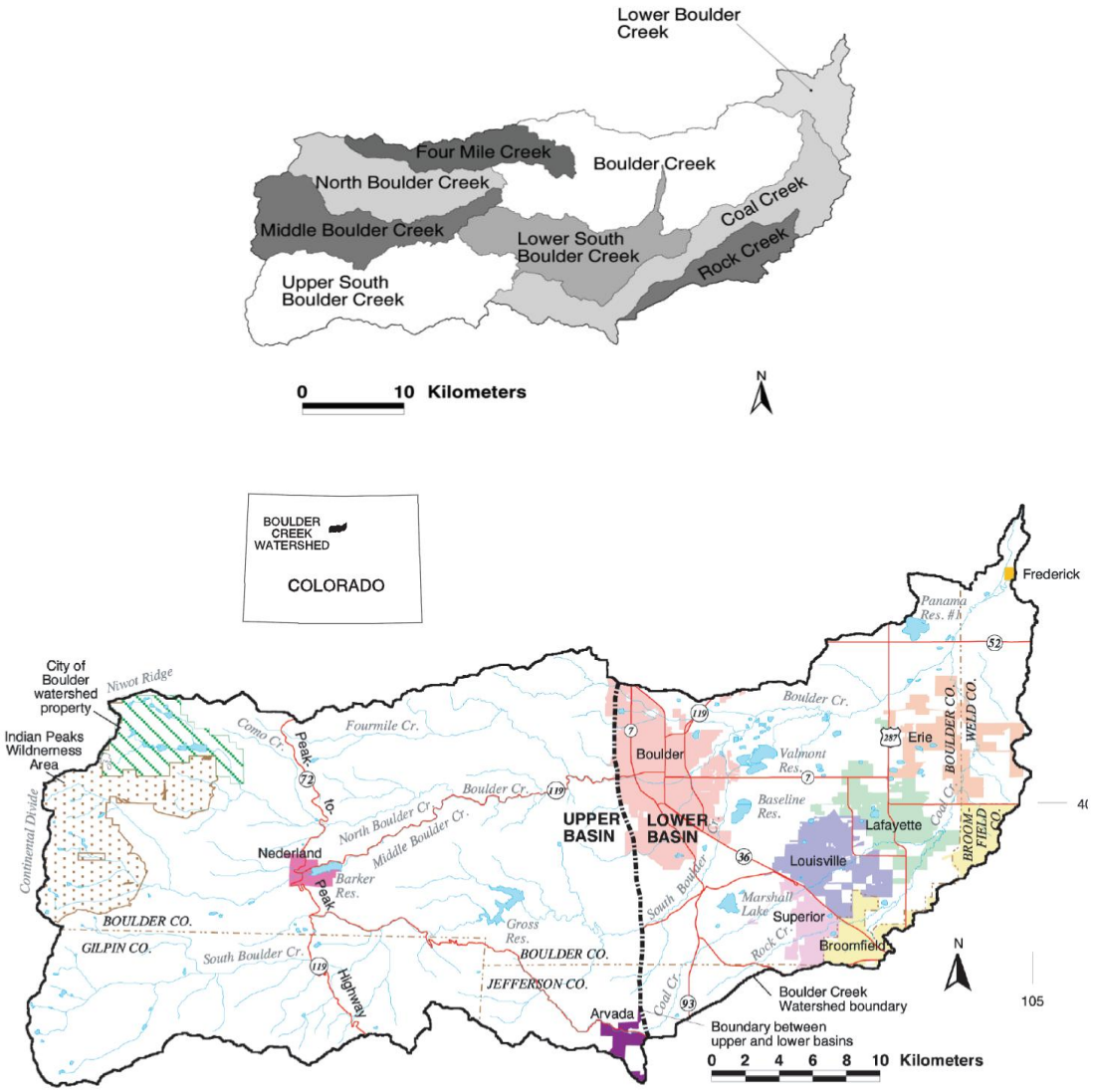


**Figure 1.6. Boulder Creek Watershed.**
*Top*: Subwatersheds of Boulder Creek, including Fourmile Creek.
*Bottom*: Detailed map of the Boulder Creek watershed.
(Murphy et al. 2000)

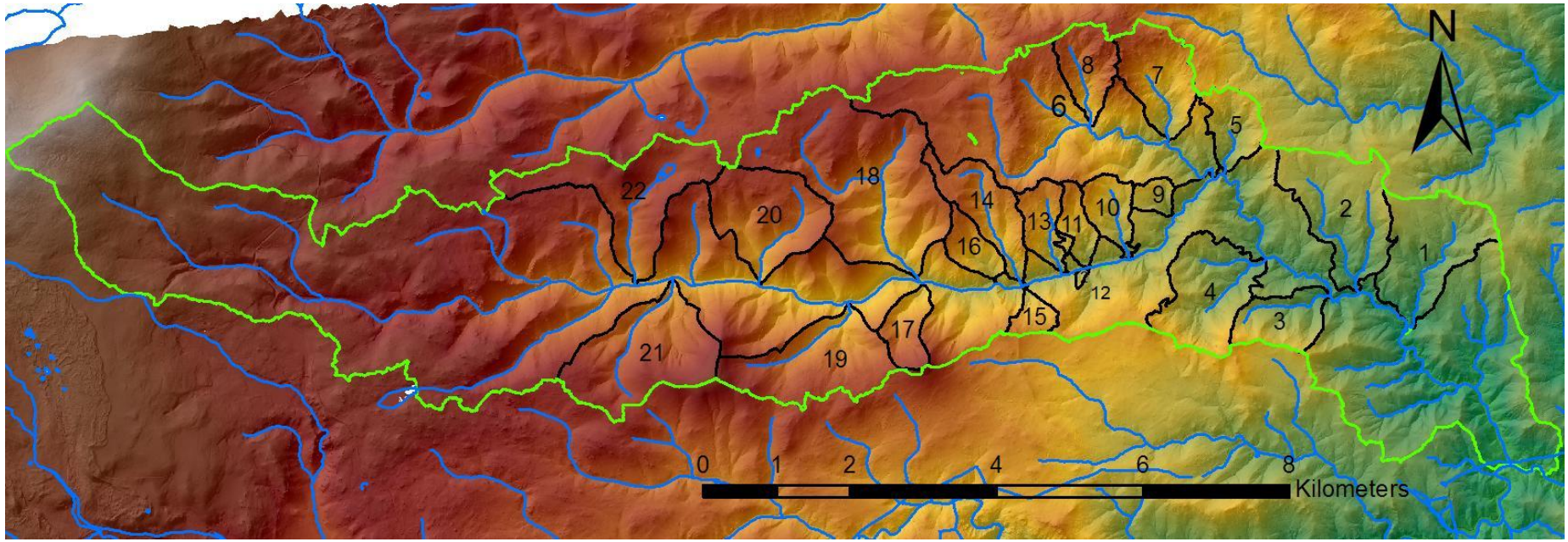


**Figure 1.7. Fourmile Creek Watershed and Tributaries.** Map of tributaries (blue) sampled in this study and their watersheds (outlined in black). The Fourmile Creek watershed is outlined in green. Background color represents elevation, with warmer colors at higher elevation.

1 – Dry Gulch
2 – Sand Gulch
3 – Arkansas Gulch
4 – Sunbeam Gulch
5 – Sweet Home Gulch
6 – Gold Run
7 – Ingram Gulch
8 – Black Hawk Gulch
9 – Melvina East Gulch
10 – Melvina Gulch
11 – Melvina West Gulch
12 – Wall Street Gulch
13 – Schoolhouse Gulch
14 – Emerson Gulch
15 – Banana Gulch
16 – Emerson West Gulch
17 – Sugarloaf Gulch
18 – Long Gulch
19 – Bald Gulch
20 – Potato Gulch
21 – Bear Gulch
22 – Todd Gulch

elevation in the basin ranges from 1,600 to 2,900 m (Graham et al. 2011). The upper Boulder Creek watershed, including Fourmile Creek, is underlain by Precambrian gneisses and schists (~1800 Ma) that are intruded by the Boulder Creek granodiorite (~1715 Ma) and the Silver Plume granite (~1422 Ma) (*Figure 1.8*) (Murphy et al. 2000; Verplank et al. 2008). Boulder Creek granodiorite, a batholith that dominates the central Colorado Front Range and underlies the lower Fourmile Creek watershed, contains primarily plagioclase, quartz, potassium feldspar, and biotite; it also has minor amounts of hornblende, muscovite, sphene, zircon, and apatite (Lovering and Goddard 1950; Verplank et al. 2008).

The Colorado Mineral Belt, a northeast-trending zone of late Cretaceous and Paleogene (68–27 Ma) intrusive dikes and sills that are associated with ore deposits, runs through the eastern Colorado Front Range along the western border of the Boulder Creek granodiorite (Lovering and Goddard 1950; Murphy et al. 2000; Kellogg et al. 2004). The intrusions that define the mineral belt are associated with a zone of crustal weakness and contain gold, silver, tungsten, copper, lead, zinc, tin, and uranium (Murphy et al. 2000; Kellogg et al. 2004). The Gold Hill mining district is located in the Fourmile Creek watershed; there, abundant gold–telluride ore deposits, along with a few pyritic gold and silver–lead ore deposits, are associated with Laramide faults called breccia reefs (*Figure 1.9*) (Lovering and Goddard 1950). Gold Hill mines began producing gold, silver, lead, copper, and zinc in 1859 (Murphy et al. 2000). In this area of Colorado, mine drainage is not very acidic because carbonate in mined ore bodies is readily available to buffer acid produced from the weathering of sulfides (Murphy et al. 2000).

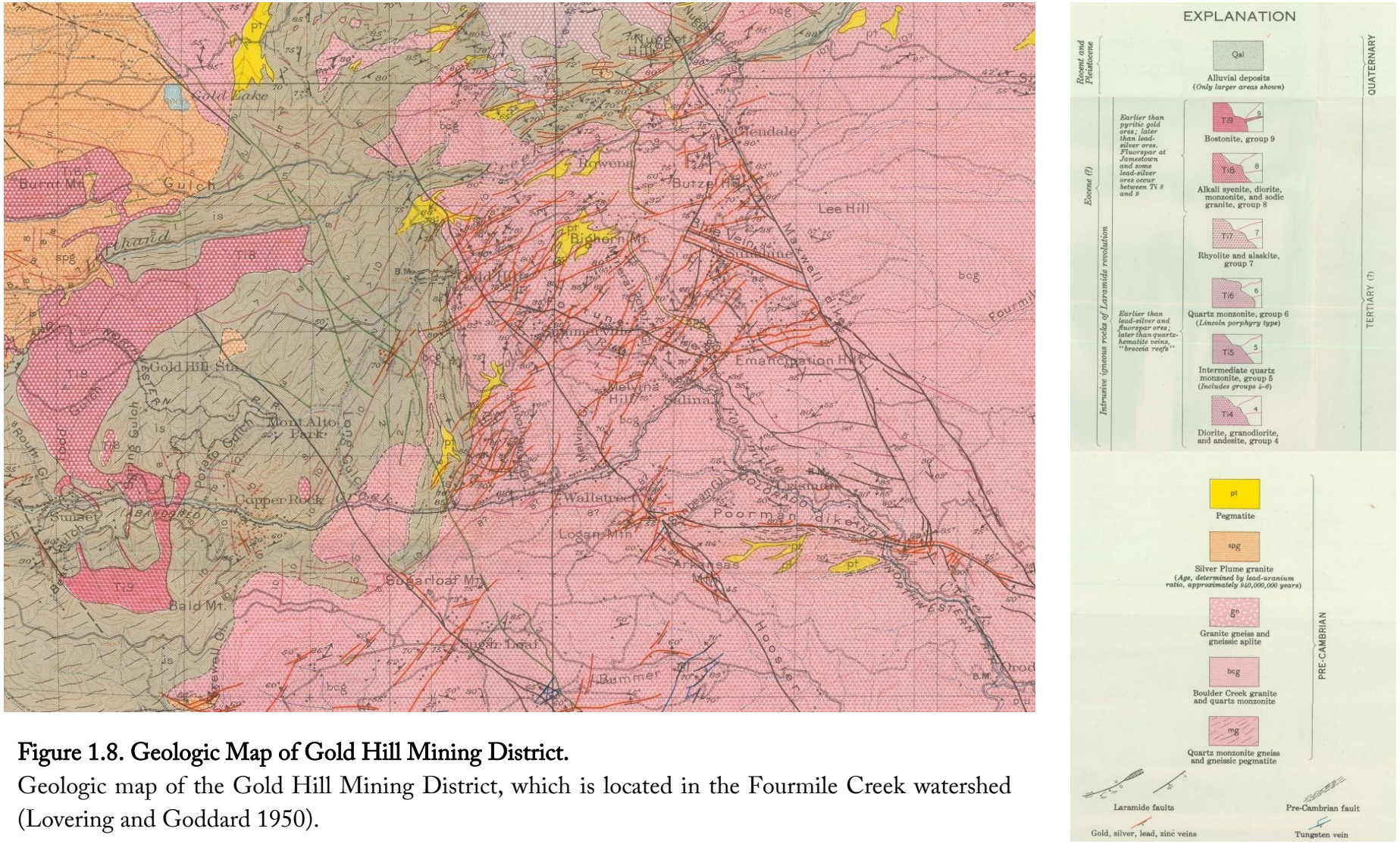


**Figure 1.8. Geologic Map of Gold Hill Mining District.**
Geologic map of the Gold Hill Mining District, which is located in the Fourmile Creek watershed (Lovering and Goddard 1950).

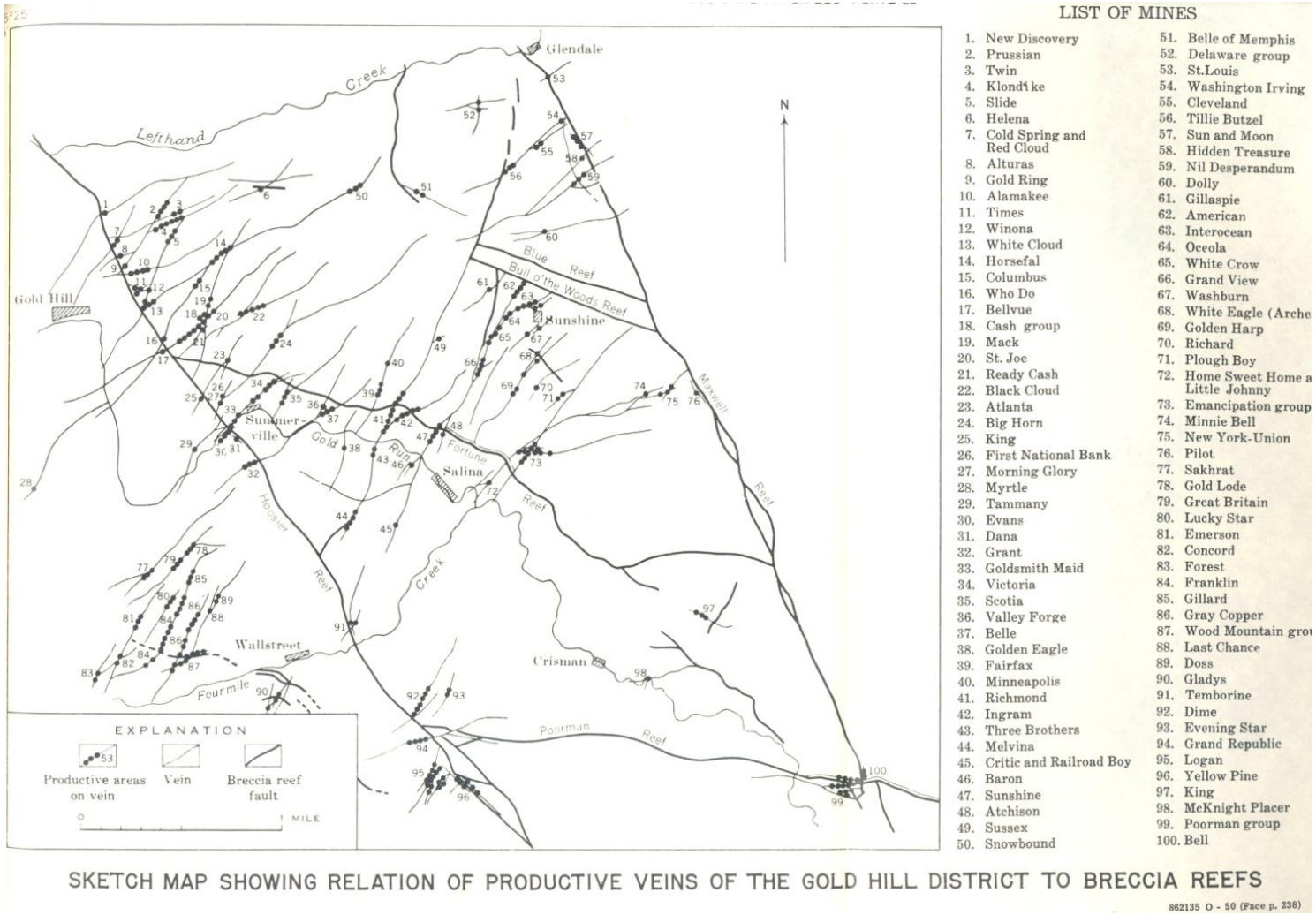


**Figure 1.9. Historic Map of Gold Hill Mining District.**

Historic map of mines, productive veins, and Laramide breccia reefs in the Gold Hill mining district (Lovering and Goddard 1950).

Soils in this area are primarily derived from in-place weathering of metamorphic and igneous bedrock; they tend to be coarse textured, sandy soils that are poorly developed, shallow, and well-drained. North-facing slopes are moister than their south-facing counterparts (Graham et al. 2011). The vegetation is dominated by Ponderosa pine (*Pinus ponderosa*) and Douglas fir (*Pseudotsuga menziesii*) (Murphy et al. 2000), and the rich understory consists of common juniper, mountain mahogany, and grasses (Graham et al. 2011).

Climate varies in the upper Boulder Creek watershed with elevation. Fourmile Creek is located in the foothills region, which in 2000 was reported to have average daily minimum and maximum temperatures of 3˚C and 16˚C, respectively (Murphy et al. 2000). The mean annual temperature is 10.7˚C and the mean summer temperature is 21.2˚C; an average of 47.5 cm of precipitation falls each year (Graham et al. 2011). Most precipitation in the Boulder Creek watershed falls as snow in the upper basin (Murphy et al. 2000).

Wildfires are common in the Colorado Front Range. The fire return interval in Ponderosa pine forests in eastern Colorado is 5–10 years. Despite active fire suppression (*Figure 1.10*), large fires are still common. Recently, two major fires have occurred in the area: the Black Tiger Fire of 1989 and the Hayman Fire of 2002 (Graham et al. 2011). During the summer, the Colorado Front Range often has high-speed winds and low humidity, conditions that are ideal for starting wildfires. In the summer of 2010, before the Fourmile Fire, temperatures were higher than normal and rainfall was below average (*Figure 1.11*). By the beginning of September, the area was experiencing short-term drought conditions (Graham et al. 2011).

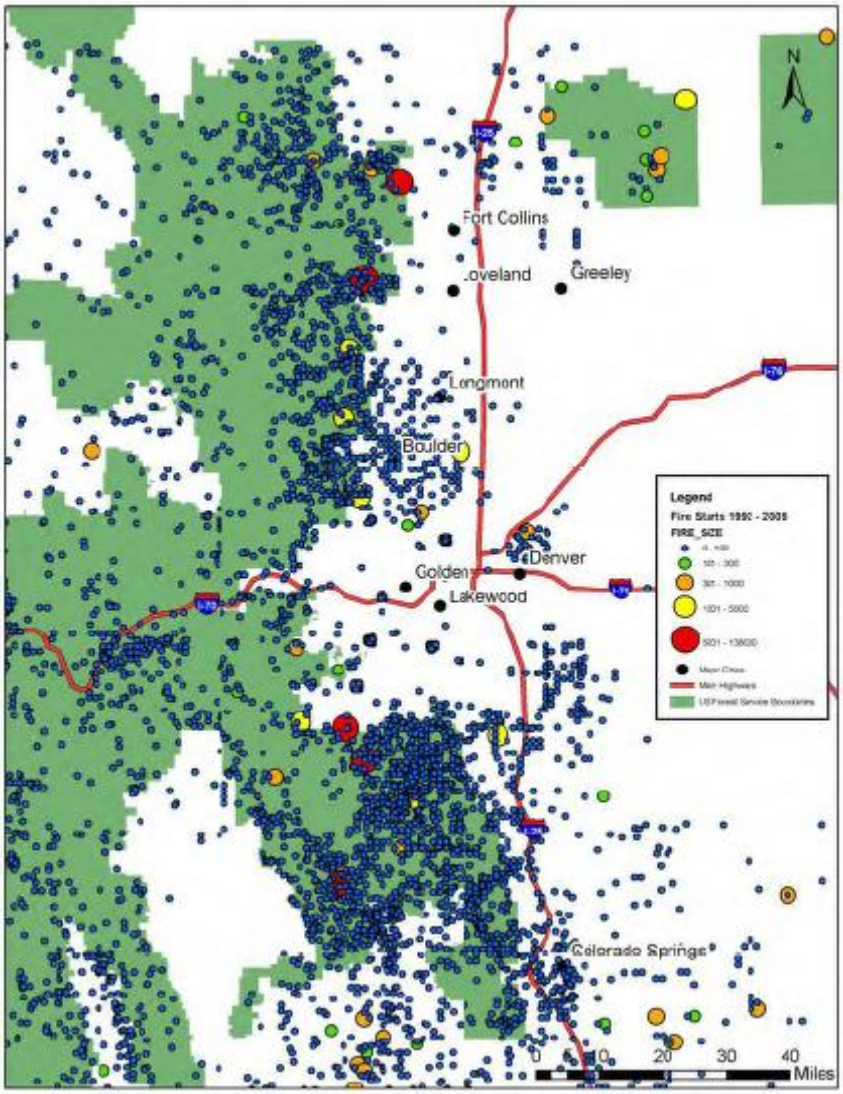


**Figure 1.10. Recent Wildfires near Boulder.**
A map of fire starting locations in the Boulder area from 1992 to 2009; the size of each point represents the size of the fire (Graham et al. 2011).


**Figure 1.11. Precipitation and Temperature in 2010.**
Precipitation and temperature patterns in the Fourmile Creek area for the year 2010 compared to average. Temperatures were above average and precipitation was below average leading up to the Fourmile Fire on Sept. 6, 2010 (Graham et al. 2011).

Starting on September 6, 2010 and burning for 10 days, the Fourmile Fire burned over 6,000 acres (26 $km^2$) (*Figure 1.12*). It was the most destructive wildfire in Colorado history in terms of cost, destroying 169 homes and costing over $217 million in damages (Murphy and Writer 2011). The burned area encompasses the Gold Hill mining district, and the fire exposed many mines and tailings piles (*Figure 1.13*). The area did not experience a major post-fire precipitation event until July 13, 2011, when a severe convective storm caused severe flooding and debris flows in the burned area (*Figure 1.14*). These conditions provide a unique opportunity to study the combined geochemical impact of wildfire and mining in a small watershed.

## 1.6. Potential Impact on Fourmile Creek Watershed

Most geochemical effects of wildfire and mining are additive; both generally increase streamwater concentrations of major solutes and trace elements (McConnell 1995; Rhoades et al. 2011; Smith et al. 2011). Conductivity is a measure of water's ability to conduct an electrical current and represents the total ionic content of a water sample (Drever 1997). By increasing the concentrations of various ions in solution, both wildfire and mining increase streamwater conductivity (Bradley 2008; Rhoades et al. 2011); thus, streamwater conductivity in burned and mined tributaries is expected to be very high. The presence of mine tailings in a watershed provides a further source of material to be eroded after wildfire, while increased hillslope erosion after wildfire causes increased delivery of mining products to streams. In an area affected by both disturbances, specific increases in streamwater solute concentrations are expected to be greater than those reported for catchments affected by only one of these disturbances.

**Figure 1.12. Burned Area Photos.**
Photos taken in the Emerson Gulch watershed, July 2011.

**Figure 1.13. Tailings Exposed by Fourmile Fire.**
Tailings piles exposed by the fire in the Emerson Gulch watershed, July 2011.

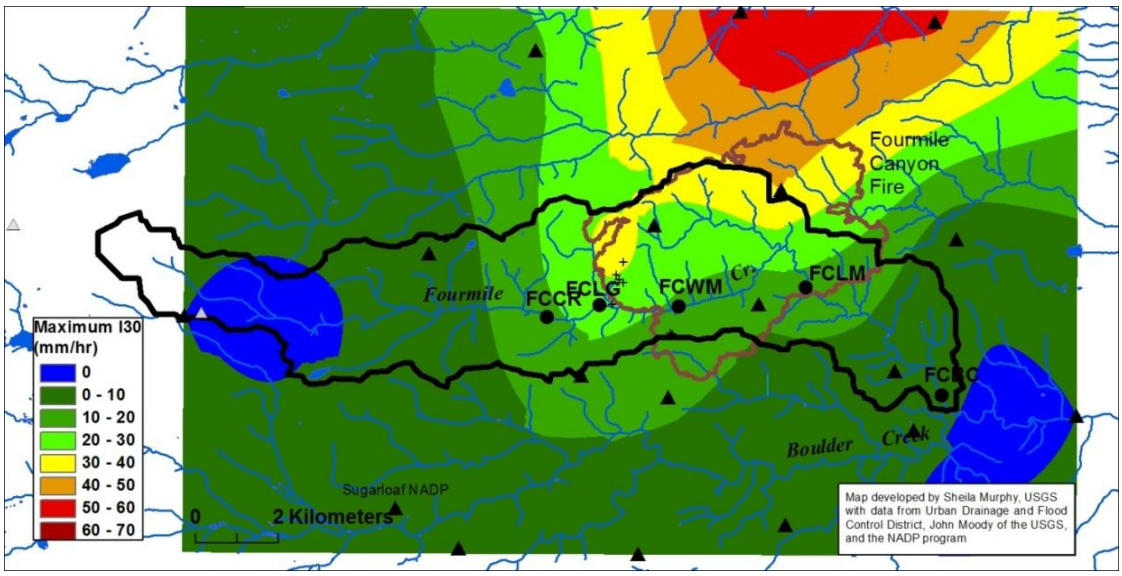


**Figure 1.14. Post-Fire Precipitation in Fourmile Watershed.**
*Top*: Map showing the maximum 30-minute rainfall intensity during the rainstorm on July 13, 2011 (S. Murphy, personal communication).
*Bottom*: Near the mouth of Melvina Gulch, a large pile of sediment that was transported downstream during flooding, July 2011.

While wildfire increases streamwater alkalinity through the production of alkaline ash (Bayley and Schindler 1991), the weathering of sulfide minerals associated with mine drainage is a source of acidity (Bradley 2007). Increased acidity is associated with decreased alkalinity, as $HCO_3^-$ is used to buffer the acid (Drever 1997). The effects of wildfire and mining on streamwater alkalinity could cancel each other out, or one may dominate over the other. The high system buffering capacity in this area due to carbonate in ore deposits further reduces the impact of acidity from mine drainage. Increased solubility of metals and other solutes in streams affected by mine drainage is a result of increased acidity, and these effects may be reduced in this watershed. Other effects of mining, including elevated $SO_4^{2-}$, are independent of changes in pH or alkalinity.

Wildfire and mining also have opposing effects on sediment mercury concentrations. Wildfire reduces mercury levels by revolatilizing any accumulated mercury (Biswas et al. 2008), although the amount released is limited by the amount stored in soils prior to burning (Biswas et al. 2007). In contrast, mining is a source of mercury in addition to atmospheric deposition (Alpers et al. 2005). Mines in the Colorado Front Rage did not commonly use mercury amalgamation, so reported impact of mining on sediment mercury is less there than in a typical mined area (Mast and Krabbenhoft 2010). Additionally, the effects of wildfire, a more recent disturbance, could mask the impact of mining on mercury.

Samples were collected shortly after the first major post-fire precipitation event. As this was nearly 10 months after the fire, the area had some time for vegetation recovery. The degree of flooding and debris flows generated by this storm, however, suggests that the area was still severely affected by the fire. As this was the

first substantial precipitation since the fire, any buildup of nutrients and cations from ash, or other changes in hillslope chemistry as a result of the fire, would likely have been flushed out during this storm, so this is an opportune time to observe the impact of the fire on streamwater and sediment chemistry. Sampling was too long after the fire to reveal the short-term impacts of ash, so this study will focus on the longer-term impacts of wildfire on the chemistry of a historically mined watershed.

# 2. METHODS

## 2.1. Field Sampling and Measurement

Streamwater was sampled from nineteen tributaries of Fourmile Creek, ten locations along Fourmile Creek, and two mine drainage sites (*Figures 3.1, 3.2a*). Arkansas Gulch, Potato Gulch, and Dry Gulch were not sampled for water because they were dry. Several Fourmile Creek sampling sites were chosen immediately upstream of the mouths of major tributaries so that the impact of tributary input could be evaluated. Samples were collected at all locations on July 25, 2011 and August 3, 2011 with the exception of two tributaries. Sunbeam Gulch had dried up between sampling dates and Melvina East Gulch was not discovered until the later date. On August 3, three additional water samples were taken in a downstream profile along Emerson Gulch. For each sample, a bottle was washed out three times with streamwater and then filled. Samples were filtered within 24 hours of collection using a separate 0.45-micron filter for each sample. Eighteen samples were shared with the USGS in Boulder and were filtered using their equipment. The remaining samples were filtered using a portable Nalgene filter. All samples were split into two bottles after filtering; 30 mL of each was acidified with nitric acid.

Streamwater conductivity was recorded using an Amber Science digital conductivity meter after collecting each water sample; many additional conductivity measurements were taken on other days and at other locations along Fourmile Creek. For every tributary, discharge at the time of sampling was recorded. Many tributaries ran through culverts; for these, the entire flow was collected and discharge was calculated as a volume per time. Where culverts were not available, it was often

**Figure 2.1. Sampled Tributary Photos.**
Four sampled tributaries of Fourmile Creek. *Top left*: Firehouse mine drainage site. *Top right*: Bald Gulch, a small unburned tributary. *Bottom left*: Gold Run, Fourmile Creek's largest tributary, which was both burned and mined. *Bottom right*: Ingram Gulch, a tributary of Gold Run that was also burned and mined. Photos taken July–August 2011.

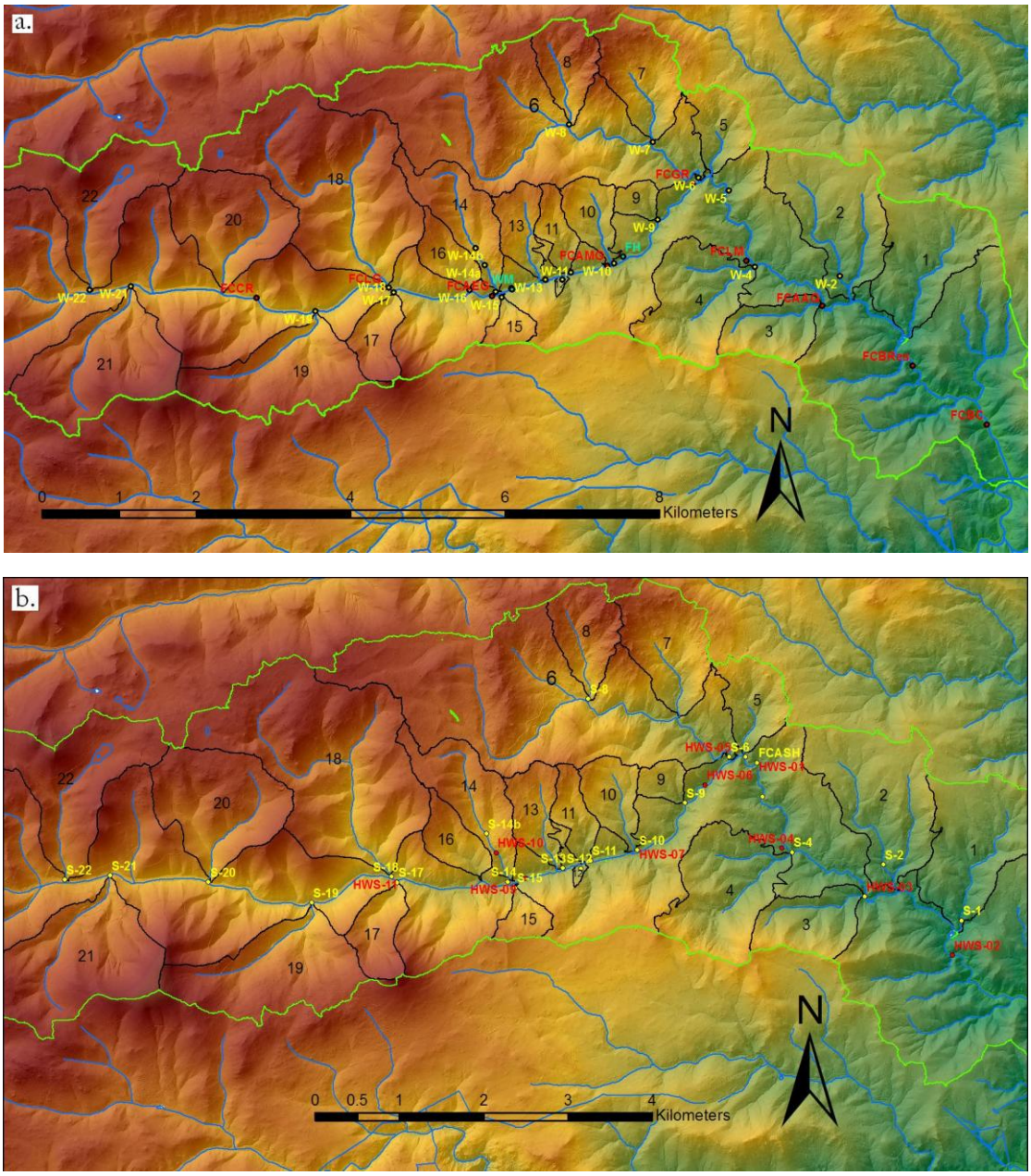


**Figure 2.2. Sample Site Maps.**

a. Map of water sampling sites. Tributary samples are shown in yellow; Fourmile Creek samples are shown in red; mine drainage sites are shown in turquoise. Sites FCWM (located near site WM) and W-14 (located at the mouth of watershed 14) are not labeled.

b. Map of sediment sampling sites. Streambed samples are shown in yellow; flood deposit samples are shown in red. All sample numbers correspond with watershed number.

possible to divert nearly the entire flow into a bucket and use the same method, estimating the percentage of flow that was lost. For tributaries with low discharge, flow was collected in a Ziploc bag and its volume measured in a graduated cylinder. For tributaries with high discharge, for which it was impossible to collect the entire flow, discharge was calculated by estimating the average width and depth of the channel and recording the velocity of a wooden dowel in the stream over a certain length. The resulting surface velocity measurement was adjusted by a factor of 0.7 to represent the average velocity (Jopling 1966), which was multiplied by average width and depth to estimate discharge. In all cases, three to five discharge measurements were averaged.

Surface streambed sediment samples were collected from all tributaries except Emerson West Gulch and Ingram Gulch (*Figure 2.2b*). These run alongside roads that had been heavily reworked in response to post-fire debris flows and flooding. The streams were diverted, and undisturbed streambed sediment could not be found (*Figure 2.3*). Samples were stored in Ziploc bags and periodically drained of liquid. Where possible, sediment that had clearly been deposited along stream banks during the July 13 flooding event was sampled (*Figure 2.4*). Flood deposit samples were collected from five tributary sampling sites and six sites along Fourmile Creek.

## 2.2. ArcGIS Analysis

Analysis in ArcGIS 10 was used to delineate the watersheds of each sampled tributary and quantify characteristics of each, including fire severity, degree of mining disturbance, underlying bedrock, and average slope. This analysis was used in conjunction with chemical analysis of tributary water and sediment samples.

**Figure 2.3. Ingram Gulch Mouth.**
Ingram Gulch runs alongside a road, making it impossible to sample undisturbed streambed sediment, July 2011.

**Figure 2.4. Black Hawk Flood Deposit.**
Undisturbed flood deposit along the banks of Black Hawk Gulch, a burned and mined tributary of Gold Run, July 2011.

A 1-m-resolution Light Detection and Ranging (LiDAR) dataset was used to produce a digital elevation model (DEM) mosaic encompassing the Fourmile Creek watershed. This DEM was used to delineate all watersheds from which samples were collected. A depressionless DEM was created using the Fill tool, which "fills" areas of internal drainage. Using the filled DEM, the Flow Direction tool was used to create a raster containing the downslope direction for each cell, and the Flow Accumulation tool was used to create a raster containing the number of cells upslope of each cell. The precise point at which each tributary enters Fourmile Creek, the pour point, was identified as the pixel with the highest flow accumulation before merging with Fourmile. A shapefile was created for each pour point and used as input for the Watershed tool along with the Flow Direction raster. After watersheds were delineated, they were converted into polygons and the area of each was calculated.

Delineation of the Wall Street watershed, basin 12 (see *Figure 1.7*), was questionable. Despite precise location of sampling and measurement sites in ArcGIS, the calculated watershed was unexpectedly small (0.028 $km^2$). This is nearly an order of magnitude smaller than the next larger analyzed basin. Its measured discharge on both dates was ~0.1 L/sec, and it is unlikely that a watershed of this size could have channelized so much water. It is possible that water was diverted into this catchment from an adjacent larger basin. To avoid uncertainty, this watershed was eliminated from analyses relying on basin characteristics.

Fire intensity in each watershed was quantified using a raster dataset compiled by the USGS. This dataset uses the differenced normalized burn ratio (dNBR) as a proxy for fire intensity. NBR values are calculated using Landsat remote sensing imagery from before and after a fire, and the difference between pre- and post-fire

images directly reflects wildfire damage to vegetation (Platt et al. 2011). More so than other approximations, dNBR has been found to accurately estimate fire intensity when compared with field measurements of burn severity, such as the composite burn index (CBI) (Cocke et al. 2005; Epting et al. 2005; Allen and Sorbel 2008; Miller et al. 2009). According to the Burned Area Reflectance Classification (BARC), burned areas are classified into four categories: unchanged (but not necessarily unburned), low intensity burn, moderate intensity burn, and high intensity burn (Platt et al. 2011). Alhough the Fourmile Fire dNBR raster had values ranging from 0 to 255, it was reclassified to correspond to the four BARC classes. The Extract by Mask tool was used to map the dNBR raster onto each watershed. From these raster masks, the percent area of the watershed that belonged to each BARC class was calculated. The total percent area burned was used as a proxy for watershed fire intensity.

In order to quantify the degree of mining disturbance in each tributary watershed, an up-to-date map of mines and tailings piles in the Fourmile basin was produced using a combination of historic mining data (U.S. Geological Survey 2011), my field observations, and Google Earth satellite imagery. The historic dataset contains a set of GPS points and was loaded into Google Earth. Starting in areas well-documented in the field, polygons were traced that outlined mines and tailings piles. Polygons were used instead of points to account for the varying sizes of mines and tailings piles. The location and size of each polygon was checked using several satellite images taken over a span of 12 years. After mapping areas that were familiar from field work, the procedure was extrapolated to the rest of the watershed. The area of each polygon was calculated, and the total area of polygons in each watershed was determined, approximating the total area disturbed by mining in each watershed. The

percentage area of each watershed that was mined or covered in tailings was used as a proxy for watershed mining intensity.

From a dataset with bedrock geology for the state of Colorado (Stoeser et al. 2005), bedrock polygons that covered the Fourmile Creek watershed were isolated and used to characterize the bedrock of each watershed. The polygons were converted into a raster in which each rock type had a different value, and the Extract by Mask tool was used to create a mask for every watershed that consisted of more than one bedrock type. From these masks, the percentage area covered by each bedrock type was calculated for each watershed.

Using the Slope tool, a slope map of the Fourmile watershed was produced, and the Extract by Mask tool was used to create a slope mask for each watershed. From these masks, the average slope of each watershed was calculated.

## 2.3. Lab Analysis of Samples

Water samples were chemically analyzed at Amherst College using alkalinity titrations, inductively coupled plasma mass spectrometry (ICP-MS), and ion chromatography (IC). Samples were analyzed at Smith College using cavity ringdown spectroscopy isotope analysis and inductively coupled plasma optical emission spectrometry (ICP-OES). Fourmile Creek samples, as well as some tributary samples, were analyzed by the USGS in Boulder using inductively coupled plasma atomic emission spectroscopy (ICP-AES) for cations and trace elements, IC for anions, and an autotitrator for alkalinity.

The alkalinity of water samples was determined by titration with 0.02 N hydrochloric acid. Drops of acid were added in ~0.1 mL increments to 8.0 mL of

sample and pH was recorded at each step. As pH declined, acid increments were reduced to ~0.01 mL. This continued until at least 10 points were recorded below a pH of 4.5. The data were used to plot the titration curve and Gran function, which is a function of pH and volume of acid added. The x-intercept of the Gran function best-fit line was used to calculate alkalinity, which, at the pH of samples in this study (>8.0), is equivalent to $HCO_3^-$ concentration.

To determine trace element concentrations, acidified water samples were analyzed using ICP-MS. Three standards and a blank were used for Ag, Al, As, Ba, Be, Bi, Cd, Co, Cr, Cs, Cu, Fe, Ga, In, Li, Mn, Ni, Pb, Rb, Se, Sr, Tl, U, V, and Zn, and an additional two standards were used to account for higher concentrations of Mn. Standards were prepared by weight in Nalgene volumetric flasks, and after adding standard solutions, flasks were filled with 3% optima acid. Yttrium was used as the internal standard. Four check solutions were interspersed throughout the run to calculate precision and accuracy. The lower detection limit for each element was determined by tripling the absolute value of the measured concentration in the blank. Concentrations of Be, Bi, Cs, In, Se, and Tl were below detection limits for nearly all samples, so these were not included in trace element analysis.

Concentrations of $Cl^-$, $F^-$, $NO_3^-$, and $SO_4^{2-}$ in unacidifed samples were determined using IC. Three standards were prepared based on expected anion concentrations, as inferred from conductivity and alkalinity measurements. Standards were prepared by weight in volumetric flasks and, after adding standard solutions, flasks were filled with deionized (DI) water. Due to very high $SO_4^{2-}$ concentrations, many samples were diluted with DI water. A check was run after every five samples and used to calculate precision and accuracy.

A Picarro isotope analyzer was used to determine the ratios of $^{18}O$ to $^{16}O$ and $^{2}H$ to $^{1}H$ in each water sample. Isotope measurements were taken six times, and the latter three measurements were averaged for analysis. Snow and water standards were run after every ten samples. Data were compared to the Global Meteoric Water Line (GMWL) and a Local Meteoric Water Line (LMWL) calculated for the Pawnee National grasslands, located ~100 km northeast of Fourmile Creek (Harvey 2005).

ICP-OES was used to determine concentrations of $Ca^{2+}$, $Mg^{2+}$, $Na^{+}$, $K^{+}$, $Sr^{2+}$, and $SiO_2$ in acidified samples. Three standards and a blank were prepared based on expected concentrations, as determined using the USGS data for samples from the same area. Standards were prepared by weight in volumetric flasks, and after adding standard solutions, flasks were filled with 3% optima nitric acid. The blank consisted of only optima acid, and if necessary, samples were diluted with optima acid. The medium standard was run as a check after every five samples and used to calculate precision and accuracy.

Sediment samples were analyzed at Amherst College using loss on ignition (LOI), Elemental Analysis (EA), Hydra-C mercury analysis, and Scanning Electron Microscopy (SEM). Samples were analyzed at University of Massachusetts Amherst using X-ray flurorescence (XRF). Unpowdered samples were used for LOI and SEM; for all other analyses, bulk samples were first powdered in a tungsten carbide shatterbox at University of Massachusetts Amherst.

To determine LOI, samples were dried in a furnace at 100˚C for >24 hours. They were weighed and transferred to another furnace at 500˚C for 2 hours. After cooling for 10 minutes, the samples were weighed again. LOI was calculated as the percent weight lost in the 500˚C furnace.

Using EA, C:N ratios were measured. Expected C concentrations were calculated using LOI data, which provide the percent organic C present in each sample. The required mass of each sample was calculated so that the amount of C would fall within the range of acetanilide standards used. Many samples had very low LOI and would thus require a large mass to reach the desired amount of C. A maximum of 5,000 μg was used for each sample, and extra acetanilide standards of lower weight were added to the sequence to ensure that the calibration curve was accurate for lower values. Weight % C and weight % N were reported for each sample, and the C:N ratio was calculated by dividing these values.

Samples were also run on the Hydra-C mercury analyzer, a cold vapor atomic adsorption spectrometer (CVAAS). NIST standard 2702 (marine sediment) was run after every six samples and used to calculate precision and accuracy. The Hg:C ratio in ppm/wt % was calculated in conjunction with EA data and used for analysis.

Six samples were bound with epoxy, made into thin sections, and carbon-coated for SEM analysis. Sediment from the three most heavily mined watersheds, as determined by ArcGIS analysis, and three entirely unmined watersheds were chosen. Samples were analyzed to determine the composition of grains with high atomic number, those that appeared brightest in a back-scattered election image. The goal of this analysis was to determine whether mined watersheds contained any reactive sulfides, and to establish any obvious differences in sediment chemistry characterizing mined versus unmined watersheds.

XRF analysis was used to determine concentrations of major oxides. Samples were ignited overnight in a furnace at 850˚C and then ground into a fine powder with a mortar and pestle. For each sample, two mixtures consisting of 0.3 ± .0003 g sample

and 1.6070–1.6075 g flux (a mixture of 47% lithium tetraborate, 36.7% lithium carbonate, and 16.3% lanthanum oxide) were weighed out. A powdered ammonium iodide tablet was stirred into each mixture before it was put into a furnace at 1050°C for six minutes. Every two minutes, the sample was removed from the furnace and stirred for ~20 seconds. After six minutes, the liquid was poured onto a graphite disc and pressed into a glass disc that would be run in the machine. Two discs were fused and run for each sample. Major analysis yielded percent concentrations of $Al_2O_3$, CaO, $Fe_2O_3$, $K_2O$, MgO, MnO, $Na_2O$, $P_2O_5$, $SiO_2$, and $TiO_2$. Two standards were run after every three samples. The two values for each sample were averaged and used for analysis unless one of the two yielded a total percentage that deviated from 100% by more than 0.5%, in which case the better measurement was used.

## 2.4. Statistical Data Analysis

Fire and mining intensity in each watershed, as determined using ArcGIS analysis, were compared with concentrations of each measured constituent in tributary water and sediment samples to determine which constituents had statistically significant correlations with watershed fire and/or mining intensity. For water samples, 18 watersheds were sampled and analyzed. With 16 degrees of freedom (calculated to be 2 fewer than the total number of values used) and a significance level of 0.05, Pearson's critical correlation coefficient is 0.468. There were 19 watersheds from which sediment samples were collected and analyzed; Pearson's critical correlation coefficient with a significance level of 0.05 and 17 degrees of freedom is 0.456. These were the thresholds used to distinguish significant correlations for analyses considering all tributary samples.

Welch two-sample *t*-tests with a confidence level of 0.95 were used to determine if there were significant differences in concentration between watersheds with predominantly Boulder Creek granodiorite bedrock and those with predominantly metamorphic bedrock. Watersheds with no more than 75% of their area covered by a single bedrock type were not considered in this analysis to isolate differences in bedrock type; this eliminated only two watersheds. The results of this analysis were corroborated with a bedrock chemistry dataset of unweathered bedrock samples from nearby Gordon Gulch and Betasso Gulch (D. Dethier, personal communication).

Tributary water samples were also analyzed in smaller groups based on their characteristics (e.g., only watersheds that were burned). The thresholds for significant correlations were individually determined for each analysis of a subset of tributary data using Pearson's critical correlation coefficient with a significance level of 0.05. Paired *t*-tests were used to determine if there were significant differences between flood deposits and streambed sediment collected from the same watershed and between tributary and Fourmile flood deposits.

## 2.5. Limitations of Analysis

Three variables from ArcGIS anaylsis were primarily used to analyze chemical data: bedrock type, fire intensity, and mining intensity. When analyzing chemical data, these variables were considered independent, but a limitation of this analysis is association between the variables. Mines were located in Boulder Creek granodiorite intrusions and not in areas with metamorphic bedrock, and the burned area closely

overlapped with the mined area. Fully distinguishing between the effects of wildfire, mining, and bedrock is difficult for tributary samples.

Watersheds were divided into two groups based on bedrock type, and samples were tested to determine if the groups had significant chemical differences. However, this analysis disregards variation in bedrock chemistry within units and ignores the Cretaceous/Paleogene granite in the upper watershed. Although this granite was not predominant in any catchment, it could still impact watershed chemistry.

Accuracy of analysis of tributary chemistry according to estimated fire and mining intensity is limited by the strength of the proxies used to represent these variables. The dNBR is itself a proxy for fire intensity, although it is widely considered the most accurate (Cocke et al. 2005; Epting et al. 2005; Allen and Sorbel 2008; Miller et al. 2009). In this study, the fire intensity in a given watershed was represented as the percent area burned, which correlates strongly with average dNBR fire intensity for each watershed ($r = 0.991$), however, this does not fully represent the distribution of fire intensity within a watershed.

Mining intensity was estimated using the percent area covered by mines and tailings piles without distinguishing between the two, thus, this proxy does not take into account the number of mines in each watershed. There was no correlation between number of mines and percent area disturbed by mining ($r = 0.318$), but it is possible that many small mines have a different impact on a watershed than a few large ones. It also does not take into account what was being mined at each site, a key factor especially in determining how much mercury mines might contribute.

# 3. RESULTS

## 3.1. ArcGIS Results

Tributary watersheds were analyzed in ArcGIS to characterize watershed mining intensity, fire intensity, bedrock, and slope (*Figure 3.1*; *Table 3.1*). Ten watersheds have no mining presence, and 12 have some degree of mining disturbance (*Figure 3.1b*). The number of mines per watershed ranges from 1 to 82, the total area disturbed by mining ranges from 133 $m^2$ to 25,375 $m^2$, and the percent area mined ranges from 0.01% to 1.66% (*Table 3.1*).

The Fourmile Fire burned part of 16 watersheds, leaving six watersheds entirely unburned (*Figure 3.1c*). Most unburned watersheds are upstream of the fire, with only one, Arkansas Gulch, located downstream. Three watersheds are burned to a small degree: Dry Gulch (0.1%), Sunbeam Gulch (13.04%), and Long Gulch (24.84%). Other watersheds have at least 67.73% total area burned (*Table 3.1*).

There are four bedrock units in the Fourmile Creek watershed: Early Proterozoic biotite gneiss and schist, Boulder Creek granodiorite (Early Proterozoic), Silver Plume granite (Middle Proterozoic), and Cretaceous/Paleogene granodiorite (*Figure 3.1d*). The lower watershed consists of Boulder Creek granodiorite, and 13 tributary watersheds have entirely Boulder Creek bedrock. Metamorphic rock runs through the upper Fourmile watershed. Eight tributary watersheds have a substantial amount of metamorphic bedrock; for six of these, it is the predominant bedrock type (*Table 3.1*). Only four watersheds have Cretaceous/Paleogene granite, which occurs as a thin unit within metamorphic rock in the upper part of the watershed. Silver Plume granite appears only in a small portion of the Todd Gulch watershed.

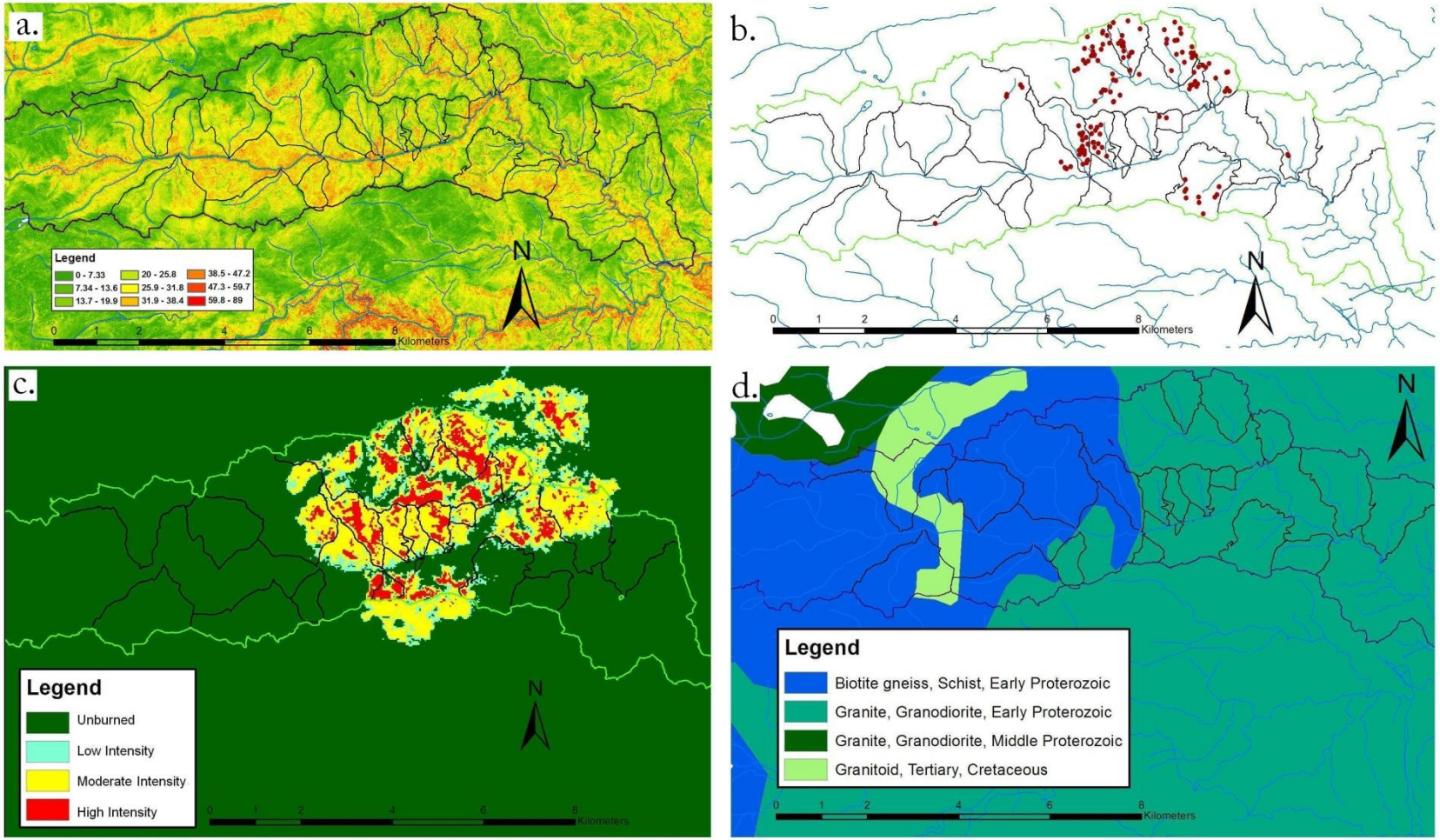


**Figure 3.1. Fourmile Watershed Maps.**

Maps showing attributes of the Fourmile Creek watershed. a. Slope map. b. Map of mines and tailings, shown here as points. c. Differenced Normalized Burn Ratio (dNBR) intensity map of Fourmile Fire. d. Simplified bedrock map.

| | Tributary Name | Watershed Area (sq. km) | Avg. Slope (°) | Down-stream Dist. from Todd (km) | Discharge (L/sec) | | % Area by Bedrock | | | | # Mines | Area Disturbed by Mining (sq. m) | % Area Disturbed by Mining | % Area Low Intensity Burn | % Area Moderate Intensity Burn | % Area High Intensity Burn | Total % Burned |
|---|---|---|---|---|---|---|---|---|---|---|---|---|---|---|---|---|---|
| | | | | | 7/25 | 8/03 | Boulder Creek granodiorite, Early Proterozoic | Biotite gneiss and schist, Early Proterozoic | Granodiorite, Tertiary / Cretaceous | Silver Plume granite, Middle Proterozoic | | | | | | | |
| 1 | Dry | 1.79 | 20.2 | 13.2 | 0.0 | 0.0 | 100.0 | 0.0 | 0.0 | 0.0 | 0 | 0 | 0.00 | 0.0 | 0.1 | 0.0 | 0.1 |
| 2 | Sand | 1.93 | 17.4 | 12.3 | 0.2 | 0.3 | 100.0 | 0.0 | 0.0 | 0.0 | 2 | 133 | 0.01 | 9.3 | 53.8 | 4.7 | 67.7 |
| 3 | Arkansas | 0.81 | 28.3 | 11.8 | 0.0 | 0.0 | 100.0 | 0.0 | 0.0 | 0.0 | 0 | 0 | 0.00 | 0.0 | 0.0 | 0.0 | 0.0 |
| 4 | Sunbeam | 1.60 | 24.9 | 10.7 | 0.1 | 0.0 | 100.0 | 0.0 | 0.0 | 0.0 | 10 | 4523 | 0.28 | 8.5 | 3.7 | 0.8 | 13.0 |
| 5 | Sweet Home | 0.66 | 24.0 | 9.1 | 1.1 | 0.4 | 100.0 | 0.0 | 0.0 | 0.0 | 7 | 2871 | 0.43 | 10.1 | 64.3 | 18.4 | 92.9 |
| 6 | Gold Run | 7.28 | 21.6 | 9.0 | 26.1 | 21.5 | 78.9 | 21.1 | 0.0 | 0.0 | 82 | 25375 | 0.35 | 14.1 | 37.2 | 19.6 | 70.9 |
| 7 | Ingram | 1.19 | 25.9 | 9.0 | 6.8 | 7.7 | 100.0 | 0.0 | 0.0 | 0.0 | 17 | 2415 | 0.20 | 5.0 | 54.6 | 36.6 | 96.3 |
| 8 | Black Hawk | 0.78 | 25.2 | 9.0 | 2.1 | 1.6 | 100.0 | 0.0 | 0.0 | 0.0 | 17 | 12964 | 1.66 | 17.9 | 50.2 | 12.9 | 81.0 |
| 9 | Melvina East | 0.23 | 20.7 | 8.1 | 0.1 | 0.1 | 100.0 | 0.0 | 0.0 | 0.0 | 2 | 291 | 0.13 | 18.7 | 71.8 | 6.2 | 96.7 |
| 10 | Melvina | 0.55 | 22.1 | 7.3 | 0.8 | 0.3 | 100.0 | 0.0 | 0.0 | 0.0 | 0 | 0 | 0.00 | 3.0 | 63.0 | 31.6 | 97.6 |
| 11 | Melvina West | 0.38 | 24.1 | 6.6 | 1.0 | 0.5 | 100.0 | 0.0 | 0.0 | 0.0 | 0 | 0 | 0.00 | 6.2 | 83.6 | 7.2 | 97.1 |
| 12 | Wall Street | 0.03 | 26.6 | 6.6 | 0.1 | 0.1 | 100.0 | 0.0 | 0.0 | 0.0 | 0 | 0 | 0.00 | 0.0 | 0.0 | 0.0 | 0.0 |
| 13 | Schoolhouse | 0.55 | 22.5 | 6.3 | 1.5 | 0.4 | 100.0 | 0.0 | 0.0 | 0.0 | 13 | 3119 | 0.57 | 1.1 | 84.2 | 14.1 | 99.4 |
| 14 | Emerson | 1.04 | 21.8 | 5.7 | 1.3 | 0.2 | 7.9 | 92.1 | 0.0 | 0.0 | 19 | 5498 | 0.53 | 4.9 | 60.2 | 32.9 | 97.9 |
| 15 | Banana | 0.26 | 22.4 | 5.7 | 1.4 | 0.7 | 100.0 | 0.0 | 0.0 | 0.0 | 0 | 0 | 0.00 | 6.5 | 23.7 | 56.2 | 86.3 |
| 16 | Emerson West | 0.45 | 25.4 | 5.3 | 0.6 | 0.4 | 22.8 | 77.2 | 0.0 | 0.0 | 5 | 1250 | 0.28 | 5.1 | 85.1 | 9.7 | 99.9 |
| 17 | Sugarloaf | 0.54 | 29.8 | 4.2 | 0.3 | 0.0 | 97.8 | 2.2 | 0.0 | 0.0 | 0 | 0 | 0.00 | 0.0 | 0.0 | 0.0 | 0.0 |
| 18 | Long | 4.08 | 21.7 | 4.1 | 2.7 | 1.4 | 0.0 | 100.0 | 0.0 | 0.0 | 4 | 1158 | 0.03 | 3.7 | 18.3 | 2.9 | 24.8 |
| 19 | Bald | 1.89 | 22.1 | 3.1 | 0.7 | 0.4 | 34.0 | 62.8 | 3.2 | 0.0 | 1 | 396 | 0.02 | 0.0 | 0.0 | 0.0 | 0.0 |
| 20 | Potato | 1.73 | 21.6 | 1.7 | 0.0 | 0.0 | 0.0 | 99.8 | 0.2 | 0.0 | 0 | 0 | 0.00 | 0.0 | 0.0 | 0.0 | 0.0 |
| 21 | Bear | 2.23 | 21.9 | 0.5 | 0.8 | 0.5 | 0.0 | 78.3 | 21.7 | 0.0 | 0 | 0 | 0.00 | 0.0 | 0.0 | 0.0 | 0.0 |
| 22 | Todd | 2.22 | 18.1 | 0.0 | 0.2 | 0.2 | 0.0 | 49.7 | 48.6 | 1.7 | 0 | 0 | 0.00 | 0.0 | 0.0 | 0.0 | 0.0 |

**Table 3.1. Tributary Watershed Properties.**
Summary of watershed properties, calculated using ArcGIS.

Tributary water and sediment chemistry were compared with calculated fire and mining intensity in corresponding watersheds. Although there is overlap between the areas affected by wildfire and mining—most burned watersheds are mined, and all but one mined watershed is burned—the intensity of these disturbances within individual watersheds does not have a significant correlation (r = 0.313; Pearson's cutoff = 0.468) (*Figure 3.2*).

## 3.2. Water Chemistry Results

All water samples were chemically classified using Piper plots (Fetter 2001). Upstream of the fire, Fourmile Creek samples are calcium bicarbonate waters, and gradually become calcium sulfate waters downstream through the disturbed area (*Figure 3.3a*). Waters are consistently calcium-type, close to the boundary between calcium-type and mixed-type. All tributary samples from unburned and/or unmined watersheds are calcium bicarbonate waters (*Figure 3.3b,c*). Some unmined tributaries are close to the boundary between calcium bicarbonate and calcium sulfate waters; these tributaries are unmined and burned. Most samples from watersheds affected by both wildfire and mining are calcium sulfate waters, although a few classify as calcium bicarbonate (*Figure 3.3d*). Disturbed tributaries have varied cation concentrations without a directed trend, while Fourmile Creek samples shift toward greater $Ca^{2+}$ levels downstream.

All water samples plot at $\delta^{18}O$ and $\delta D$ values below the LMWL and GMWL on an oxygen–deuterium isotope plot (*Figure 3.4*). There are two distinct clusters of points, one of Fourmile Creek samples and one of tributary samples; Fourmile Creek has lower $\delta^{18}O$ and $\delta D$ than tributaries. There is no correlation between watershed

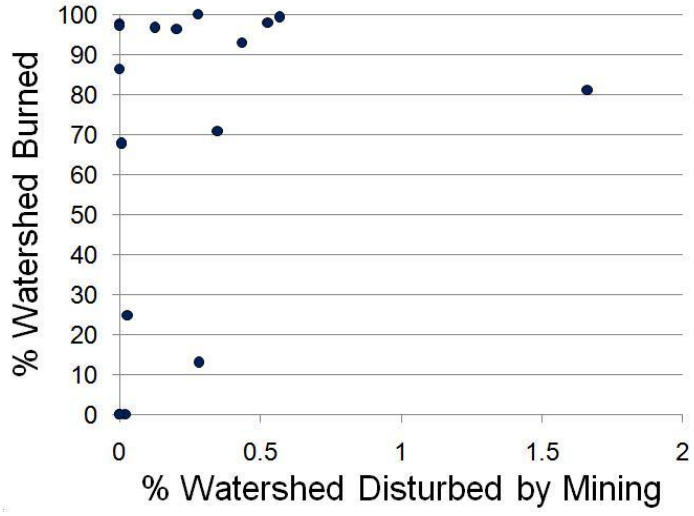


**Figure 3.2. Watershed Fire and Mining Intensity.**
There is no correlation between watershed fire and mining intensity.

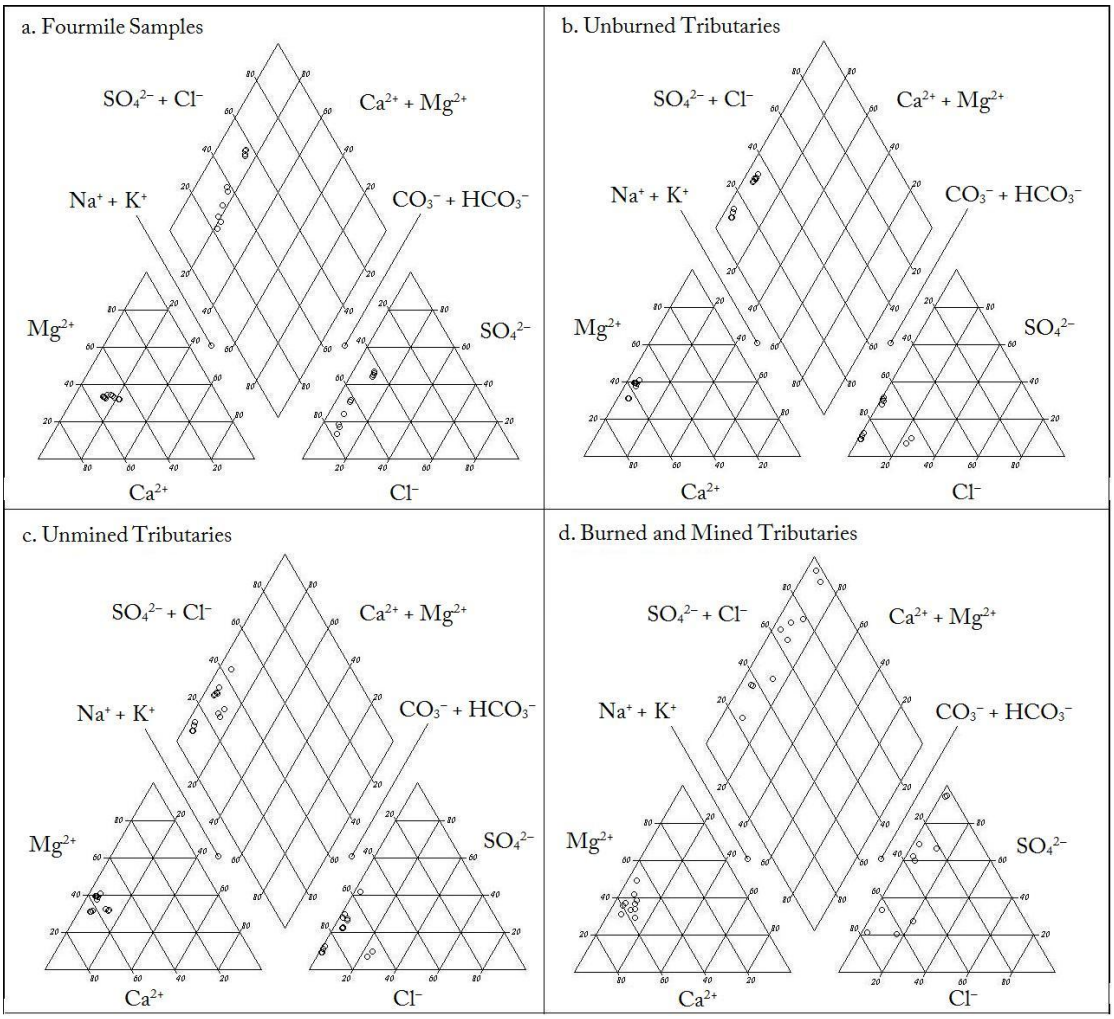


**Figure 3.3. Piper Plots.**
Piper plots for Fourmile Creek samples (a), samples from unburned tributaries (b), samples from unmined tributaries (c), and samples from tributaries that were both burned and mined (d).

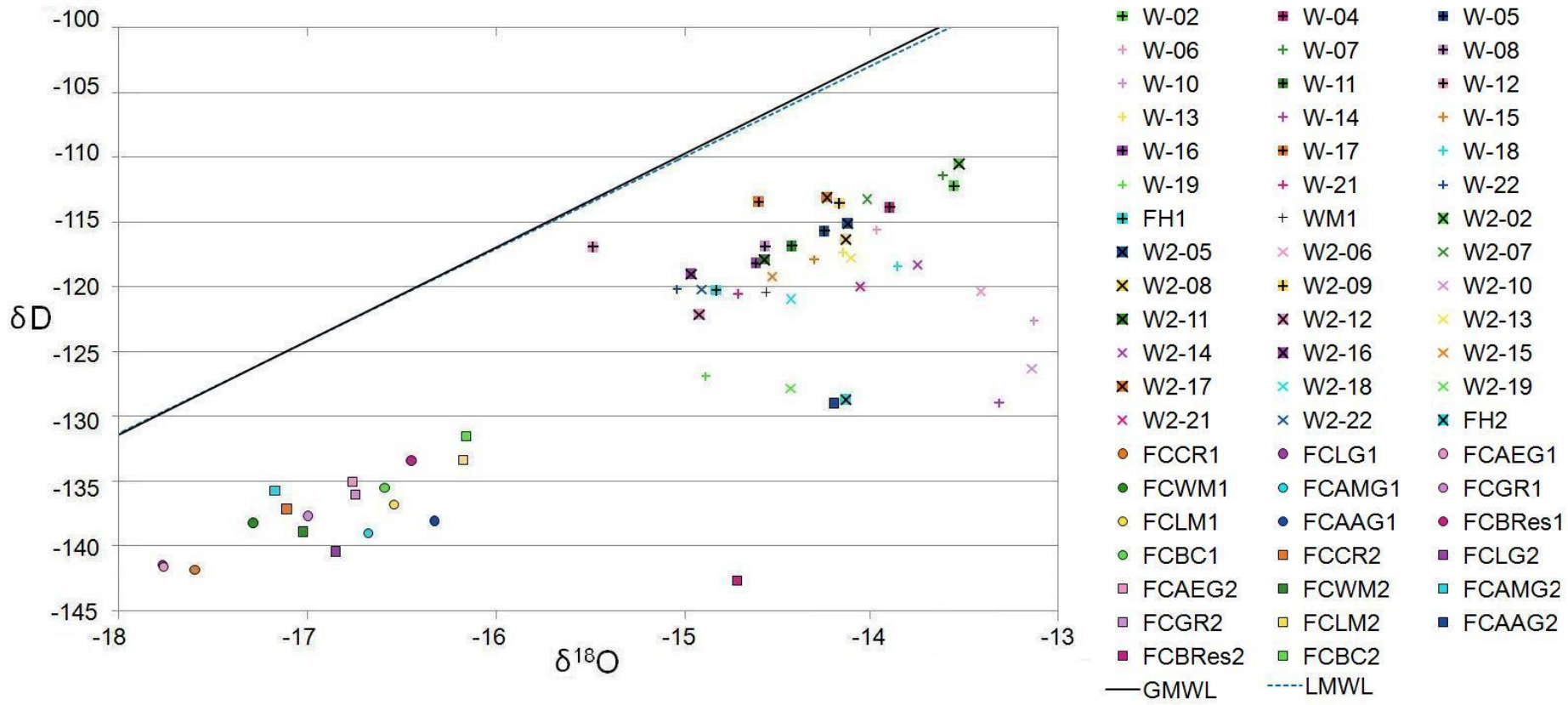


**Figure 3.4. Oxygen–Deuterium Isotope Plot.**

Plot of oxygen and deuterium isotopes for all water samples compared to the global meteoric water line (GMWL) and a local meteoric water line (LMWL).

disturbance and location on the isotope plot for tributary samples. For all samples, there is a positive correlation between conductivity and $\delta^{18}O$ (*Figure 3.5a*). Downstream along Fourmile Creek, $\delta^{18}O$ increases (*Figure 3.5b*), and between sampling dates, $\delta^{18}O$ increases at most sites.

For most tributaries and all sites along Fourmile Creek, discharge substantially decreased between sampling dates. On both dates, Fourmile discharge remains relatively constant downstream through the study area (*Figure 3.6*).

### *3.2.1. Tributary Water Chemistry*

Tributary conductivity correlates with watershed fire intensity (r = 0.664; Pearson's cutoff = 0.456) but not with mining intensity (r = 0.175) (*Figure 3.7*). The average conductivity in burned watersheds is 564 μS/cm, compared to 259 μS/cm in unburned watersheds, and the average in mined watersheds is 569 μS/cm, compared to 338 μS/cm in unmined watersheds. One outlier—Sunbeam Gulch, the tributary with the highest conductivity (1332 μS/cm)—was not considered in this analysis because the stream runs through a densely populated area and its conductivity could be disproportionately heightened by waste from nearby houses.

Concentrations of all major solutes except $HCO_3^-$ and $Sr^{2+}$ are higher, on average, in mined compared to unmined watersheds, and all except $Sr^{2+}$ are higher in burned than in unburned watersheds (*Table 3.2*). The largest differences are for $SO_4^{2-}$; the average concentration of $SO_4^{2-}$ in burned watersheds is 6.2 times that of unburned watersheds, and in mined watersheds is 4.2 times that of unmined watersheds. Concentrations of all major solutes increase by a greater margin in burned over unburned watersheds than in mined over unmined watersheds (*Table 3.2*).

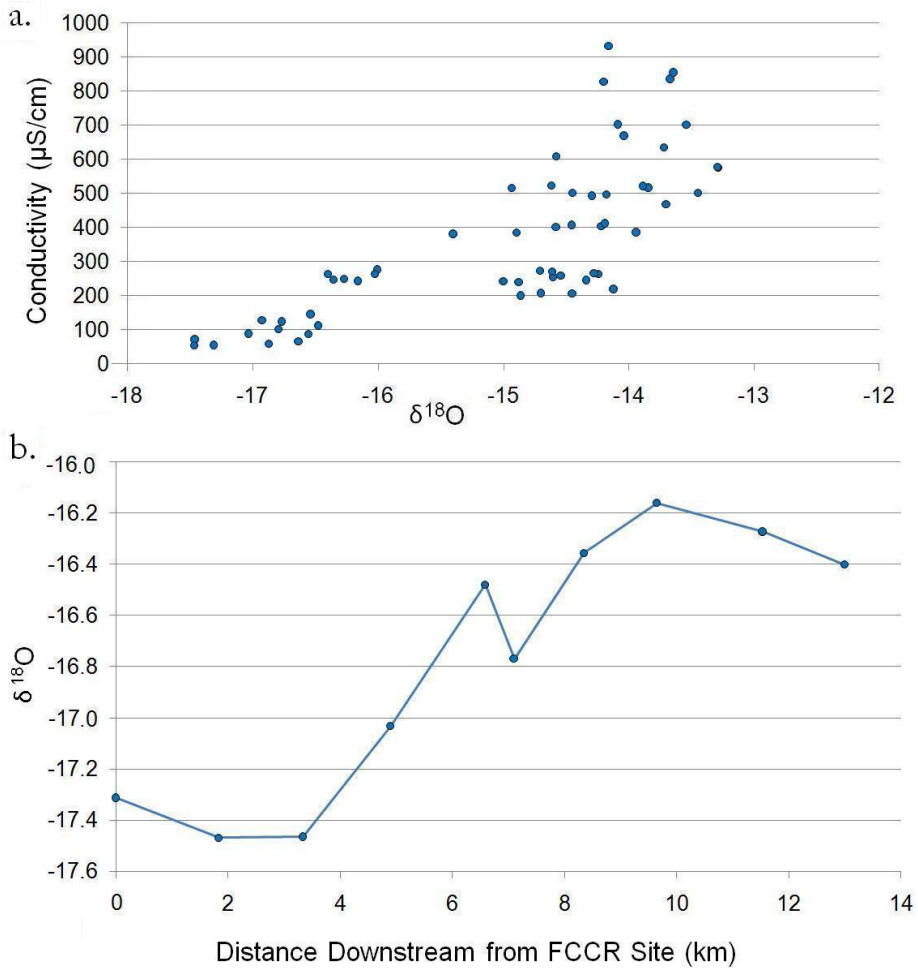


**Figure 3.5. Oxygen Isotope Plots.**

a. Conductivity positively correlates with $\delta^{18}O$ in all water samples.

b. Downstream along Fourmile Creek, $\delta^{18}O$ increases.

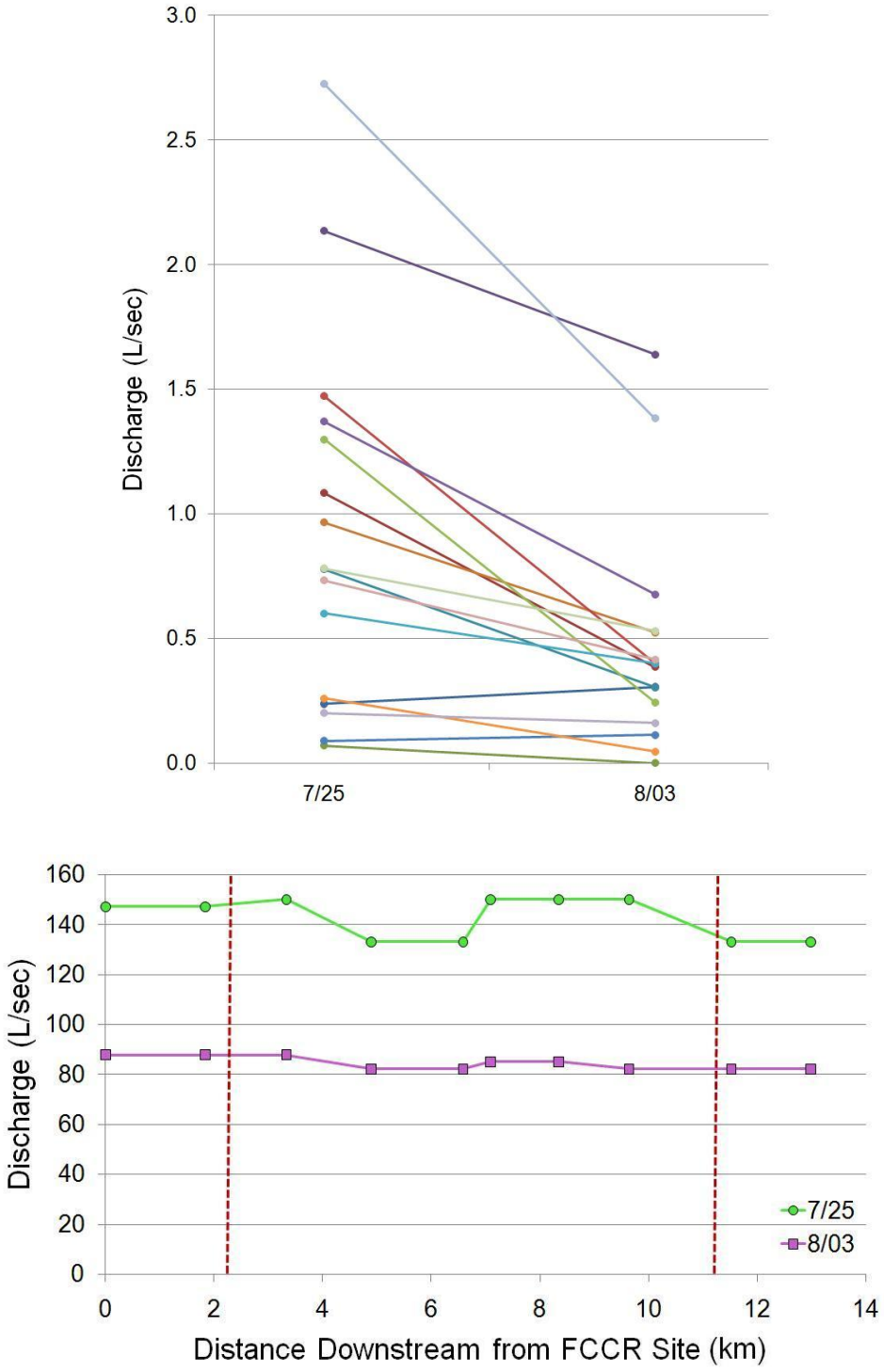


**Figure 3.6. Fourmile Creek and Tributary Discharge.**

*Top*: The discharge of most tributaries decreases between sampling dates. Gold Run and Ingram Gulch, whose discharges are substantially higher than all other tributaries, are not included on this plot.

*Bottom*: Discharge of Fourmile Creek in studied area on both sampling dates (S. Murphy, personal communication).

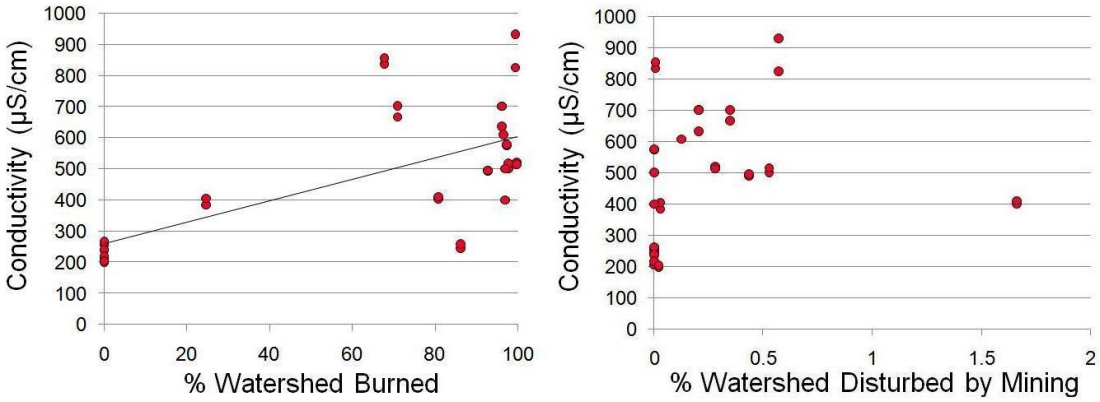


**Figure 3.7. Tributary Conductivity.**
Tributary conductivity correlates significantly with fire intensity (r = 0.664; Pearson's cutoff = 0.468) but not with mining intensity (r = 0.175).

| | Average Mined Conc. (ppm) | Average Unmined Conc. (ppm) | Difference (ppm) | Ratio of Mined to Unmined | | Average Burned Conc. (ppm) | Average Unburned Conc. (ppm) | Difference (ppm) | Ratio of Burned to Unburned |
|---|---|---|---|---|---|---|---|---|---|
| $Ca^{2+}$ | 59.2 | 40.0 | 19.1 | 1.48 | | 59.9 | 30.4 | 29.5 | 1.97 |
| $Cl^{-}$ | 20.9 | 6.0 | 15.0 | 3.51 | | 19.1 | 4.8 | 14.3 | 3.95 |
| $F^{-}$ | 0.6 | 0.4 | 0.2 | 1.54 | | 0.6 | 0.2 | 0.4 | 2.62 |
| $HCO_3^{-}$ | 139.1 | 148.7 | -9.6 | 0.94 | | 153.0 | 115.0 | 38.0 | 1.33 |
| $K^{+}$ | 3.9 | 3.2 | 0.7 | 1.23 | | 4.3 | 1.7 | 2.6 | 2.49 |
| $Mg^{2+}$ | 24.6 | 14.4 | 10.2 | 1.71 | | 24.2 | 11.4 | 12.8 | 2.12 |
| $Na^{+}$ | 7.1 | 4.2 | 2.9 | 1.68 | | 7.5 | 1.8 | 5.7 | 4.07 |
| $NO_3^{-}$ | 1.9 | 1.0 | 0.8 | 1.84 | | 1.9 | 0.7 | 1.2 | 2.84 |
| $SiO_2$ | 14.2 | 12.7 | 1.5 | 1.12 | | 15.7 | 8.2 | 7.4 | 1.91 |
| $SO_4^{2-}$ | 148.9 | 35.7 | 113.2 | 4.17 | | 137.2 | 22.1 | 115.1 | 6.21 |
| $Sr^{2+}$ | 0.5 | 0.7 | -0.2 | 0.66 | | 0.5 | 0.6 | -0.1 | 0.88 |

**Table 3.2. Major Solute Concentrations.**
Average concentrations of major solutes in mined watersheds compared to unmined watersheds and burned compared to unburned watersheds.

Tributary concentrations of most major solutes ($Ca^{2+}$, $Mg^{2+}$, $K^{+}$, $Na^{+}$, $F^{-}$, $NO_3^{-}$, $SO_4^{2-}$, and $SiO_2$) positively correlate with watershed fire intensity, but notably, $HCO_3^{-}$ does not (r = 0.192) (*Figure 3.8*; *Table 3.3*). Although the average $SO_4^{2-}$ concentration is much higher in burned watersheds, the correlation between $SO_4^{2-}$ and fire intensity is relatively weak (r = 0.615; Pearson's cutoff = 0.468). Major cations ($Ca^{2+}$, $Mg^{2+}$, $K^{+}$, and $Na^{+}$) correlate with $SO_4^{2-}$ but not with other anions (*Table 3.3*). Only $SO_4^{2-}$ has a positive correlation with mining intensity, and this correlation is also relatively weak (r = 0.510); $HCO_3^{-}$ has a weak negative correlation (r = -0.510) with mining intensity (*Figure 3.9*).

Compared to unmined watersheds, mined watersheds have higher concentrations of most trace elements, and the same is true for burned compared to unburned watersheds (*Table 3.4*). Increases of $Cd^{+}$, $Ni^{2+}$, and $Zn^{2+}$ are particularly high in mined relative to unmined watersheds; these increase by factors of 44, 21, and 27, respectively, in mined watersheds. Mining intensity correlates with increased $Al^{3+}$, $Cd^{+}$, $Co^{2+}$, $Cr^{3+}$, $Cu^{+}$, $Fe^{2+}$, $Mn^{2+}$, and $Zn^{2+}$, while fire intensity correlates positively with $Rb^{+}$ and $V^{2+}$ and negatively with $Ba^{2+}$ and $Ga^{3+}$.

When grouped by date sampled, tributary correlations of most major solutes are the same as when considering all samples together. On both dates, fire intensity correlates positively with $Ca^{2+}$, $Mg^{2+}$, $K^{+}$, $F^{-}$, $NO_3^{-}$, and $SO_4^{2-}$ and mining correlates with increased $SO_4^{2-}$ and decreased $HCO_3^{-}$. Although fire intensity correlates positively with $Na^{+}$ and $SiO_2$ on the earlier date, it does not correlate with either on the second. Correlations with most solutes are stronger on the earlier date.

When comparing tributary samples from different dates, most concentrations increase from the first to the later date. Of the 17 tributaries sampled on both dates,

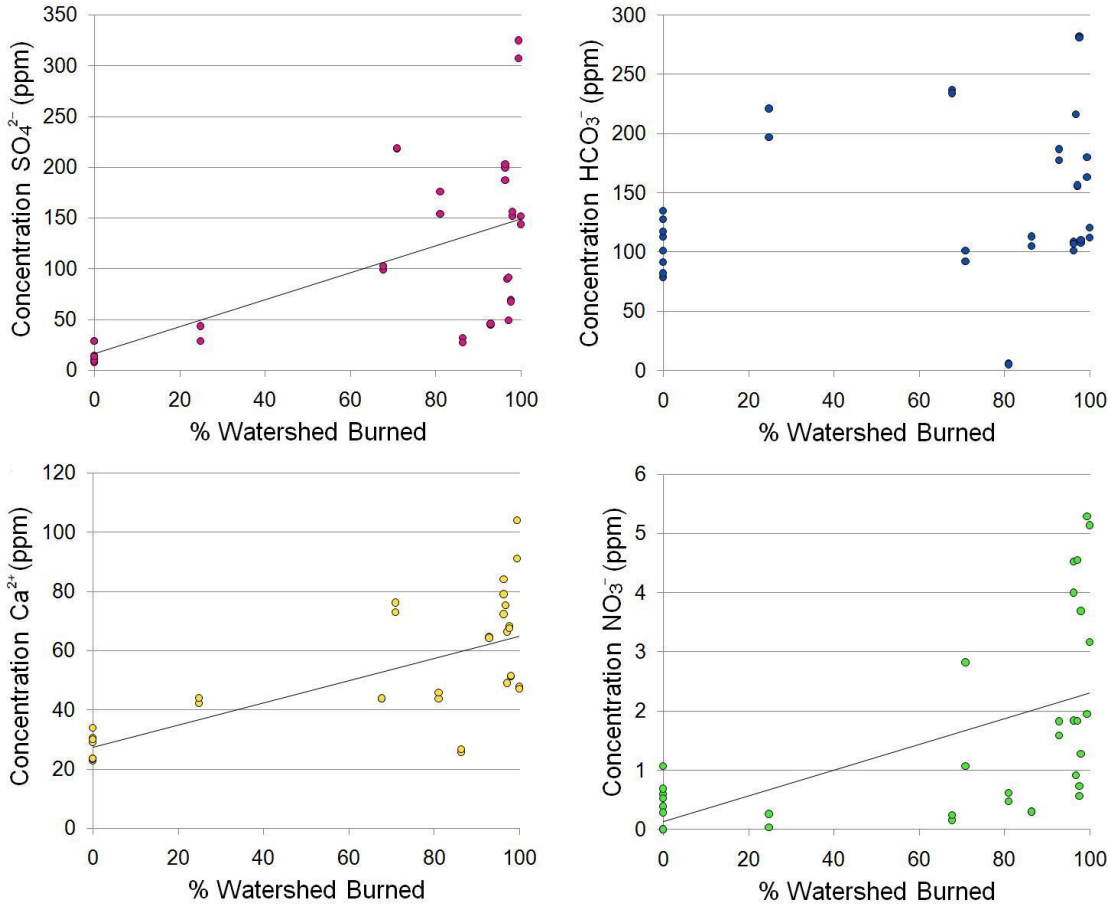


**Figure 3.8. Fire Intensity and Major Solutes.**
Tributary streamwater concentrations of $SO_4^{2-}$, $HCO_3^-$, $Ca^{2+}$, and $NO_3^-$ plotted against watershed fire intensity.

| | Mining Intensity | Fire Intensity | $SO_4^{2-}$ | $HCO_3^-$ |
|---|---|---|---|---|
| SC | 0.18 | **0.66** | **0.79** | 0.41 |
| $F^-$ | 0.19 | **0.72** | **0.63** | 0.13 |
| $Cl^-$ | -0.09 | 0.26 | 0.32 | 0.22 |
| $NO_3^-$ | 0.13 | **0.55** | **0.60** | -0.11 |
| $SO_4^{2-}$ | **0.51** | **0.62** | x | -0.14 |
| $HCO_3^-$ | **-0.51** | 0.19 | -0.14 | x |
| $Ca^{2+}$ | 0.23 | **0.70** | **0.79** | 0.29 |
| $K^+$ | 0.20 | **0.81** | **0.52** | 0.36 |
| $Mg^{2+}$ | 0.30 | **0.65** | **0.87** | 0.21 |
| $Na^+$ | -0.05 | **0.48** | **0.58** | 0.42 |
| $SiO_2$ | 0.10 | **0.50** | 0.41 | 0.28 |
| $Sr^{2+}$ | -0.28 | 0.08 | 0.09 | 0.31 |

**Table 3.3. Major Solute Correlations.**
Correlation r-values for conductivity (SC) and major solutes with mining intensity, fire intensity, $SO_4^{2-}$ concentration, and $HCO_3^-$ concentration. Values that exceed Pearson's critical coefficient (0.468) are in bold.

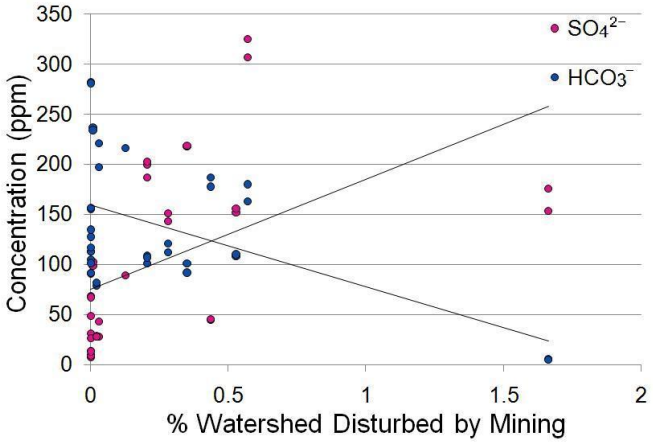


**Figure 3.9. Mining Intensity and Major Solutes.**
Tributary $SO_4^{2-}$ has a weak yet statistically significant positive correlation (r = 0.510; Pearson's cutoff = 0.468) with mining intensity, while $HCO_3^-$ has a weak negative correlation (r = -0.510).

| | Average Unmined Conc. (ppb) | Average Mined Conc. (ppb) | | Average Unburned Conc. (ppb) | Average Burned Conc. (ppb) |
|---|---|---|---|---|---|
| $Ag^+$ | 0.05 | 0.05 | | 0.03 | 0.06 |
| $Al^{3+}$ | 32.12 | 75.32 | | 43.89 | 63.54 |
| $As^{3+}$ | 0.81 | 4.82 | | 0.10 | 5.23 |
| $Ba^{2+}$ | 136.78 | 63.44 | | 137.40 | 74.12 |
| $Cd^+$ | 0.02 | 0.66 | | 0.01 | 0.66 |
| $Co^{2+}$ | 0.12 | 1.03 | | 0.12 | 1.03 |
| $Cr^{3+}$ | 0.17 | 0.52 | | 0.17 | 0.53 |
| $Cu^+$ | 6.91 | 10.10 | | 8.28 | 9.43 |
| $Fe^{2+}$ | 37.62 | 78.38 | | 51.66 | 68.18 |
| $Ga^{3+}$ | 38.79 | 14.92 | | 33.93 | 17.69 |
| $Li^+$ | 2.11 | 8.01 | | 1.15 | 7.42 |
| $Mn^{2+}$ | 27.24 | 235.24 | | 4.76 | 218.16 |
| $Ni^{2+}$ | 0.39 | 7.98 | | 0.27 | 8.03 |
| $Pb^{2+}$ | 0.90 | 2.04 | | 0.93 | 2.02 |
| $Rb^+$ | 0.52 | 3.20 | | 0.31 | 3.30 |
| $U^{4+}$ | 1.71 | 6.69 | | 1.16 | 7.01 |
| $V^{2+}$ | 0.59 | 0.54 | | 0.08 | 0.81 |
| $Zn^{2+}$ | 4.42 | 119.83 | | 4.56 | 102.69 |

**Table 3.4. Trace Element Concentrations.**
Streamwater concentrations of most trace elements are higher in burned over unburned and in mined over unmined watersheds. The increases are generally greater in mined watersheds.

$NO_3^-$ decreases in 12, and $K^+$ and $SiO_2$ decrease in 10. All other major solutes increase in the majority of tributaries (*Table 3.5*). Concentrations of $NO_3^-$ change by the largest margin; the average change in $NO_3^-$ between sampling dates is 1.06 ppm, a difference of 39%. For all other major solutes, the average change is less than 12%. The average change in concentration of major solutes for each tributary does not correlate with fire intensity, mining intensity, average slope, change in discharge between dates, or absolute discharge; it is also unaffected by bedrock type. Changes in $NO_3^-$ correlate with fire intensity.

According to *t*-test results, tributary concentrations of $Ca^{2+}$, $Cl^-$, $K^+$, and $Sr^{2+}$ are significantly greater in watersheds with predominantly Boulder Creek granodiorite bedrock than those with predominantly metamorphic bedrock in a bulk analysis of all samples and on the earlier sampling date, but not on the later date (*Figure 3.10*). No other major solutes significantly change with bedrock type, while some trace metals ($Cr^{3+}$, $Li^+$, $Rb^+$, and $V^{2+}$) are also significantly higher in granitic watersheds in bulk analysis and on the earlier date. Of the major solutes affected by bedrock, $Ca^{2+}$ has the largest increase in concentration and $Cl^-$ has the biggest percent increase in granitic watersheds over metamorphic watersheds. Slope does not have a significant impact on streamwater chemistry.

Along Emerson Gulch, all major solutes except $NO_3^-$, $HCO_3^-$, and $SiO_2$ increase downstream (*Figure 3.11*); $SO_4^{2-}$ and $Ca^{2+}$ increase most dramatically. Concentrations of $NO_3^-$ are low, but increase by a large factor, from 1.0 ppm to 3.8 ppm, between the first two sites and decrease from 3.8 ppm to 2.3 ppm between the second two. Some trace elements ($Al^{3+}$, $As^{3+}$, $Cd^+$, $Rb^+$, and $U^{4+}$) increase downstream and $Ni^{2+}$ decreases downstream, but most fluctuate without a consistent trend.

| | | $F^-$ | $Cl^-$ | $NO_3^-$ | $SO_4^{2-}$ | $HCO_3^-$ | $Ca^{2+}$ | $K^+$ | $Mg^{2+}$ | $Na^+$ | $SiO_2$ | $Sr^{2+}$ |
|---|---|---|---|---|---|---|---|---|---|---|---|---|
| 2 | Sand | **-0.01** | 0.67 | 0.09 | 3.70 | **-2.96** | 0.17 | 0.00 | 2.48 | **-0.78** | 0.02 | 0.00 |
| 5 | Sweet Home | **-0.04** | **-5.42** | **-0.24** | 0.73 | 9.22 | **-0.27** | **-0.08** | 2.23 | 0.11 | **-0.39** | 0.00 |
| 6 | Gold Run | 0.08 | 1.30 | **-1.75** | 1.00 | 9.10 | 3.30 | **-0.18** | 1.80 | 1.20 | 0.20 | 0.02 |
| 7 | Ingram | 0.16 | 6.30 | **-2.68** | 16.00 | 6.00 | 6.70 | **-0.11** | 1.80 | 1.70 | **-0.70** | 0.06 |
| 8 | Black Hawk | 0.02 | 0.33 | **-0.15** | 22.06 | **-0.66** | 2.00 | **-0.80** | 3.38 | **-0.13** | **-0.93** | 0.02 |
| 10 | Melvina | 0.03 | **-0.15** | **-0.17** | **-1.40** | **-1.00** | **-0.70** | **-0.33** | 0.00 | 0.00 | **-0.30** | **-0.01** |
| 11 | Melvina West | **-0.07** | 0.31 | **-2.72** | **-42.09** | 0.99 | **-17.39** | 0.17 | **-4.79** | **-1.72** | **-0.32** | **-0.65** |
| 12 | Wall Street | 0.04 | 0.03 | 0.49 | 5.60 | 2.91 | **-2.25** | **-0.91** | **-3.66** | 0.29 | **-0.43** | **-0.05** |
| 13 | Schoolhouse | 0.07 | 0.20 | **-3.34** | 18.00 | 17.00 | 12.90 | 0.38 | 8.20 | 0.50 | **-0.10** | 0.18 |
| 14 | Emerson | 0.04 | 0.15 | **-2.41** | 4.00 | 2.00 | 0.30 | 0.05 | 1.20 | 0.26 | 0.00 | 0.01 |
| 15 | Banana | 0.04 | 0.32 | 0.00 | **-4.80** | 8.00 | 1.10 | 0.00 | 0.28 | 0.31 | 0.00 | 0.02 |
| 16 | Emerson West | **-0.24** | **-0.78** | **-1.97** | **-7.93** | 8.57 | **-0.76** | **-0.80** | **-2.01** | 0.49 | 1.03 | 0.01 |
| 17 | Sugarloaf | **-0.02** | **-0.19** | 0.29 | **-0.72** | 7.19 | 1.09 | 0.30 | 0.39 | 0.05 | 0.10 | 0.02 |
| 18 | Long | 0.03 | 0.39 | **-0.23** | **-14.90** | 24.00 | 1.70 | 0.05 | 1.00 | 0.23 | 0.40 | 0.03 |
| 19 | Bald | 0.00 | 0.14 | 0.69 | **-0.17** | 3.21 | 0.34 | **-0.07** | 0.08 | 0.02 | **-0.20** | 0.01 |
| 21 | Bear | 0.02 | **-0.20** | **-0.68** | 0.09 | 4.42 | 0.68 | **-0.23** | 0.36 | -0.01 | **-0.19** | 0.02 |
| 22 | Todd | **-0.04** | 0.13 | **-0.08** | **-2.42** | 10.03 | **-3.35** | **-0.23** | **-1.07** | **-0.05** | **-0.89** | **-0.08** |

**Table 3.5. Changes in Concentration between Sampling Dates.**
Differences in concentration between sampling dates in tributaries, in ppm. Negative values, representing a decrease between the first and second day, are in bold.

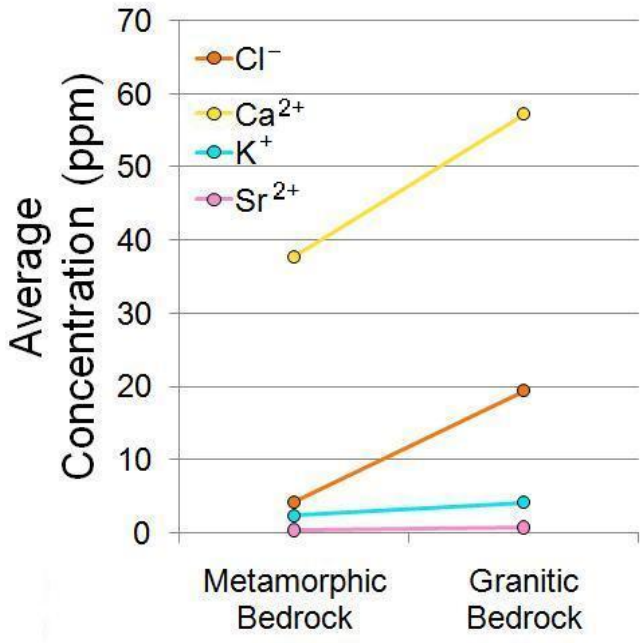


**Figure 3.10. Bedrock Type and Major Solutes.**
Concentrations of $Ca^{2+}$, $Cl^-$, $K^+$, and $Sr^{2+}$ are greater in tributaries draining watersheds with predominantly Boulder Creek granodiorite bedrock than those with primarily metamorphic bedrock.

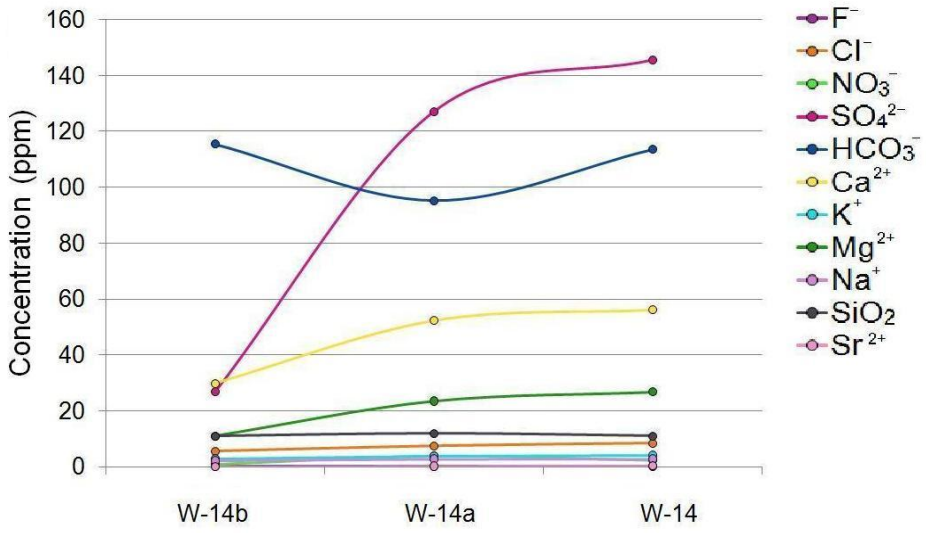


**Figure 3.11. Emerson Gulch Transect.**
Streamwater concentrations of solutes downstream along Emerson Gulch. W-14b is located in upper Emerson Gulch and W-14 is located near its mouth.

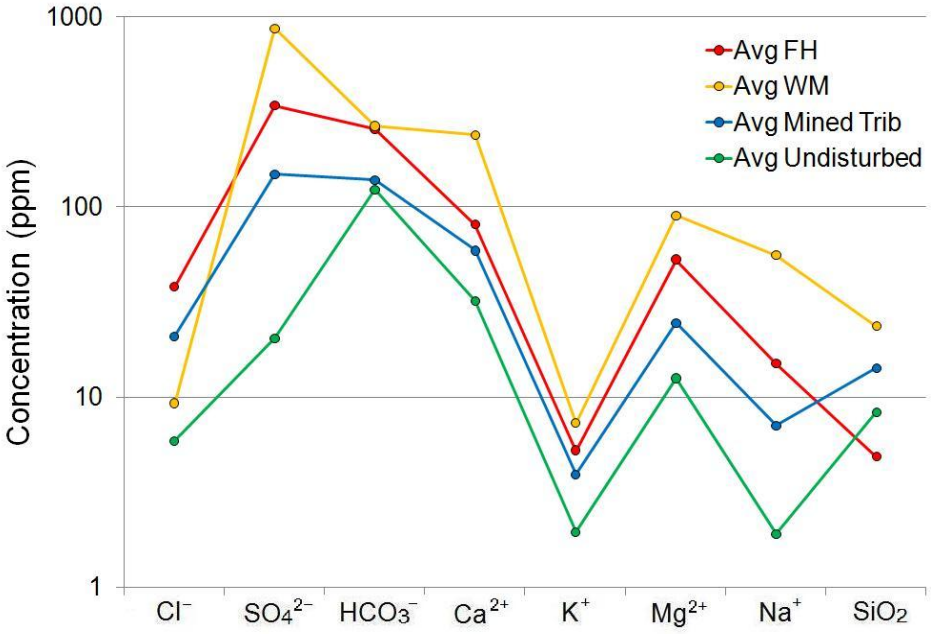


**Figure 3.12. Mine Drainage Chemistry.**
Average concentrations of Wood Mine (WM) and Firehouse (FH) mine drainage, compared with concentrations of the average mined tributary and the average undisturbed tributary on a log scale.

In addition to mined tributaries, two mine drainage sites were sampled, Wood Mine and Firehouse. Although they have low discharge, samples have very high conductivity. Values average 1271 μS/cm for Firehouse and 1880 μS/cm for Wood Mine over both sampling dates, compared with 569 μS/cm in the average mined tributary and 272 μS/cm in the average undisturbed tributary. Major cations and $SO_4^{2-}$ are substantially higher in mine drainage sites, particularly Wood Mine, than in mined tributaries (*Figure 3.12*); however, there is variability in composition between mine drainage sites. Wood Mine has higher $NO_3^-$ and $SiO_2$ than the average mined tributary, while Firehouse has lower values than undisturbed tributaries for these solutes. Firehouse has high $Cl^-$ levels, but Wood Mine has lower $Cl^-$ than the average mined tributary (*Figure 3.12*).

Concentrations of most trace metals are higher in Firehouse drainage than in the average undisturbed tributary. Notably, $Cu^+$ correlates with mining intensity but has lower concentrations than the average undisturbed tributary in both Firehouse and Wood Mine. Compared to the average mined tributary, concentrations of $Ag^+$, $As^{3+}$, $Co^{2+}$, $Li^+$, $Rb^+$, and $U^{4+}$ are higher in Firehouse, and $Li^+$ and $Rb^+$ are higher in Wood Mine.

### *3.2.2. Fourmile Creek Water Chemistry*

While its discharge is constant, Fourmile Creek's conductivity increases downstream with a notable rise after input from Gold Run (*Figure 3.13*), the largest tributary in terms of discharge by an order of magnitude. Not surprisingly, concentrations of major solutes ($Ca^{2+}$, $Mg^{2+}$, $Na^+$, $K^+$, $Sr^{2+}$, $Cl^-$, $F^-$, $SO_4^{2-}$, $HCO_3^-$, and $SiO_2$) increase steadily downstream, steeply rising after input from Gold Run (*Figure 3.14*). On both dates, concentrations for all major solutes except $NO_3^-$ follow the

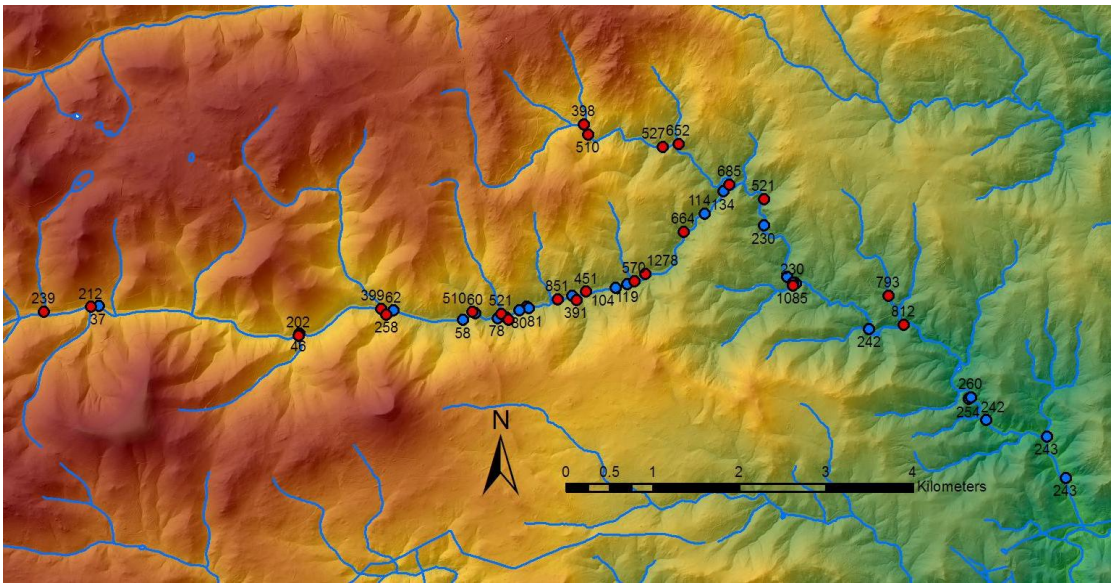


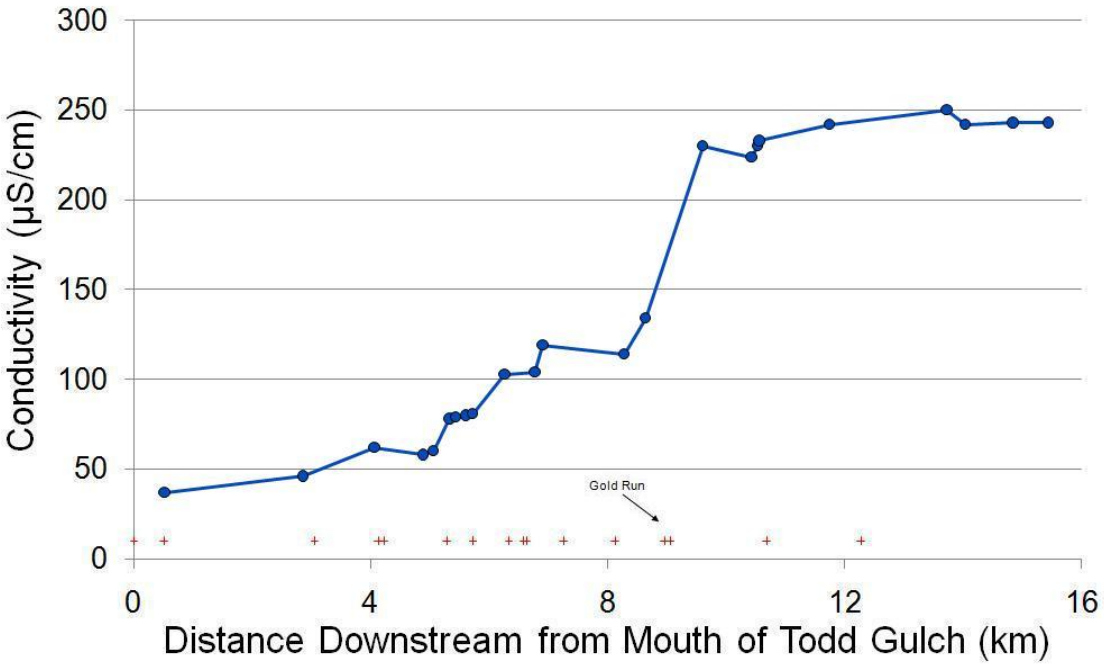


**Figure 3.13. Fourmile Creek Conductivity.**

*Top*: Map of average conductivity measurements, in µS/cm, taken along Fourmile Creek (blue bullets) and at the mouths of tributaries (red bullets).

*Bottom*: Plot of Fourmile Creek conductivity measurements downstream. Red crosses along the bottom show locations of the mouths of tributaries.

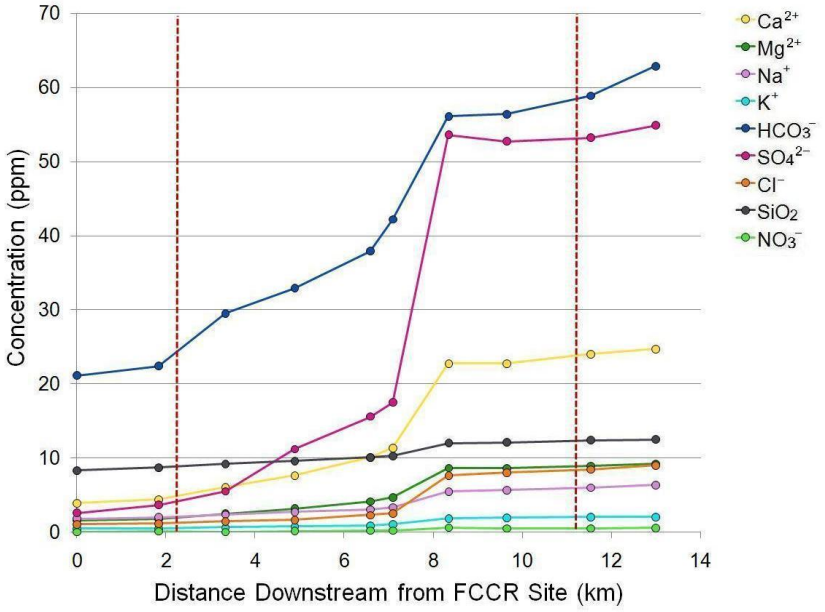


**Figure 3.14. Major Solutes in Fourmile Creek.**
Streamwater concentrations of major solutes downstream along Fourmile Creek on the first sampling date. Red dashed lines indicate the burned area.

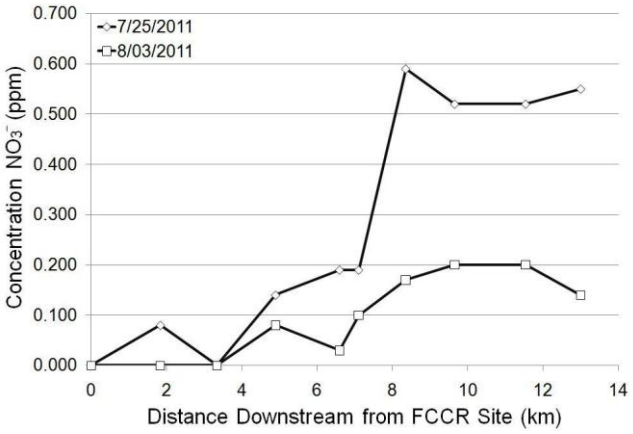


**Figure 3.15. Nitrate in Fourmile Creek.**
Concentrations of $NO_3^-$ downstream along Fourmile Creek on both sampling dates.

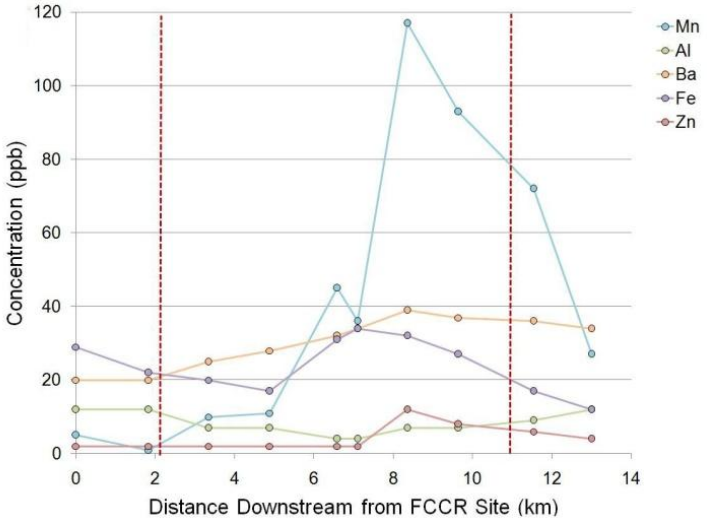


**Figure 3.16. Trace Elements in Fourmile Creek.**
Stream water concentrations of trace elements downstream along Fourmile Creek on the first sampling date. Red dashed lines indicate the burned area.

same downstream pattern, and on the second sampling date, concentrations of all but $NO_3^-$ are slightly higher. Concentrations of $NO_3^-$ do not increase consistently downstream, and between some sampling sites drop before spiking up again. Nitrate sharply increases after Gold Run on the earlier date, but on the second, a distinct Gold Run signal is not discernable (*Figure 3.15*). Trace element data were available for $Al^{3+}$, $Ba^{2+}$, $Fe^{2+}$, $Mn^{2+}$, and $Zn^{2+}$ in Fourmile samples; concentrations of these elements downstream do not vary consistently, and only $Mn^{2+}$ and $Zn^{2+}$ spike after input from Gold Run (*Figure 3.16*).

Upstream of the disturbed area, $SiO_2$ is the second most abundant solute after $HCO_3^-$. Concentrations of $SiO_2$ and $HCO_3^-$ increase downstream at a much slower rate than other solutes, so that their relative abundances drop while those of $Ca^{2+}$ and $SO_4^{2-}$ increase. Concentrations of all solutes, including $Ca^{2+}$ and $SO_4^{2-}$, level off downstream of the disturbed area. Relative abundances change most dramatically after input from Gold Run and stay relatively constant downstream from there.

## 3.3. Sediment Chemistry Results

All sediment samples contain approximately 70% $SiO_2$. Watershed fire intensity correlates with higher percentages of $Al_2O_3$, CaO, MgO, and $Na_2O$ in streambed sediment and lower percentages of $K_2O$ and $SiO_2$ (*Figure 3.17*). Mining intensity correlates only with increased MnO ($r = 0.643$), and notably does not correlate with a change in $Fe_2O_3$ ($r = -0.317$) (*Figure 3.18*). SEM analysis also does not demonstrate a difference in iron oxide abundance between mined and unmined watersheds based on visual inspection. There are no significant differences in major oxides based on underlying bedrock composition or average slope.

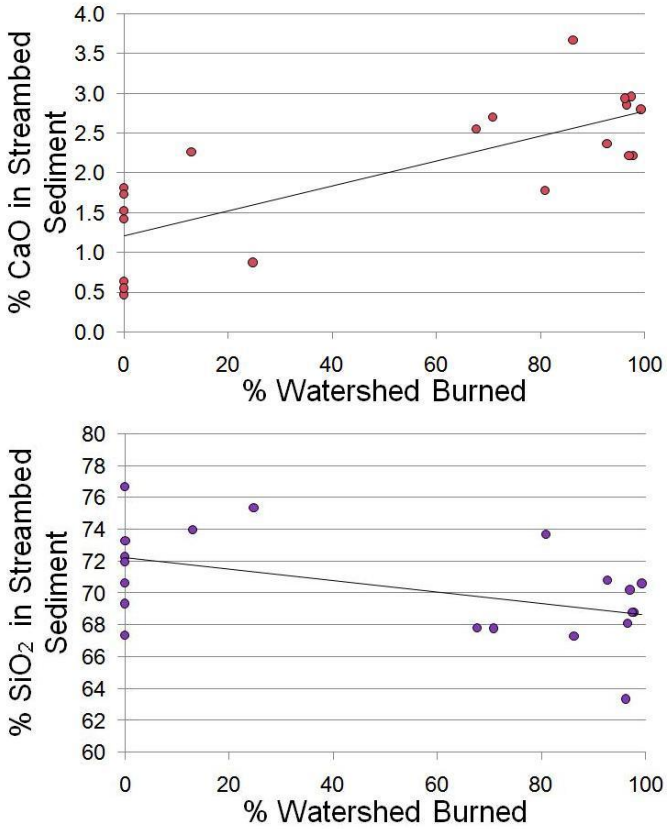


**Figure 3.17. Fire Intensity and Major Oxides.** Watershed fire intensity has a significant positive correlation with CaO ($r = 0.778$; Pearson's cutoff = 0.433) and a negative correlation with $SiO_2$ in tributary streambed sediment ($r = -0.504$).

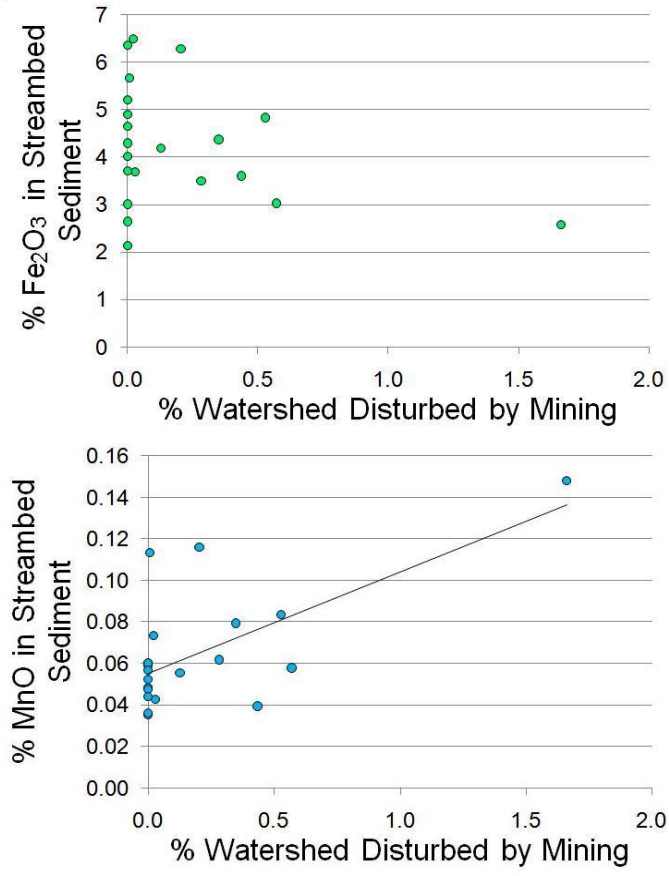


**Figure 3.18. Mining Intensity and Major Oxides.** Watershed mining intensity has a weak yet statistically significant positive correlation with MnO ($r = 0.643$; Pearson's cutoff = 0.433) in tributary streambed sediment. It does not correlate with any other major oxides, including $Fe_2O_3$ ($r = -0.317$).

For five burned tributaries, flood deposit was also collected, and there are no significant differences in composition between flood deposit and streambed sediment from the same watershed. Six flood deposit samples were taken along Fourmile Creek. As there was no flooding upstream of the disturbed area, all but one of these are from within the disturbed area, and sample FCBRes is downstream. When compared to tributary flood sediment, Fourmile flood sediment has significantly higher MgO, $P_2O_5$, and $TiO_2$. Considering Fourmile flood deposits downstream, all major elements except $K_2O$ and $Na_2O$ spike, whether an increase or decrease, at site FCASH, just downstream from the mouth of Gold Run (*Figure 3.19*). Site FCASH is a turning point in overall downstream trends; $Al_2O_3$, CaO, $Fe_2O_3$, MgO, MnO, $P_2O_5$, and $TiO_2$ decrease over the first three sites and increase over the last three, switching at site FCASH. Not surprisingly, $SiO_2$ increases over the first three sites and decreases over the last three to balance the analysis.

Although Hg:C ratios do not correlate with fire or mining intensity, mined watersheds have a higher average Hg:C ratio (114.4 ppm/wt %) than unmined watersheds (23.0 ppm/wt %), and burned watersheds have a higher average Hg:C ratio (95.0 ppm/wt %) than unburned watersheds (19.7 ppm/wt %). Bald Gulch has a very large weight % C, and although its Hg concentration is the highest measured (191 ppb) its Hg:C ratio is relatively low (22.6 ppm/wt %). On the other hand, Gold Run, Schoolhouse Gulch, and Black Hawk Gulch have low weight % C, and their Hg:C ratios are the largest calculated (510.0, 214.3, and 167.4 ppm/wt %, respectively). There is no correlation between fire intensity and Hg:C ratio in unmined watersheds (*Figure 3.20*).

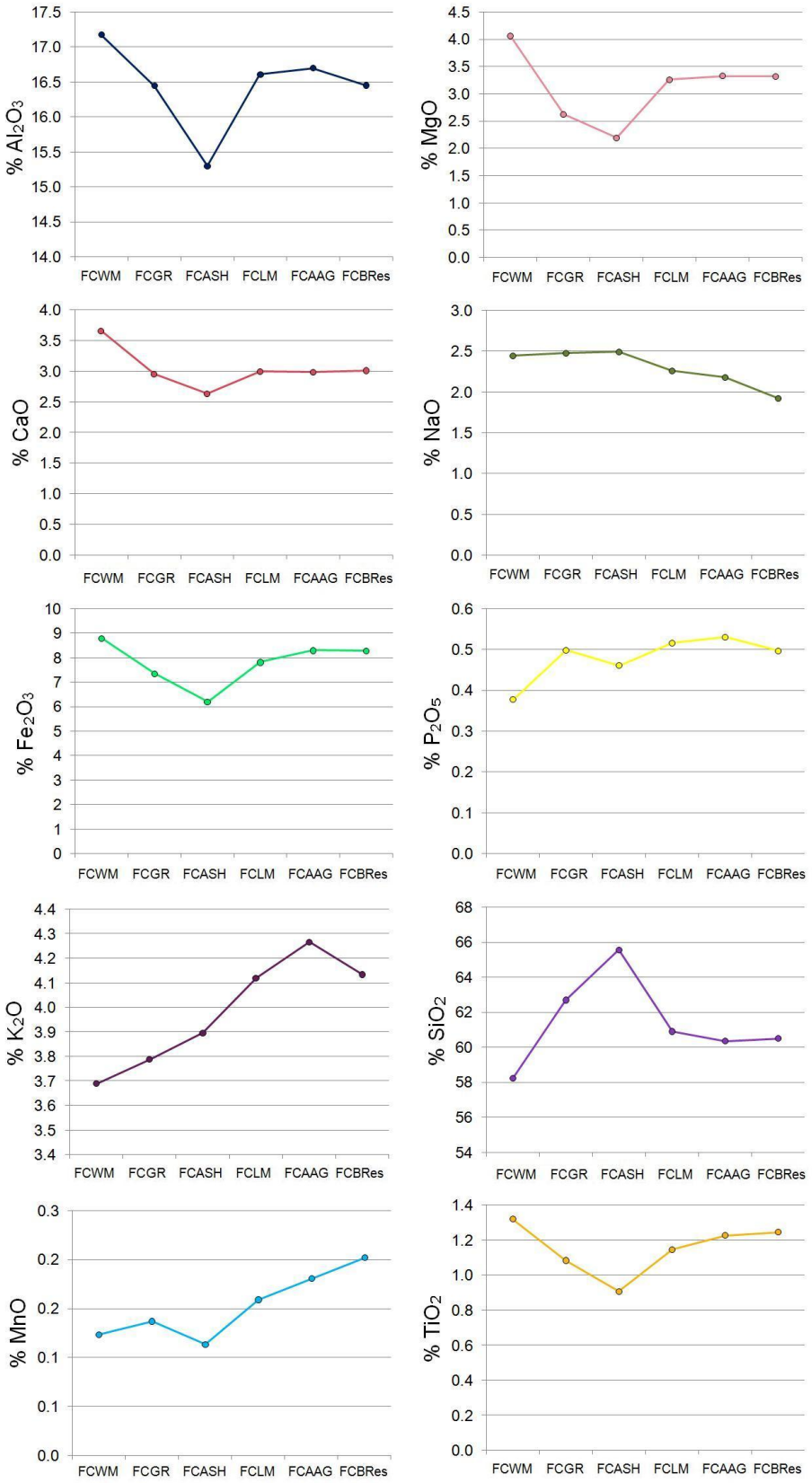


**Figure 3.19. Fourmile Creek Flood Deposit Chemistry.**
Downstream changes in concentration of flood deposits at six sites along Fourmile Creek. All are within the burned area except FCBRes, which is downstream.

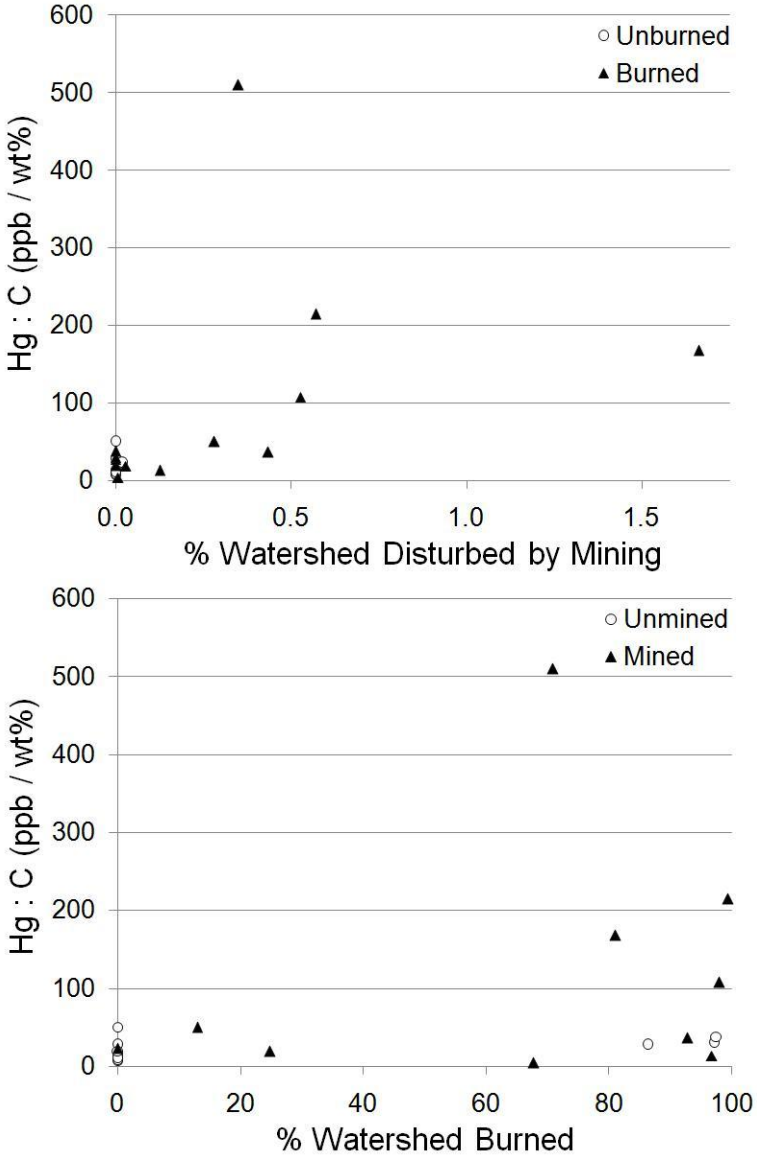


**Figure 3.20. Mercury in Tributary Sediment.**
Hg:C ratios do not correlate with watershed fire or mining intensity.

| | Unburned | Burned | % Change | | Unmined | Mined | % Change |
|---|---|---|---|---|---|---|---|
| C (wt %) | 3.79 | 0.64 | -83.15 | | 1.78 | 1.42 | -20.42 |
| N (wt %) | 0.21 | 0.04 | -80.17 | | 0.09 | 0.10 | 3.76 |
| C:N | 19.89 | 16.26 | -18.24 | | 21.48 | 13.47 | -37.31 |

**Table 3.6. Carbon and Nitrogen in Tributary Sediment.**
Streambed sediment weight % C, weight % N, and C:N ratios compared between burned/unburned and mined/unmined watersheds.

Fire intensity weakly correlates with decreased weight % C in stream sediment ($r = -0.474$; Pearson's cutoff = 0.456), but not with changes in weight % N. Average weight % C is 83% lower and weight % N is 80% lower in burned compared to unburned watersheds (*Table 3.6*). On average, there is little difference between average weight % C and weight % N in mined and unmined watersheds (*Table 3.6*), but mining intensity correlates with decreased C:N ratio. Underlying bedrock and slope have no bearing on these data.

# 4. DISCUSSION

Isotopic composition of streamwater is not affected by wildfire or mining, but yields information about water sources. Fourmile Creek had lower $\delta^{18}O$ and $\delta D$ than its tributaries (see *Figure 3.4*), suggesting that a greater portion of Fourmile Creek water is sourced from isotopically light groundwater. Groundwater in this region is primarily sourced from snowmelt, which has relatively low conductivity, $\delta^{18}O$, and $\delta D$ (Campbell et al. 1995). Tributaries, on the other hand, are primarily sourced from spring and summer rainwater, and have higher $\delta^{18}O$ and $\delta D$ as a result. Observed $\delta^{18}O$ trends are consistent with this theory. The conductivity of water samples correlates with $\delta^{18}O$; Fourmile Creek has lower conductivity than its tributaries partly because a greater portion of its water is from dilute groundwater. Downstream along Fourmile Creek, $\delta^{18}O$ increases, reflecting greater input from tributaries carrying meteoric water.

On the second sampling date, $\delta^{18}O$ and $\delta D$ in all samples are slightly higher than on the earlier date, indicating decreased groundwater dilution. The discharge at all sites decreases substantially between sampling dates in response to a lack of precipitation (see *Figure 3.6*). The combination of evaporation, lack of meteoric water input, and less dilution by groundwater explains the increases in solute concentrations and conductivity over time in most samples.

Piper plots (see *Figure 3.3*) are a simple way to demonstrate the profound impact of wildfire and mining on streamwater chemistry; overall these disturbances contribute a large supply of $SO_4^{2-}$ that shifts compositions away from waters in which bicarbonate is the dominant anion. Cation concentrations in affected tributaries show

greater dispersal than in undisturbed tributaries, reflecting increases in cations that change their relative abundances. Fourmile Creek has increased $Ca^{2+}$ downstream, which demonstrates that $Ca^{2+}$ most closely follows patterns of $SO_4^{2-}$ increase.

## 4.1. Water Chemistry

### *4.1.1. Tributary Water Chemistry*

Many studies have reported increased conductivity in streams affected by wildfire (Earl and Blinn 2003; Rhoades et al 2011; Smith et al. 2011). In this study, tributary conductivity correlates with fire intensity as expected. Studies have also found streams affected by mine drainage to have increased conductivity (McConnell 1995; Sullivan and Drever 2001; Tripole et al. 2006). The high conductivity measured in mine drainage sites (>1200 μS/cm) suggests that mining in this area contributes increased ion concentrations to streamwater. On average, conductivity is higher in mined compared to unmined watersheds, but it does not correlate with the intensity of mining within each watershed. The presence of wildfire in mined watersheds dominates the magnitude of conductivity increase and likely masks any correlation between mining intensity and conductivity.

Similarly, the dramatic effects of wildfire on streamwater chemistry obscure the impact of mining on individual constituents. Concentrations of most major solutes are greater in mined compared to unmined watersheds, but only $SO_4^{2-}$ (positively) and $HCO_3^-$ (negatively) correlate with mining intensity. In other studies, mine drainage has been reported to increase solute concentrations across the board (McConnell 1995; Tripole et al. 2006). Sampled mine drainage has high concentrations of most major solutes, particularly $SO_4^{2-}$ and major cations, which

implies that mining in the area is a source of these ions. Although major cations do not correlate with mining intensity, they do correlate with fire intensity. This suggests that fire dominates the magnitude of increase for these ions and masks any correlation with mining intensity. Additionally, there are substantial differences in composition of major and trace elements between mine drainage sites (see *Figure 3.12*). The varying composition of mine drainage partly accounts for the lack of correlation between mining intensity and solutes other than $HCO_3^-$ and $SO_4^{2-}$.

Average $SO_4^{2-}$ concentrations in this study are 4.2 times higher in mined watersheds than in unmined watersheds (see *Table 3.2*). This value is within the limits of reported $SO_4^{2-}$ increases in response to mine drainage, which increase by as high a factor as 15 (McConnell 1995; Tripole et al. 2006). Burned watersheds in this study have an average $SO_4^{2-}$ concentration that is 6.2 times greater than unburned watersheds. Reported post-fire increases in streamwater $SO_4^{2-}$ vary, but many report increases by up to a factor of three (Bayley and Schindler 1991; Mast and Clow 2008; Smith et al. 2011). The large $SO_4^{2-}$ increase here is a result of the combined effects of wildfire and mining. Wildfire increases the supply of $SO_4^{2-}$ through oxidation of sulfur in organic matter (Smith et al. 2011); wildfire also increases exposure and weathering of sulfide minerals associated with mining. The combination of wildfire and mining explains the weak correlation of $SO_4^{2-}$ with fire and mining intensity, as $SO_4^{2-}$ is simultaneously responding to two strong signals.

In bulk analysis of all tributaries, $SO_4^{2-}$ correlates with concentrations of major cations ($Ca^{2+}$, $Mg^{2+}$, $Na^+$, and $K^+$), and other anions do not. When only considering data from burned tributaries, $SO_4^{2-}$ alone correlates with $Ca^{2+}$ and $Mg^{2+}$, but not with $K^+$ or $Na^+$ (*Figure 4.1*). This confirms the finding that after wildfire, increased $SO_4^{2-}$

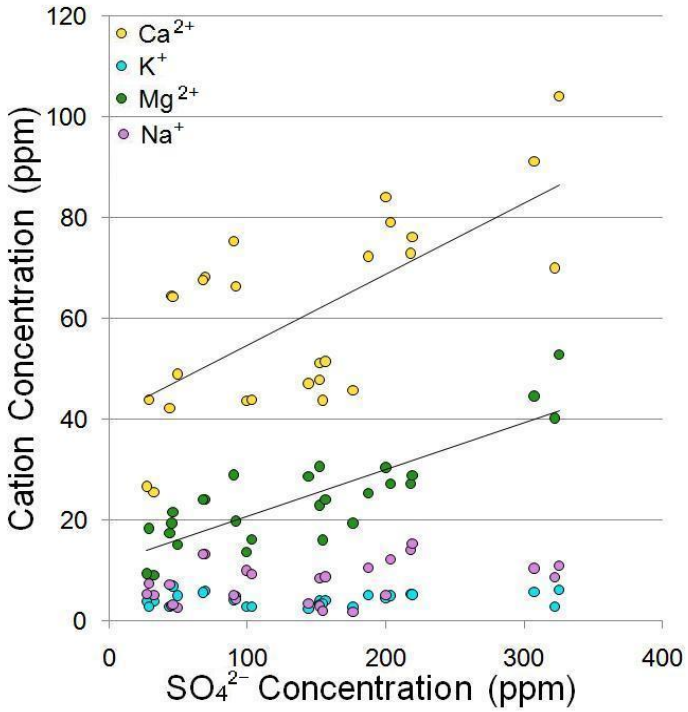


**Figure 4.1. Sulfate and Cations.**
In burned watersheds, $SO_4^{2-}$ correlates with divalent cations ($Ca^{2+}$ and $Mg^{2+}$) but not with monovalent cations ($Na^+$ and $K^+$).

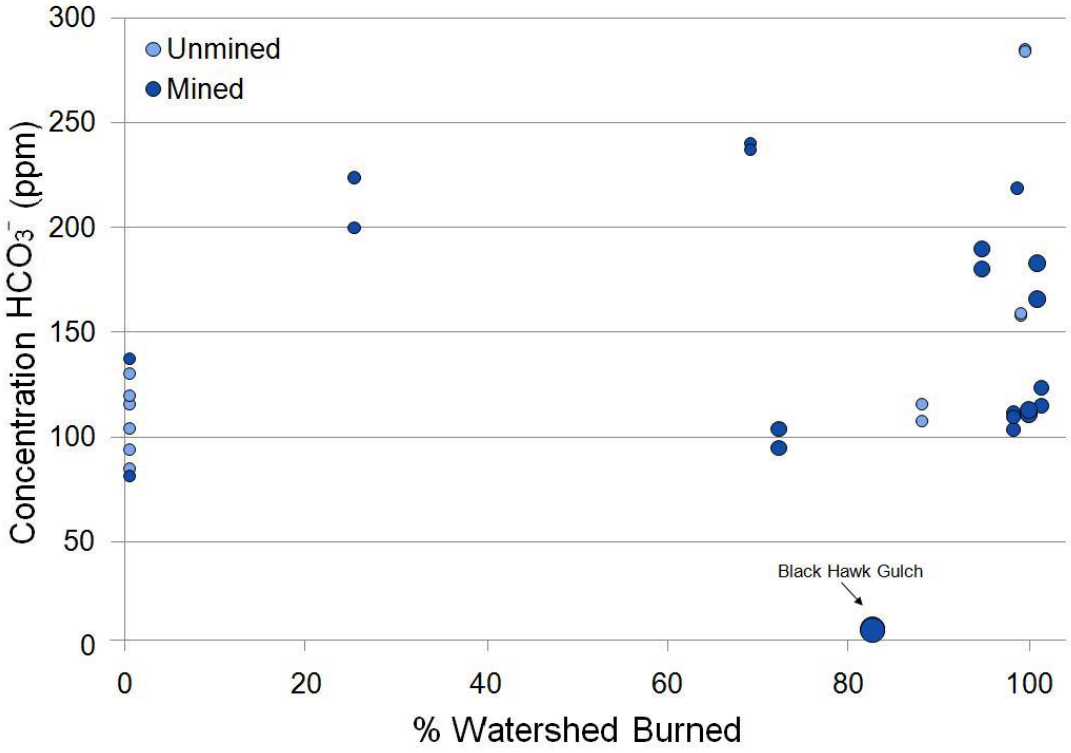


**Figure 4.2. Alkalinity in Burned and Mined Tributaries.**
Concentrations of $HCO_3^-$ plotted against watershed fire intensity; the size of each point represents the mining intensity in that watershed.

export from oxidized organic matter is associated with export of divalent cations more so than with export of monovalent cations (Bayley and Schindler 1991). The correlation between $SO_4^{2-}$ and divalent cations also holds in mined tributaries. Sulfide minerals associated with mining generally contain transition metals rather than base cations (Blowes et al. 2005). Through cation exchange with these highly reactive transition elements, increased $SO_4^{2-}$ in mined watersheds could indirectly be coupled with increased concentrations of divalent cations. Alternatively, the correlation in mined watersheds could be a result of wildfire in those basins. Considering only samples from undisturbed tributaries, no pair of solutes has a significant correlation, which implies that consistent correlation among solutes, such as that of divalent cations and $SO_4^{2-}$, is a product of mining and/or wildfire disturbance.

Wildfire and mining have opposing effects on streamwater alkalinity; while wildfire is associated with increased alkalinity, mining is associated with decreased alkalinity. Although $HCO_3^-$ concentrations in this study are on average 38 ppm higher in burned than in unburned tributaries, fire intensity does not correlate with increased alkalinity. This is because $HCO_3^-$ from wildfire is contributing to the buffering of acidity from mine tailings. While most $HCO_3^-$ concentrations fall between 100 and 200 ppm, samples from Black Hawk Gulch have $HCO_3^-$ concentrations of ~5 ppm on both sampling dates (*Figure 4.2*). Most mined watersheds have between 0.1 and 0.5% of their area disturbed by mining, but Black Hawk has 1.66% of its area disturbed; this is nearly triple the next highest value of 0.58%. Even though 81% of the watershed burned, contributing increased alkalinity, the abundance of mines and tailings caused alkalinity in this watershed to act as an acid buffer and prevented it from reaching streamwater. Thus, the full extent of

increased alkalinity after wildfire is not observed in watersheds that are also mined. Among the six unmined watersheds in this study, the correlation between alkalinity and fire intensity is not significant (r = 0.589; Pearson's cutoff = 0.811), but it is stronger than when all samples are considered (r = 0.098; Pearson's cutoff = 0.468).

There is a weak negative correlation between alkalinity and mining intensity in this study. The presence of wildfire, which increases alkalinity, as well as a high system buffering capacity due to carbonate in ore bodies (Murphy et al. 2000), explains why this trend is not as strong as otherwise would be expected.

While wildfire dominates the concentrations of major solutes in streamwater, mining has a stronger impact on trace elements, which makes sense, as tailings piles are a direct source of these elements (McConnell 1995; Sullivan and Drever 2001; Kim et al. 2007; Bradley 2008). Although the impact of mining on trace elements is more commonly observed and better documented, a few studies report that ash from wildfire contains trace elements such as $Cu^{+}$, $Fe^{2+}$, $Mn^{2+}$, and $Zn^{2+}$ and contributes to higher concentrations of these elements in the streamwater, sediment, and soil of burned watersheds (Certini 2005; Gonzalez Parra 2006; Smith et al. 2011). Wildfire increases sediment transport downslope, and if there is a pre-existing source of trace elements on hillslopes, such as tailings piles, it will also contribute increased trace element concentrations in burned watersheds. In this study, mined and burned watersheds have greater concentrations of most trace elements compared to unmined and unburned watersheds (see *Table 3.4*), but many more trace elements correlate with mining intensity than with fire intensity. The magnitude of trace element increase in mined and burned watersheds is controlled by the degree of mining

disturbance in a watershed, implying that mine tailings, rather than ash from wildfire, are the primary source of trace elements in these watersheds.

Within Emerson Gulch, concentrations of most major solutes increase downstream, and not surprisingly, those affected most strongly by wildfire and mining ($SO_4^{2-}$ and $Ca^{2+}$) have the greatest increases (see *Figure 3.11*). The fact that concentrations far upstream of the mouth are low and increase downstream demonstrates that these solutes are sourced from hillslopes throughout the catchment. Having a greater density of sampling sites within Emerson Gulch and comparing these data with similar data for other tributaries would be useful to further evaluate the distribution of solute sources within tributary catchments.

Slope was expected to have an impact on tributary water chemistry in some capacity (Swanson 1981). In a burned watershed, if there are steeper slopes, there will be a greater erosional response to wildfire, and thus increased sediment and solute delivery to streams. Slopes in this mountainous area are generally steep, however, so there may not be an effective difference between watersheds. The average slope of a watershed, the proxy for slope used in this study, is not a complete representation of slope variability within a basin. If slope has an impact on geomorphic and hydrologic processes here, it is overshadowed by wildfire and mining in chemical data.

Watersheds with Boulder Creek granodiorite bedrock have consistently higher streamwater concentrations of $Ca^{2+}$, $Cl^-$, $K^+$, and $Sr^{2+}$ than those with metamorphic bedrock. Boulder Creek granodiorite contains carbonate-rich ore deposits, which weather readily to provide increased streamwater $Ca^{2+}$ and $HCO_3^-$ (Drever 1997; Murphy et al. 2000). Granitic rocks in the area contain trace levels of $Sr^{2+}$, which can easily substitute for $Ca^{2+}$ (Lovering and Goddard 1950). While it is consistent with

these observations that granitic bedrock would provide a greater supply of $Ca^{2+}$ and $Sr^{2+}$, $Cl^-$ is not typically sourced from bedrock interactions (Drever 1997).

Although the burned and mined area is mostly within granitic bedrock, $SO_4^{2-}$ concentrations do not significantly differ between watersheds with different bedrock type. As $SO_4^{2-}$ was the solute affected most dramatically by wildfire and mining, this suggests that the increases in $Ca^{2+}$, $Cl^-$, $K^+$, and $Sr^{2+}$ are not necessarily a product of wildfire or mining. Furthermore, $Sr^{2+}$ is on average lower in burned and mined watersheds compared to unburned and unmined watersheds, and is significantly higher in granitic watersheds. The effects of bedrock on streamwater chemistry, although relatively minor, appear to be distinct from wildfire and mining disturbance. It is, however, possible that wildfire and mining obscure the impact of bedrock on other solutes.

Chemical data for bedrock samples of Boulder Creek granodiorite and metasediment from nearby watersheds were compared (D. Dethier, personal communication); granodiorite samples are fairly consistent in composition, but metamorphic samples have highly variable composition (*Table 4.1*). This makes it difficult to speculate how the chemical composition of bedrock in the Fourmile Creek basin specifically varies between tributary watersheds, and in turn, how these differences might impact streamwater chemistry.

Although the *t*-test values for $Ca^{2+}$, $Cl^-$, $K^+$, and $Sr^{2+}$ in watersheds with different bedrock were strong on the first sampling date, they were weaker and/or not statistically significant on the later date. This was a consistent trend across many variables—correlations with fire and mining intensity tended to be stronger on the earlier date. The impacts of wildfire and mining are expected to be clearer on the

| | | Metamorphic Bedrock | | | Granitic Bedrock | | |
|---|---|---|---|---|---|---|---|
| | | Average | Min | Max | Average | Min | Max |
| $SiO_2$ | % | 65.53 | 60.64 | 70.01 | 64.08 | 48.76 | 69.53 |
| $Al_2O_3$ | % | 15.81 | 14.95 | 16.68 | 15.80 | 14.09 | 18.56 |
| $Fe_2O_3$ | % | 5.75 | 4.00 | 7.54 | 5.60 | 3.34 | 10.11 |
| MgO | % | 1.18 | 0.23 | 2.28 | 2.43 | 1.61 | 5.52 |
| CaO | % | 2.41 | 0.30 | 5.89 | 3.87 | 2.05 | 8.19 |
| $Na_2O$ | % | 2.33 | 0.83 | 3.80 | 3.10 | 2.55 | 3.79 |
| $K_2O$ | % | 5.02 | 1.78 | 9.50 | 3.20 | 1.95 | 4.88 |
| $TiO_2$ | % | 0.53 | 0.24 | 0.86 | 0.57 | 0.35 | 0.93 |
| P2O5 | % | 0.25 | 0.04 | 0.69 | 0.24 | 0.17 | 0.55 |
| MnO | % | 0.04 | 0.01 | 0.07 | 0.06 | 0.04 | 0.12 |
| Sr | ppm | 471.6 | 169.4 | 997.8 | 695.7 | 400.5 | 1046.0 |

**Table 4.1. Bedrock Chemistry Data.**
Summary of bedrock chemistry for samples from nearby watersheds (D. Dethier, personal communication).

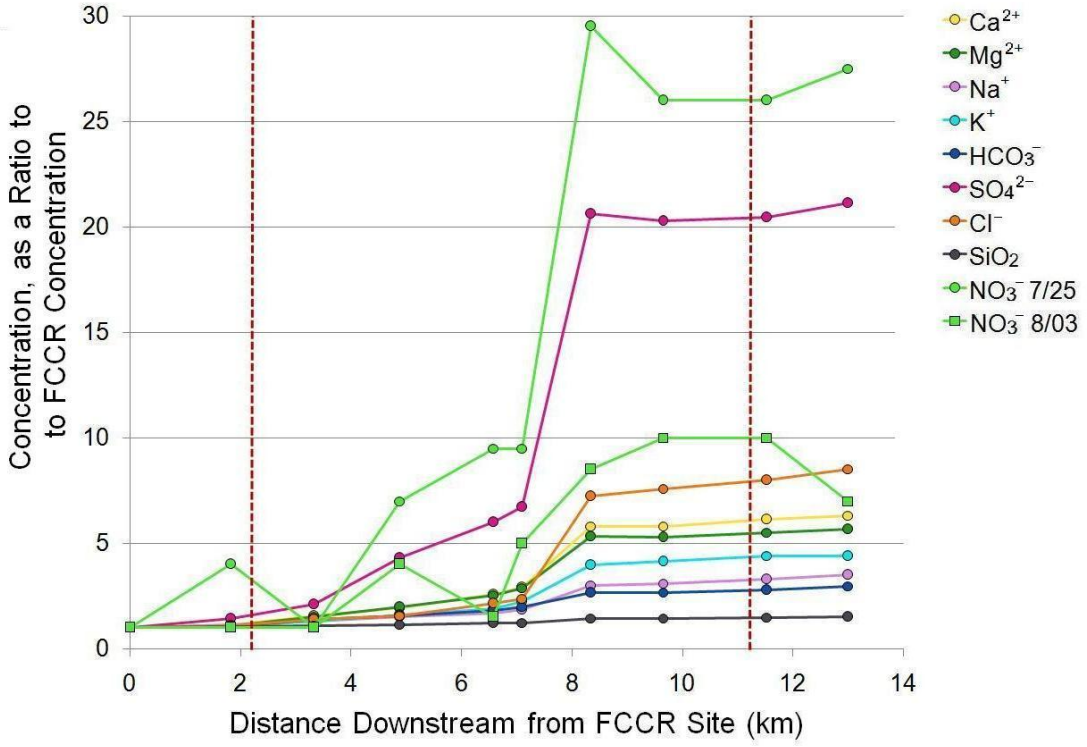


**Figure 4.3. Downstream Changes in Major Solutes.**
Streamwater concentrations of major solutes on the first sampling date plotted as ratios to upstream, undisturbed concentrations at site FCCR. Patterns are similar on the later date for all except $NO_3^-$, which is shown for both dates.

earlier date, soon after the rainstorm that caused increased solute delivery to streams. Bedrock effects should be constant and may be difficult to discern due to strong wildfire and mining input.

### *4.1.2. Fourmile Creek Water Chemistry*

Patterns of increased major solutes and conductivity downstream along Fourmile Creek are controlled by input from burned and mined tributaries. The influence of Gold Run, Fourmile Creek's largest tributary in terms of discharge by an order of magnitude, is clear in the spikes of most solutes and conductivity in Fourmile Creek downstream of the mouth of Gold Run (see *Figure 3.14*).

Downstream concentrations of major solutes were considered as ratios of concentration at each sampling site to concentration at site FCCR, the sampling site farthest upstream. This site best represents undisturbed waters upstream of the burned and mined area, and considering downstream data using this ratio shows the magnitude of downstream changes through the disturbed area. Those most affected by wildfire and mining in tributaries change by the largest margin downstream; concentrations of $SO_4^{2-}$ downstream of the disturbed area are 21.1 times those at site FCCR (*Figure 4.3*). While $HCO_3^-$ and $SiO_2$ also increase downstream, they do so at a slower rate, and their magnitudes of increase are much smaller. As Fourmile Creek exits the disturbed area, concentrations of most solutes level off and relative abundances shift slightly toward their upstream, undisturbed values. Outside the disturbed area, tributary input does not affect Fourmile Creek streamwater chemistry as strongly as it does within the disturbed area.

Changes in concentration of major solutes between adjacent Fourmile sampling sites were compared to tributary discharge input between sites and changes in Fourmile Creek discharge between sites. There is a strong positive correlation between incoming tributary discharge and change in concentration of all major solutes except $NO_3^-$. The only solute that correlates with changes in discharge of Fourmile Creek is $SiO_2$, which decreases as Fourmile discharge increases. Thus, Fourmile Creek losing or gaining discharge from other sources, such a groundwater, does not have a large impact on solute chemistry. Fourmile Creek discharge stays relatively constant through the studied area (see *Figure 3.6*), and tributaries do not substantially contribute to Fourmile discharge. Even so, differences in concentration of major ions between Fourmile sites correlate strongly with the individual mass flux of ions from tributary input between sites, calculated by multiplying tributary discharge by ion concentration (*Figure 4.4*). All but $NO_3^-$ ($r = 0.847$) have an r-value greater than 0.9. Changes in solute chemistry downstream along Fourmile Creek are primarily due to tributary input, even though tributaries contribute minimally to flow volume, which is consistent with tributaries having a much higher solute load than Fourmile Creek.

Trace elements in Fourmile Creek have variable downstream trends. While wildfire and mining contribute increased concentrations of trace elements, the effects are less consistent and of smaller magnitude than effects on major elements. This explains why trace element concentrations in Fourmile Creek do not reflect tributary input as strongly. Concentrations of $Mn^{2+}$ and $Zn^{2+}$ spike after input from Gold Run (see *Figure 3.16*), implying that input from burned and mined tributaries do influence trace elements in Fourmile Creek, although the effects are less persistent.

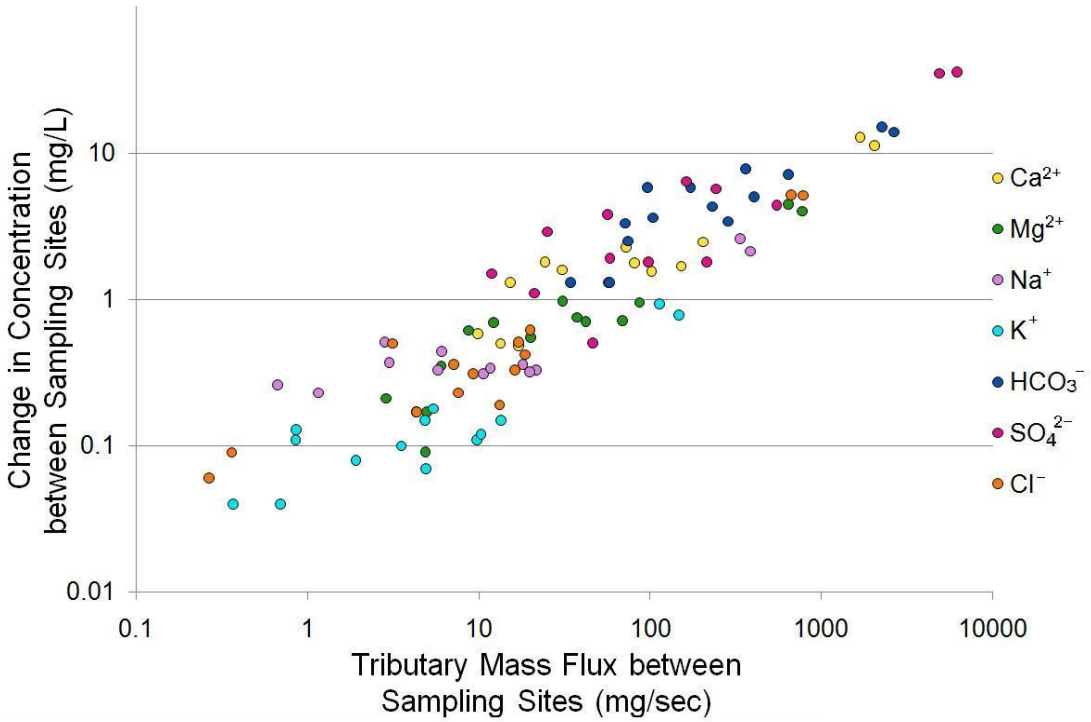


**Figure 4.4. Tributary Mass Flux and Fourmile Creek Concentrations.**
The mass flux of tributary input between Fourmile Creek sampling sites for each major ion (the sum of the ion's mass fluxes for all tributaries entering between sites) plotted against the change in Fourmile Creek concentration for each ion between sites.

### *4.1.3. Nitrate*

Nitrate is an exception in tributary and Fourmile Creek streamwater chemistry analysis. In Fourmile Creek, $NO_3^-$ is the only solute for which concentration does not continually increase downstream and is the only solute to have different downstream patterns between sampling dates (see *Figures 4.14, 5.3*). Unlike all other major solutes, it does not correlate with discharge from incoming tributaries. This could be because $NO_3^-$ concentrations are very low, although $F^-$, $K^+$, and $Sr^{2+}$ have similar concentrations and do correlate with tributary input.

As expected, tributary $NO_3^-$ concentrations correlate with fire intensity but not with mining intensity. Mining has not been reported to have an impact on $NO_3^-$, as there is generally no N in mined ore deposits (Sullivan and Drever 2001; Blowes et al. 2005). Wildfire increases streamwater $NO_3^-$ as a result of oxidized N-species in organic matter; the magnitude of increase varies greatly depending on many factors (Ice et al. 2004; Johnson et al. 2007; Mast and Clow 2008).

Tributary $NO_3^-$ concentrations and downstream patterns along Fourmile Creek change substantially between sampling dates compared to all other solutes, implying that $NO_3^-$ responds to additional short-term factors more strongly than other solutes. Many studies have found the post-fire response of streamwater N-species to be particularly dependent on short-term precipitation patterns (Johnson et al. 2007; Bladon et al. 2008; Betts and Jones 2009; Rhoades et al. 2011). The lack of precipitation between sampling dates may have had a particular impact on $NO_3^-$ in burned watersheds. Additionally, more so than other studied solutes, $NO_3^-$ concentrations respond to changes in biological activity (Betts and Jones 2009). Nitrogen is often a limiting nutrient in stream ecosystems, and can thus be taken up

rapidly, which could cause concentrations to fluctuate on short time scales (Lohman et al. 1991). Sewage from nearby houses could also affect $NO_3^-$ and might not have a consistent impact from day to day. Within the burned area, the majority of structures were destroyed, but some houses survived, particularly in the Gold Run watershed. The area upstream of the burn is sparsely populated, so wastewater effects are minimal there, but downstream of the burned area there are houses along Fourmile Creek and its tributaries, especially Sunbeam Gulch. The disproportionately high conductivity (1332 μS/cm) and alkalinity (254 ppm) in Sunbeam Gulch suggest that wastewater from houses affects streamwater chemistry.

## 4.2. Sediment Chemistry

Fire intensity correlates with increased percentages of most major oxides in streambed sediment along with a decrease in the percentage of $SiO_2$ (see *Figure 3.17*). This suggests that the sediment load transported downslope after the fire includes a lesser percentage of $SiO_2$ and a greater percentage of other major oxides than material coming down hillslopes into stream channels in undisturbed catchments. Forest biomass is typically rich in aluminum, calcium, iron, magnesium, manganese, phosphorous, and potassium; to a lesser extent, it can also contain sodium (Drever 1997). Wildfire burns vegetation and leaves behind an increased supply of these major oxides, which can then be adsorbed onto fine material and entrained in sediment that is deposited on the streambed. This explains the positive correlation between fire intensity and percentages of $Al_2O_3$, CaO, $K_2O$, $Na_2O$, MgO, and $P_2O_5$ in streambed sediment, and why the percentage of $SiO_2$ decreases with fire intensity, diluted by higher levels of these other oxides.

Mining overall has little to no impact on major oxides in streambed sediment. It was expected that mined watersheds would have higher $Fe_2O_3$ than unmined watersheds, as streams affected by mine drainage typically have abundant ferric precipitates (Bradley 2008). However, neither SEM nor XRF analysis showed this to be the case (see *Figure 3.18*). This could reflect the fact that all sediment samples were taken near the mouths of tributaries, as mining-related iron precipitates may be quickly deposited adjacent to mine sites, so that they are not visible downstream.

Tributary flood deposits have compositions statistically indistinguishable from streambed sediment for all measured constituents. Post-fire flooding caused increased sediment delivery to streams, and either it did not impact the composition of that sediment, or it impacted it to such a great degree that streambed sediment still mirrored flood deposits nearly two weeks after the storm event. In contrast, Fourmile Creek flood deposits have significantly different composition from tributary flood deposits. This is as expected, as Fourmile Creek flood deposits reflect a combination of input from all upstream tributaries and headwaters. Fourmile Creek also has significantly greater flow, and has the power to wash sediment away more quickly than its small tributaries. Thus, sediment deposited along Fourmile Creek will have different characteristics (e.g., grain size) than sediment deposited along tributaries.

As input from burned and mined tributaries dominates downstream trends in Fourmile Creek streamwater chemistry, downstream trends in flood deposit chemistry were expected to reflect tributary input. Unlike solutes in streamwater, major oxides in flood deposit samples do not have a steady downstream trend, but they do change after input from Gold Run. The downstream patterns for most major oxides switch direction after Gold Run (see *Figure 3.19*); in contrast, streamwater from Gold Run

magnifies pre-existing downstream trends. The small number of flood deposit samples makes it difficult to evaluate the effects of tributary contribution as accurately as for streamwater.

The Hg:C ratio is generally accepted as the most accurate way to represent and analyze mercury data, because it accounts for mercury being readily absorbed by organic carbon (Sunderland et al. 2006). Bald Gulch demonstrates this well; the unmined watershed had an inexplicably high Hg concentration (191 ppb), but when corrected for a large weight % C, the Hg:C ratio was low. In general, the impact of wildfire is to decrease Hg in burned watersheds through the volatilization of accumulated Hg in soils (Smith et al. 2011), although the amount released is limited by the amount stored in soils prior to burning (Biswas et al. 2007). In contrast, mining provides a source of Hg in addition to atmospheric deposition (Alpers et al. 2005). Mines in the Colorado Front Range did not commonly use mercury amalgamation, so the impact of mining on sediment Hg is less than in a typical mined area (Mast and Krabbenhoft 2010).

There is no significant correlation between Hg:C ratio and fire or mining intensity. Because wildfire and mining have opposing effects on Hg, a strong trend with either was not expected. All unmined watersheds have low Hg:C ratios (<50 ppm/wt %), and of the five most heavily mined watersheds, four have Hg:C ratios over 100 ppm/wt %; these are the four highest values (*Figure 4.5*). This implies that mining is a source of mercury in these watersheds. A trend of decreasing Hg:C with fire intensity is not observed, and Hg:C ratios are higher on average in burned than in unburned watersheds. As most burned watersheds were also mined, this suggests that mining dominates the influence on Hg in these watersheds. Gold Run, which has the

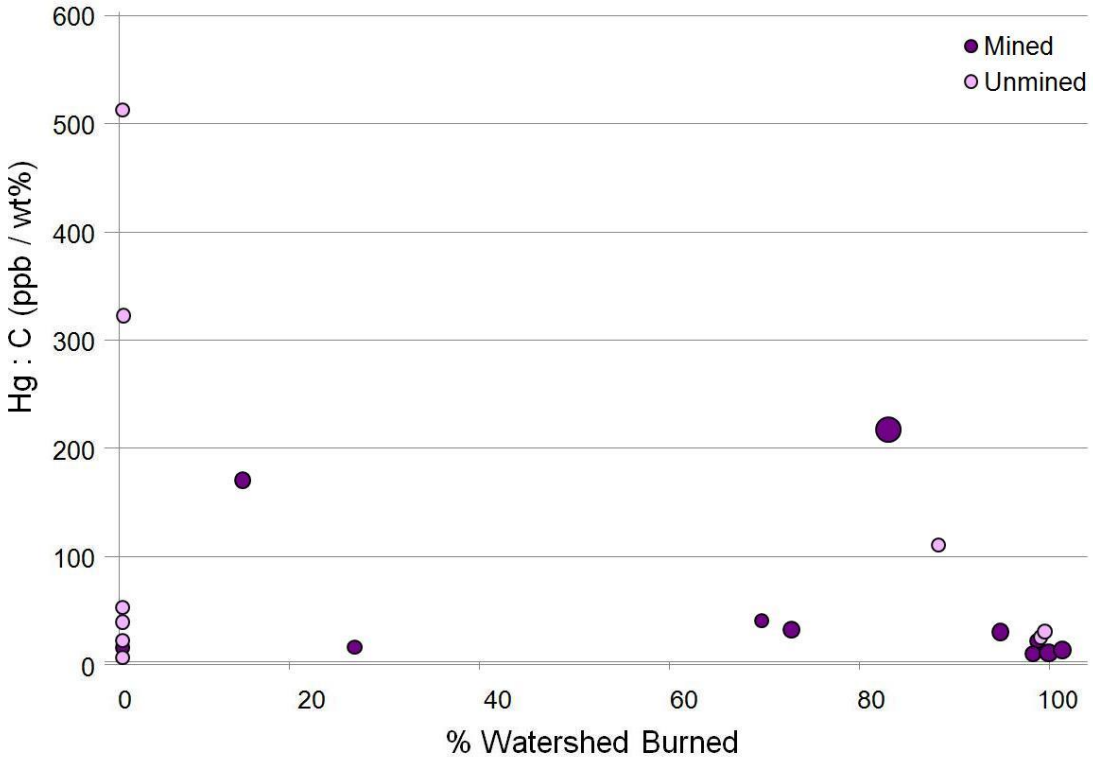


**Figure 4.5. Hg:C Ratios in Burned and Mined Tributaries.**
Hg:C ratios plotted against watershed fire intensity; the size of each point represents the mining intensity in that watershed.

highest Hg:C ratio (510.0 ppm/wt %), is heavily mined but has a smaller percent area burned (70.1%) than the other heavily mined watersheds. The lesser presence of fire in this watershed coupled with severe mining could explain the very high Hg:C ratio. However, accurately evaluating the effects of wildfire on mercury is difficult without knowing pre-fire mercury concentrations.

Fire weakly correlates with decreased weight % C in streambed sediment, and on average, both weight % C and weight % N are ~80% lower in burned compared to unburned watersheds (see *Table 3.6*). Severe wildfires consume most if not all C and N stored in the O horizon (Baird et al. 1999; Betts and Jones 2009), which greatly reduces nutrient delivery to streams; the decreases observed in this study are consistent with these findings.

Mining intensity correlates with decreased C:N ratios, but not with changes in weight % C or N. Shrestra and Lal (2011) found that mining caused decreased C:N ratios in soils, but also observed changes in C and N pools. They explain the decreased C:N ratio as a product of drastic reduction in soil organic C due to mining. Weight % C was 20% lower in mined watersheds, but this a relatively small decrease that could partially be a product of wildfire in these basins. While the correlation between mining intensity and C:N ratio is statistically significant, it might not be meaningful. Sediment trace element data were not available, but would be expected to reflect the influence of mining with increased concentrations of heavy metals.

# 5. CONCLUSION

The chemistry of Fourmile Creek and its tributaries is heavily influenced by the Fourmile Fire in addition to historical mining. Burned watersheds on average have much higher concentrations of almost every major solute than unburned watersheds; the same is true for mined and unmined watersheds, although the differences are not as great. Wildfire is associated with dramatic increases in $Ca^{2+}$, $Mg^{2+}$, $Na^{+}$, $K^{+}$, $NO_3^{-}$, and $SO_4^{2-}$ in tributary streamwater, while mining causes large increases in $SO_4^{2-}$ and smaller decreases in alkalinity as $HCO_3^{-}$. Increased $SO_4^{2-}$ in burned watersheds coincided with increased export of divalent cations in particular.

In Fourmile Creek, water classification shifts from calcium bicarbonate to calcium sulfate waters downstream through the disturbed area as the large input of $SO_4^{2-}$ from burned and mined tributaries changes the relative abundances of major anions. Although these tributaries do not contribute substantial discharge to Fourmile Creek, downstream concentration changes along Fourmile Creek strongly reflect the influence of these tributaries. Major solute concentrations in Fourmile Creek increase at a higher rate through the disturbed area than they do upstream or downstream. In particular, most solutes dramatically spike in concentration after input from Gold Run, the largest tributary. Changes in concentration along Fourmile Creek between sampling sites correlate strongly with tributary input.

Differences in bedrock have a minor impact on water chemistry, as watersheds with predominantly Boulder Creek granodiorite bedrock have higher concentrations of $Ca^{2+}$, $Cl^{-}$, $K^{+}$, and $Sr^{2+}$ than watersheds with metamorphic bedrock. Slope does not have a significant effect. Nitrate is the only solute to change concentration patterns between sampling dates, showing that it responds to other signals in addition to fire

and mining. Biological processes and sewage from nearby houses may play a role in the fluctuating concentrations of $NO_3^-$ over the short time scale of this study.

Tributary sediment chemistry reflects the impact of wildfire with increased concentrations of major oxides and decreased levels of C and N in burned watersheds. There is no compositional difference between flood deposits from the storm event and streambed sediment. Downstream along Fourmile Creek, flood deposits show changes in composition after input from Gold Run, but do not have a consistent downstream trend. Mining does not impact major oxides or nutrients in streambed sediment, but does contribute increased mercury.

The coincidence of wildfire and mining causes different effects than in watersheds affected by only one of these disturbances. Wildfire typically increases alkalinity, but acidity from mine drainage partially cancels out this effect. Sulfate increases in burned watersheds are greater than often observed after wildfire, which is due to additional $SO_4^{2-}$ from mining. Severe wildfire in a catchment reduces or completely eliminates ground vegetation cover, increasing the supply of major elements from burned organic matter and making it easier for these to be eroded and transported to streams. Mining is associated with tailings piles, which provide an additional supply of material to be eroded after a fire. Wildfire dominates the short-term geochemistry of the Fourmile Creek watershed, and its effects are exacerbated by the presence of historical mining.

## 5.1. Future Work

These results represent a snapshot in time of water and sediment chemistry of samples collected over a period of less than two weeks. A longer-term evaluation of

stream and sediment chemistry would allow for full characterization of the impact of these disturbances, and could answer several other questions. How long will the effects observed in this study persist? Does the presence of historical mining affect the speed of watershed recovery after wildfire? How do specific precipitation events influence long-term watershed recovery? A better quantification of variations in bedrock chemistry and analysis of housing density in the area might provide better insight into how these variables specifically affect watershed chemistry.

Sediment sampling along Fourmile Creek itself only included six flood deposits, but additional sampling and analysis of streambed sediment would be useful to evaluate the potential impact of burned and mined tributary input on Fourmile Creek sediment chemistry. A bulk analysis of sediment samples is provided here; an analysis of sieved samples would provide additional insight, as it would isolate the composition of fine-grained material. Trace element data for bulk and sieved samples would also be valuable, as the effect of mining on sediment chemistry would be most evident in these data.

It is rare for a severe wildfire to coincide so closely with historical mining, and studying how these disturbances combine to chemically affect the Fourmile Creek catchment can provide new insight into the mechanisms through which wildfire and mining affect watershed chemistry. This could allow for prediction of how areas affected by other geochemical disturbances might respond to wildfire, which will be especially useful in the future as wildfire regimes are expected to shift with climate change.

# 6. REFERENCES


Allen, J.L., and Sorbel, B., 2008, Assessing the differenced Normalized Burn Ratio's ability to map burn severity in the boreal forest and tundra ecosystems of Alaska's national parks: International Journal of Wildland Fire, v. 17, p. 463–475.

Alpers, C.N., Hunerlach, M.P., May, J.T., Hothem, R.L., Taylor, H.E., Antweiler, R.C., De Wild, J.F., and Lawler, D.A., 2005, Geochemical characterization of water, sediment, and biota affected by mercury contamination and acidic drainage from historical gold mining, Greenhorn Creek, Nevada County, California, 1999–2001: U.S. Geological Survey Scientific Investigations Report 2004–5251, 278 p.

Baird, M., Zabowski, D., and Everett, R.L., 1999, Wildfire effects on carbon and nitrogen in inland coniferous forests: Plant and Soil, v. 209, p. 233–243.

Bayley, S.E., and Schindler, D.W., 1991, The role of fire in determining stream water chemistry in northern coniferous forests *in* Mooney, H.A., Medina, E., Schindler, D.W., Schulze, E.-D., and Walker, B.H., editors, Ecosystem experiments, Scope Forty-Five: Chichester, U.K., John Wiley and Sons, p. 141–165.

Benavides-Solorio, J., and MacDonald, L.H., 2001, Post-fire runoff and erosion from simulated rainfall on small plots, Colorado Front Range: Hydrological Processes, v. 15, p. 2931–2952.

Bergeron, Y., and Flannigan, M.D., 1995, Predicting the effects of climate change on fire frequency in the southeastern Canadian boreal forest: Water, Air and Soil Pollution, v. 82, p. 437–444.

Betts, E.F., and Jones, J.B., 2009, Impact of wildfire on stream nutrient chemistry and ecosystem metabolism in boreal forest catchments of interior Alaska: Arctic, Antarctic, and Alpine Research, v. 41, no. 4, p. 407–417.

Biswas, A., Blum, J.D., Klaue, B., and Keeler, G.J., 2007, The release of mercury from Rocky Mountain forest fires: Global Biogeochemistry Cycles, p. 21.

Biswas, A., Blum, J.D., and Keeler, G.J., 2008, Mercury storage in surface soils in a central Washington forest and estimated release during the 2001 Rex Creek Fire: Science of the Total Environment, v. 404, p. 129–138.

Bladon, K.D., Silins, U., Wagner, M.J., Stone, M., Emelko, M.B., Mendoza, C.A., Devito, K.J., and Boon, S., 2008, Wildfire impacts on nitrogen concentration and production from headwater streams in southern Alberta's Rocky Mountains: Canadian Journal of Forest Research, v. 38, p. 2359–2371.

Blowes, D.W., Ptacek, C.J., Jambor, J.L., and Weisener, C.G., 2005, The Geochemistry of Acid Mine Drainage *in* Lollar, B.S., editor, 2005, Environmental Geochemistry: Oxford, UK, Elsevier Ltd, p. 149–204.

Bradley, H.A., 2008, Sediment chemistry and benthic macro-invertebrate communities within an acid mine drainage impacted stream: Earth & Environment, v. 3, p. 1–31.

Campbell, D.H., Clow, D.W., Ingersoll, G.P., Mast, M.A., Spahr, N.E., and Turk, J.T., 1995, Processes controlling the chemistry of two snowmelt-dominated streams in the Rocky Mountains: Water Resources Research, v. 31, no. 11, p. 2811–2821.

Campbell, R.E., Baker Jr., M.B., Ffolliot, P.F., Larson, F.R., and Avery, C.C., 1977, Wildfire effects on a ponderosa pine ecosystem: An Arizona case study: USDA For. Serv. Resp. Pap. RM-191., Fort Collins, CO: U.S. Department of Agriculture, Forest Service, Rocky Mountain Forest and Range Experiment Station, 12 p.

Certini, G., 2005, Effects of fire on properties of forest soils: A review: Oecologia, v.143, p. 1–10.

Chorover, J., Vitousek, P.M., Everson, D.A., Esperanza, A.M., and Turner, D., 1994, Solution chemistry profiles of mixed-conifer forests before and after fire: Biogeochemistry, v. 26, p. 115–144.

Cocke, A.E., Fulé, P.Z., and Crouse, J.E., 2005, Comparison of burn severity assessments using Differenced Normalized Burn Ratio and ground data: International Journal of Wildland Fire, v. 14, p. 189–198.

DeBano, L.F., 2000, The role of fire and soil heating on water repellency in wildland environments: A review: Journal of Hydrology, v. 231, p. 195–206.

Drever, J.I., 1997, The Geochemistry of Natural Waters: Surface and Groundwater Environments: Upper Saddle River, New Jersey, Prentice-Hall, Inc., 436 p.

Dyrness, C.T., Vancleve, K., and Levison, J.D., 1989, The effect of wildfire on soil chemistry in four forest types in interior Alaska: Canadian Journal of Forest Research, v. 19, no. 11, p. 1389–1396.

Earl, S.R., and Blinn, D.W., 2003, Effects of wildfire ash on water chemistry and biota in South-Western U.S.A. streams: Freshwater Biology, v. 48, p. 1015–1030.

Epting, J., Verbyls, F., and Sorbel, B., 2005, Evaluation of remotely sensed indices for assessing burn severity in interior Alaska using Landsat TM and ETM+: Remote Sensing of Environment, v. 96, p. 328–339.

Fetter, C.W., 2001, Applied Hydrogeology, Fourth Edition: Upper Saddle River, New Jersey, Prentice-Hall, Inc., 598 p.

Gabet, E.J., 2003, Sediment transport by dry ravel: Journal of Geophysical Research, v. 108, p. 22.

Gonzalez Parra, J., 1996, Forms of Mn in soils affected by a forest fire: The Science of the Total Environment, v. 181, p. 231–236.

Graham, R., Finney, M., McHugh, C., Cohen, J., Stratton, R., Bradshaw, L., Nikolov, N., and Calkin, D., 2011, Fourmile Canyon Fire: Preliminary Findings: U.S. Department of Agriculture Forest Service, 99 p.

Hall, R.J., Likens, G.E., Fiance, S.B., and Hendrey, G.R., 1980, Experimental acidification of a stream in the Hubbard Brook experimental forest, New Hampshire: Ecology, v. 61, no. 4, p. 976–989.

Harvey, F.E., 2005, Stable hydrogen and oxygen isotope composition of precipitation in northeastern Colorado: Journal of the American Water Resources Association, v. 41, no. 2, p. 447–459.

Hessl, A.E., 2011, Pathways for climate change effects on fire: Models, data, and uncertainties: Progress in Physical Geography, v. 35, no. 3, p. 393–407.

Ice, G.C., Neary, D.G., and Adams, P.W., 2004, Effects of wildfire on soils and watershed processes: Journal of Forestry, p. 16–20.

Inbar, M., Tamir, M., and Wittenberg, L., 1998, Runoff and erosion processes after a forest fire in Mount Carmel, a Mediterranean area: Geomorphology, v. 24, p. 17–33.

Johnson, D., Murphy, J.D., Walker, R.F., Glass, D.W., and Miller, W.W., 2007, Wildfire effects on forest carbon and nutrient budgets: Ecological Engineering, v. 31, p. 183–192.

Jopling, A.V., 1966, Some principle and techniques used in reconstructing the hydraulic parameters of a paleo-flow regime: Journal of Sedimentary Petrology, v. 36, no. 1, p. 5–49.

Kellogg, K.S., Bryant, B., Reed Jr., J.C., 2004, The Colorado Front Range—Anatomy of a Laramide uplift *in* Nelson, E.P., and Erslev, E.A., editors, Field Trips in the Southern Rocky Mountains, USA: Boulder, Colorado, The Geological Society of America, Inc., p. 89–108.

Khanna, P.K., and Raison, R.J., 1986, Effect of fire intensity on solution chemistry of surface soil under a Eucalyptus pauciflora forest: Australian Journal of Soil Research, v. 24, p. 423–434.

Kim, J.G., Ko, K.-S., Kim, T.H., Lee, G.H., Song, Y., Chon, C.-M., and Lee, J.-S., 2007, Effect of mining and geology on the chemistry of stream water and sediment in a small watershed: Geosciences Journal, v. 11, no. 2, p. 175–183.

Kunze, M.D., and Stednick, J.D., 2006, Streamflow and suspended sediment yield following the 2000 Bobcat fire, Colorado: Hydrological Processes, v. 20, p. 1661–1681.

Lavoie, M., Paré, D., and Bergeron, Y., 2005, Impact of global climate change and forest management on carbon sequestration in northern forested peatlands: Environmental Review, v. 13, p. 199–240.

Lin, C., Wu, Y., Lu, W., Chen, A., and Liu, Y., 2007, Water chemistry and ecotoxicity of an acid mine drainage-affected stream in subtropical China during a major flood event: Journal of Hazardous Materials, v. 142, p. 199–207.

Lohman, K., Jones, J.R., and Baysinger-Daniel, C., 1991, Experimental evidence for nitrogen limitation in a northern Ozark stream: Journal of the North American Benthological Society, v. 10, no. 1, p. 14–23.

Lovering, T.S., and Goddard, E.N., 1950, Geology and ore deposits of the Front Range, Colorado: U.S. Geological Survey Professional Paper 223, 319 p.

Malmer, A., 2004, Streamwater quality as affected by wild fires in natural and manmade vegetation in Malaysian Borneo: Hydrological processes, v. 18, p. 853–864.

Mast, M.A., and Clow, D.W., 2008, Effects of 2003 wildfires on stream chemistry in Glacier National Park, Montana: Hydrological processes, v. 22, p. 5013–5023.

Mast, M.A., and Krabbenhoft, D.P., 2010, Comparison of mercury, bottom sediment, and zooplankton in two Front Range reservoirs in Colorado, 2008–09: U.S. Geological Survey, Scientific Investigations Report 2010–5037, 20 p.

McConnell, J., 1995, Seasonal and mining influences on stream-water chemistry, Rambler Mines area: Implications for exploration and environmental monitoring: Newfoundland Department of Natural Resources Geological Survey, Report 95–1, p. 129–137.

Miller, J.D., Knapp, E.E., Key, C.H., Skinner, C.N., Isbell, C.J., Creasy, R.M., and Sherlock, J.W., 2009, Calibration and validation of the relative differenced Normalized Burn Ratio (RdNBR) to three measures of fire severity in the Sierra Nevada and Klamath Mountains, California, USA: Remote Sensing of Environment, v. 113, p. 645–656.

Minshall, G.W., Brock, J.T., and Varley, J.D., 1989, Wildfires and Yellowstone's stream ecosystems: Bioscience, v. 39, no. 10, p. 707–715.

Moody, J.A., and Martin, D.A., 2001, Initial hydrologic and geomorphic response following a wildfire in the Colorado Front Range: Earth Surface Processes and Landforms, v. 26, p. 1049–1070.

Moody, J.A., Martin, D.A., and Cannon, S.H., 2008a, Post-wildfire erosion response in two geologic terrains in the Western USA: Geomorphology, v. 95, p. 103–118.

Moody, J.A., Martin, D.A., Haire, S.L., and Kinner, D.A., 2008b, Linking runoff response to burn severity after a wildfire: Hydrological Processes, v. 22, p. 2063–2074.

Murphy, S.F., Verplanck, P.L., and Barber, L.B., editors, 2000, Comprehensive water quality of the Boulder Creek Watershed, Colorado, under high-flow and low-flow conditions: U.S. Geological Survey Water-Resources Investigations Report 03–4045, 198 p.

Murphy, S.F., and Writer, J.H., 2011, Evaluating the effects of wildfire on stream processes in a Colorado Front Range watershed, USA: Applied Geochemistry, v. 26, p. S363–S364.

Platt, R.V., Schoennagel, T., Veblen, T.T., and Sherriff, R.L., 2011, Modeling wildfire potential in residential parcels: A case study of the north-central Colorado Front Range: Landscape and Urban Planning, v. 102, p. 117–126.

Rhoades, C.C., Entwistle, D., and Butler, D., 2011, The influence of wildfire extent and severity on streamwater chemistry, sediment and temperature following the Hayman Fire, Colorado: International Journal of Wildland Fire, v. 20, p. 430–442.

Richter, D.D., Ralston, C.W., and Harms, W.R., 1982, Prescribed fire: Effects on water quality and forest nutrient cycling: Science, v. 215, p. 661–662.

Reneau, S.L., Katzman, D., Kuyumijan, G.A., Lavine, A., and Malmon, D.V., 2007, Sediment delivery after a wildfire: Geology, v. 35, no. 2, p. 151–154.

Ruddy, B.C., Stevens, M.R., Verdin, K.L., and Elliott, J.G., 2010, Probability and volume of potential postwildfire debris flows in the 2010 Fourmile burn area, Boulder County, CO: U.S. Geological Survey Open-File Report 2010–1244, 13 p.

Shrestha, R.K., and Lal, R., 2011, Changes in physical and chemical properties of soil after surface mining and reclamation: Geoderma, v. 161, p. 168–176.

Sibold, J.S., and Veblen, T.T., 2006, Relationships of subalpine forest fires in the Colorado Front Range with interannual and multidecadal-scale climatic variation: Journal of Biogeography, v. 33, p. 833–842.

Smith, H.G., Sheridan, G.J., Lane, P.N.J., Nyman, P., and Haydon, S., 2011, Wildfire effects on water quality in forest catchments: A review with implications for water supply: Journal of Hydrology, v. 396, p. 170–192.

Spencer, C.N., and Hauer, F.R., 1991, Phosphorous and nitrogen dynamics in streams during a wildfire: Journal of the North American Benthological Society, v. 10, no. 1, p. 24–30.

Spencer, C.N., Gabel, K.O., Hayer, F.R., 2003, Wildfire effects on stream food webs and nutrient dynamics in Glacier National Park, USA: Forest Ecology and Management, v. 178, p. 141–153.

Stoeser, D.B., Green, G.N., Morath, L.C., Heran, W.D., Wilson, A.B., Moore, D.W., Van Gosen, B.S., Preliminary integrated geology map databases for the United States: Central States: Montana, Wyoming, Colorado, New Mexico, North Dakota, South Dakota, Nebraska, Kansas, Oklahoma, Texas, Iowa, Missouri, Arkansas, and Louisiana: U.S. Geological Survey Open-File Report 2005–1351: http://pubs.usgs.gov/of/2005/1351/ (accessed October 2011).

Sullivan, A.B., and Drever, J.I., 2001, Spatiotemporal variability in stream chemistry in a high-elevation catchment affected by mine drainage: Journal of Hydrology, v. 252, p. 237–250.

Sunderland, E.M., Gobas, F.A.P.C., Branfireun, B.A., and Heyes, A., 2006, Environmental controls on the speciation and distribution of mercury in coastal sediments: Marine Chemistry, v. 102, p. 111–123.

Swanson, F.J., 1981, Fire and geomorphic processes *in* Mooney, H.A., Bonnicksen, T.M., Christensen, N.L., Lotan, J.E., and Reiners, W.A., editors, Proceedings of the conference on fire regimes and ecosystem properties, USDA Forest Service General Technical Report WO–26, p. 401–420.

Swetnam, T.W., and Anderson, R.S., 2008, Fire climatology in the western United States: Introduction to special issue: International Journal of Wildland Fire, v. 17, p. 1–7.

Tomkins, K.M., Humphreys, G.S., Wilkinson, M.T., Fink, D., Hesse, P.P., Doerr, S.H., Shakesby, R.A., Wallbrink, P.J., and Blake, W.H., 2007, Contemporary versus long-term denudation along a passive plate margin: The role of extreme events: Earth Surface Processes and Landforms, v. 32, p. 1013–1031.

Tripole, S., Gonzalez, P., Vallania, A., Garbagnati, M., and Mallea, M., 2006, Evaluation of the impact of acid mine drainage on the chemistry and the macrobenthos in the Carolina stream (San Luis–Argentina): Environmental Monitoring and Assessment, v. 114, p. 377–389.

U.S. Geological Survey, 2011, Mineral Resources Online Spatial Data: http://tin.er.usgs.gov/mrds/ (accessed October 2011).

Verplank, P.L., Murphy, S.F., Birkeland, P.W., Pitlick, J., Barber, L.B., and Schmidt, T.S., 2008, Boulder Creek: A stream ecosystem in an urban landscape *in* Raynolds, R.G., editor, 2008, Roaming the Rocky Mountains and Environs: Boulder, Colorado, The Geological Society of America, Inc., p. 217–233.

Westerling, A.L., Hidalgo, H.G., Cayan, D.R., and Swetnam, T.W., 2006, Warming and earlier spring increase western U.S. forest wildfire activity: Science, v. 313, p. 940–943.

Westerling, A.L., 2008, Climate and wildfire in the western United States, California Applications Program White Paper, Climate Research Division, Scripps Institution of Oceanography, NOAA Regional Integrated Science and Assessment Program, 25 p.

# 7. APPENDICES

## 7.1. Field Measurements

Field measurements of conductivity and discharge for water sampling sites. Discharges for all Fourmile sites and conductivity measurements at sites FCCR, FCLG, FCWM, FCLM, and FCBC are courtesy of Sheila Murphy, USGS Boulder. See Figure 2.2a for a map of all water sample locations.

### *7.1.1. Fourmile Creek Water Samples*

| Sample Location | Date Sampled | Sample Name | Discharge (L/sec) | Conductivity (µS/cm) |
|---|---|---|---|---|
| Fourmile Creek at Copper Rock | 7/25 | FCCR1 | 147.2 | 54 |
| | 8/03 | FCCR2 | 87.8 | 58 |
| Fourmile Creek upstream of Long Gulch | 7/25 | FCLG1 | 147.2 | 52 |
| | 8/03 | FCLG2 | 87.8 | 64 |
| Fourmile Creek upstream of Wood Mine | 7/25 | FCWM1 | 150.1 | 87 |
| | 8/03 | FCWM2 | 87.8 | 100 |
| Fourmile Creek upstream of Logan Mill Road | 7/25 | FCLM1 | 133.1 | 245 |
| | 8/03 | FCLM2 | 82.1 | 262 |
| Fourmile Creek upstream of Boulder Creek | 7/25 | FCBC1 | 133.1 | 262 |
| | 8/03 | FCBC2 | 82.1 | 275 |
| Fourmile Creek upstream of Emerson Gulch | 7/25 | FCAEG1 | 150.1 | 70 |
| | 8/03 | FCAEG2 | 85.0 | 86 |
| Fourmile Creek upstream of Melvina Gulch | 7/25 | FCAMG1 | 150.1 | 111 |
| | 8/03 | FCAMG2 | 85.0 | 126 |
| Fourmile Creek upstream of Gold Run | 7/25 | FCGR1 | 150.1 | 123 |
| | 8/03 | FCGR2 | 82.1 | 144 |
| Fourmile Creek upstream of Arkansas Gulch | 7/25 | FCAAG1 | 133.1 | 242 |
| | 8/03 | FCAAG2 | 82.1 | 262 |
| Fourmile Creek downstream of Resevoir | 7/25 | FCBRes1 | 133.1 | 248 |
| | 8/03 | FCBRes2 | 82.1 | 272 |

### *7.1.2. Tributary Water Samples*

| Tributary Name | Date Sampled | Sample Name | Discharge (L/sec) | Conductivity (µS/cm) |
|---|---|---|---|---|
| Sand | 7/25 | W-02 | 0.24 | 835 |
| Gulch | 8/03 | W2-02 | 0.30 | 854 |
| Sunbeam | 7/25 | W-04 | 0.07 | 1332 |
| Gulch | x | x | x | x |
| Sweet Home | 7/25 | W-05 | 1.08 | 492 |
| Gulch | 8/03 | W2-05 | 0.39 | 496 |
| Gold | 7/25 | W-06 | 26.09 | 668 |
| Run | 8/03 | W2-06 | 21.47 | 701 |
| Ingram | 7/25 | W-07 | 6.83 | 634 |
| Gulch | 8/03 | W2-07 | 7.74 | 702 |
| Black Hawk | 7/25 | W-08 | 2.14 | 402 |
| Gulch | 8/03 | W2-08 | 1.64 | 411 |
| Melvina East | x | x | x | x |
| Gulch | 8/03 | W-09 | 0.14 | 608 |
| Melvina | 7/25 | W-10 | 0.78 | 574 |
| Gulch | 8/03 | W2-10 | 0.30 | 577 |
| Melvina West | 7/25 | W-11 | 0.96 | 501 |
| Gulch | 8/03 | W2-11 | 0.52 | 401 |
| Wall Street | 7/25 | W-12 | 0.09 | 380 |
| Gulch | 8/03 | W2-12 | 0.11 | 383 |
| Schoolhouse | 7/25 | W-13 | 1.47 | 826 |
| Gulch | 8/03 | W2-13 | 0.40 | 931 |
| Emerson | 7/25 | W-14 | 1.30 | 501 |
| Gulch | 8/03 | W2-14 | 0.24 | 516 |
| Banana | 7/25 | W-15 | 1.37 | 244 |
| Gulch | 8/03 | W2-15 | 0.68 | 257 |
| Emerson West | 7/25 | W-16 | 0.60 | 522 |
| Gulch | 8/03 | W2-16 | 0.40 | 514 |
| Sugarloaf | 7/25 | W-17 | 0.26 | 254 |
| Gulch | 8/03 | W2-17 | 0.05 | 264 |
| Long | 7/25 | W-18 | 2.73 | 385 |
| Gulch | 8/03 | W2-18 | 1.38 | 406 |
| Bald | 7/25 | W-19 | 0.73 | 199 |
| Gulch | 8/03 | W2-19 | 0.42 | 205 |
| Bear | 7/25 | W-21 | 0.78 | 206 |
| Gulch | 8/03 | W2-21 | 0.53 | 218 |
| Todd | 7/25 | W-22 | 0.20 | 240 |
| Gulch | 8/03 | W2-22 | 0.16 | 238 |

*7.1.3. Other Water Samples*

| Sample Location | Date Sampled | Sample Name | Discharge (L/sec) | Conductivity (µS/cm) |
|---|---|---|---|---|
| Wood Mine Drainage | 7/25 | WM1 | 0.01 | 1855 |
| | x | x | x | x |
| Firehouse Mine Drainage | 7/25 | FH1 | x | x |
| | 8/03 | FH2 | x | 1271 |
| Upper Emerson Gulch | x | x | x | x |
| | 8/03 | W-14b | x | 270 |
| Middle Emerson Gulch | x | x | x | x |
| | 8/03 | W-14a | x | 467 |

## 7.2. Major Solute Data

Concentrations of major solutes ($Ca^{2+}$, $Mg^{2+}$, $Na^{+}$, $K^{+}$, $Sr^{2+}$, $SO_4^{2-}$, $F^{-}$, $Cl^{-}$, $HCO_3^{-}$, $NO_3^{-}$, and $SiO_2$) for all Fourmile Creek samples, tributary samples, and mine drainage samples. Data for all Fourmile Creek samples and for samples W-06, W2-06, W-07, W2-07, W-10, W2-10, W-13, W2-13, W-14, W2-14, W-15, W2-15, W-18, W2-18, WM1, and WM2 are courtesy of Sheila Murphy, USGS Boulder.

| Sample | $F^-$ | $Cl^-$ | $NO_3^-$ | $SO_4^{2-}$ | $HCO_3^-$ | $Ca^{2+}$ | $K^+$ | $Mg^{2+}$ | $Na^+$ | $SiO_2$ | $Sr^{2+}$ |
|---|---|---|---|---|---|---|---|---|---|---|---|
| | ppm | ppm | ppm | ppm | ppm | ppm | ppm | ppm | ppm | ppm | ppm |
| FCAAG1 | 0.27 | 8.04 | 0.52 | 52.70 | 56.40 | 22.70 | 1.90 | 8.63 | 5.64 | 12.10 | 0.21 |
| FCAAG2 | 0.30 | 8.88 | 0.20 | 54.90 | 66.40 | 25.00 | 1.95 | 9.53 | 6.22 | 12.90 | 0.25 |
| FCAEG1 | 0.19 | 1.48 | <0.02 | 5.50 | 29.50 | 6.08 | 0.61 | 2.51 | 2.38 | 9.20 | 0.08 |
| FCAEG2 | 0.22 | 2.14 | <0.02 | 6.80 | 34.90 | 7.24 | 0.72 | 3.01 | 2.83 | 10.30 | 0.10 |
| FCAMG1 | 0.20 | 2.29 | 0.19 | 15.60 | 37.90 | 10.10 | 0.88 | 4.16 | 3.06 | 10.10 | 0.12 |
| FCAMG2 | 0.24 | 2.67 | 0.03 | 17.00 | 44.30 | 11.10 | 1.00 | 4.67 | 3.60 | 11.00 | 0.15 |
| FCBC1 | 0.27 | 9.03 | 0.55 | 54.90 | 62.90 | 24.70 | 2.02 | 9.25 | 6.36 | 12.50 | 0.23 |
| FCBC2 | 0.32 | 9.49 | 0.14 | 54.40 | 71.40 | 26.10 | 2.25 | 9.78 | 7.06 | 13.20 | 0.26 |
| FCBRes1 | 0.28 | 8.46 | 0.52 | 53.20 | 58.90 | 24.00 | 2.03 | 8.98 | 6.01 | 12.40 | 0.22 |
| FCBRes2 | 0.32 | 9.39 | 0.20 | 54.80 | 69.70 | 25.50 | 2.06 | 9.62 | 6.73 | 12.80 | 0.25 |
| FCCR1 | 0.18 | 1.06 | <0.02 | 2.60 | 21.10 | 3.91 | 0.46 | 1.63 | 1.82 | 8.32 | 0.05 |
| FCCR2 | 0.21 | 1.77 | <0.02 | 3.50 | 25.80 | 4.88 | 0.61 | 2.05 | 2.23 | 9.11 | 0.07 |
| FCGR1 | 0.21 | 2.52 | 0.19 | 17.50 | 42.20 | 11.40 | 1.03 | 4.71 | 3.37 | 10.30 | 0.14 |
| FCGR2 | 0.25 | 3.17 | 0.10 | 19.90 | 50.10 | 12.90 | 1.08 | 5.28 | 3.77 | 11.20 | 0.17 |
| FCLG1 | 0.19 | 1.15 | 0.08 | 3.70 | 22.40 | 4.39 | 0.50 | 1.80 | 2.05 | 8.71 | 0.06 |
| FCLG2 | 0.22 | 1.83 | <0.02 | 5.00 | 27.10 | 5.46 | 0.65 | 2.26 | 2.49 | 9.84 | 0.08 |
| FCLM1 | 0.27 | 7.67 | 0.59 | 53.60 | 56.10 | 22.70 | 1.82 | 8.70 | 5.49 | 12.00 | 0.22 |
| FCLM2 | 0.31 | 8.37 | 0.17 | 55.20 | 65.20 | 25.80 | 2.02 | 9.75 | 6.36 | 13.00 | 0.26 |
| FCWM1 | 0.20 | 1.67 | 0.14 | 11.20 | 32.90 | 7.63 | 0.73 | 3.21 | 2.74 | 9.61 | 0.09 |
| FCWM2 | 0.23 | 2.31 | 0.08 | 10.60 | 38.50 | 8.83 | 0.82 | 3.70 | 3.16 | 10.70 | 0.12 |
| W-02 | 0.50 | 55.10 | 0.16 | 99.08 | 237.10 | 43.70 | 6.25 | 27.18 | 18.40 | 5.78 | 0.38 |
| W-04 | 1.15 | 78.19 | 1.25 | 322.03 | 254.14 | 69.98 | 5.87 | 80.61 | 14.77 | 4.77 | 1.64 |
| W-05 | 0.49 | 27.03 | 1.83 | 44.88 | 177.52 | 64.54 | 6.89 | 19.33 | 3.00 | 13.29 | 0.47 |
| W-06 | 0.53 | 29.30 | 2.82 | 218.00 | 91.90 | 72.90 | 5.32 | 27.10 | 14.10 | 19.90 | 0.48 |
| W-07 | 0.62 | 31.70 | 4.52 | 187.00 | 101.00 | 72.30 | 5.05 | 25.30 | 10.50 | 18.50 | 0.48 |
| W-08 | 0.49 | 3.49 | 0.62 | 153.99 | 5.61 | 43.76 | 3.46 | 15.98 | 1.68 | 12.24 | 0.03 |
| W-09 | 0.52 | 6.82 | 0.91 | 89.72 | 216.08 | 75.29 | 4.87 | 27.15 | 4.10 | 11.81 | 0.97 |
| W-10 | 0.63 | 9.29 | 0.73 | 69.00 | 282.00 | 68.30 | 5.93 | 24.00 | 13.20 | 25.20 | 0.60 |
| W-11 | 0.63 | 4.79 | 4.55 | 91.34 | 155.36 | 66.39 | 5.84 | 17.21 | 3.44 | 13.15 | 1.51 |
| W-12 | 0.41 | 2.18 | 1.26 | 46.62 | 150.71 | 44.83 | 3.99 | 17.90 | 2.56 | 7.09 | 1.07 |
| W-13 | 0.58 | 10.20 | 5.29 | 307.00 | 163.00 | 91.10 | 5.72 | 44.60 | 10.40 | 21.30 | 0.85 |
| W-14 | 0.28 | 6.16 | 3.69 | 152.00 | 108.00 | 51.20 | 3.95 | 22.90 | 8.48 | 21.10 | 0.31 |
| W-14a | 0.26 | 7.15 | 3.78 | 127.21 | 95.29 | 52.38 | 3.83 | 23.67 | 2.80 | 12.00 | 0.22 |
| W-14b | 0.15 | 5.68 | 1.00 | 26.90 | 115.60 | 29.93 | 2.96 | 11.15 | 2.07 | 11.10 | 0.06 |
| W-15 | 0.27 | 3.75 | 0.30 | 31.70 | 105.00 | 25.60 | 3.77 | 9.05 | 5.02 | 17.50 | 0.16 |
| W-16 | 0.93 | 9.75 | 5.14 | 151.56 | 112.13 | 47.89 | 3.21 | 29.06 | 2.88 | 11.02 | 0.15 |
| W-17 | 0.19 | 1.02 | 0.00 | 14.35 | 127.48 | 28.94 | 1.65 | 12.17 | 1.28 | 7.10 | 0.30 |
| W-18 | 0.24 | 3.66 | 0.26 | 43.30 | 197.00 | 42.20 | 2.74 | 17.30 | 7.11 | 20.10 | 0.40 |

| Sample | $F^-$ | $Cl^-$ | $NO_3^-$ | $SO_4^{2-}$ | $HCO_3^-$ | $Ca^{2+}$ | $K^+$ | $Mg^{2+}$ | $Na^+$ | $SiO_2$ | $Sr^{2+}$ |
|---|---|---|---|---|---|---|---|---|---|---|---|
| | ppm | ppm | ppm | ppm | ppm | ppm | ppm | ppm | ppm | ppm | ppm |
| W-19 | 0.12 | 0.49 | 0.00 | 28.67 | 78.78 | 23.26 | 0.95 | 6.82 | 1.57 | 7.85 | 0.06 |
| W2-02 | 0.49 | 55.78 | 0.24 | 102.78 | 234.14 | 43.87 | 6.32 | 27.48 | 18.58 | 5.80 | 0.37 |
| W2-05 | 0.46 | 21.61 | 1.58 | 45.60 | 186.73 | 64.27 | 6.81 | 18.94 | 3.10 | 12.90 | 0.46 |
| W2-06 | 0.61 | 30.60 | 1.07 | 219.00 | 101.00 | 76.20 | 5.14 | 28.90 | 15.30 | 20.10 | 0.50 |
| W2-07 | 0.78 | 38.00 | 1.84 | 203.00 | 107.00 | 79.00 | 4.94 | 27.10 | 12.20 | 17.80 | 0.53 |
| W2-08 | 0.51 | 3.82 | 0.47 | 176.05 | 4.95 | 45.76 | 3.30 | 16.71 | 1.73 | 11.31 | 0.05 |
| W-21 | 0.19 | 0.89 | 1.07 | 9.24 | 112.68 | 22.78 | 1.41 | 9.56 | 1.49 | 8.79 | 0.44 |
| W2-10 | 0.66 | 9.14 | 0.56 | 67.60 | 281.00 | 67.60 | 5.60 | 24.00 | 13.20 | 24.90 | 0.59 |
| W2-11 | 0.56 | 5.10 | 1.83 | 49.25 | 156.36 | 48.99 | 4.98 | 15.00 | 2.54 | 12.83 | 0.87 |
| W2-12 | 0.45 | 2.22 | 1.75 | 52.23 | 153.62 | 42.58 | 3.86 | 16.88 | 2.44 | 6.66 | 1.02 |
| W2-13 | 0.65 | 10.40 | 1.95 | 325.00 | 180.00 | 104.00 | 6.10 | 52.80 | 10.90 | 21.20 | 1.03 |
| W2-14 | 0.32 | 6.31 | 1.28 | 156.00 | 110.00 | 51.50 | 4.00 | 24.10 | 8.74 | 21.10 | 0.32 |
| W2-15 | 0.31 | 4.07 | 0.30 | 26.90 | 113.00 | 26.70 | 3.77 | 9.33 | 5.33 | 17.50 | 0.18 |
| W2-16 | 0.70 | 8.97 | 3.17 | 143.63 | 120.70 | 47.13 | 2.41 | 28.61 | 2.79 | 12.05 | 0.16 |
| W2-17 | 0.18 | 0.83 | 0.29 | 13.64 | 134.66 | 30.03 | 1.68 | 12.55 | 1.31 | 7.21 | 0.31 |
| W2-18 | 0.27 | 4.05 | 0.03 | 28.40 | 221.00 | 43.90 | 2.79 | 18.30 | 7.34 | 20.50 | 0.43 |
| W2-19 | 0.12 | 0.63 | 0.69 | 28.50 | 82.00 | 23.60 | 0.97 | 6.89 | 1.58 | 7.65 | 0.07 |
| W-22 | 0.18 | 19.65 | 0.60 | 10.33 | 91.29 | 33.89 | 1.55 | 10.07 | 2.16 | 11.05 | 1.25 |
| W2-21 | 0.22 | 0.69 | 0.39 | 9.34 | 117.10 | 23.45 | 1.37 | 9.92 | 1.47 | 8.60 | 0.46 |
| W2-22 | 0.14 | 19.77 | 0.52 | 7.90 | 101.31 | 30.55 | 1.32 | 9.00 | 1.94 | 10.17 | 1.16 |
| FH1 | 1.13 | 38.12 | 0.29 | 356.16 | 254.52 | 82.20 | 5.29 | 52.47 | 15.75 | 4.91 | 2.54 |
| FH2 | 1.81 | 37.89 | 0.39 | 327.89 | 260.28 | 79.93 | 5.16 | 53.32 | 14.16 | 4.81 | 2.46 |
| WM1 | 0.78 | 9.91 | 3.00 | 920.00 | 254.00 | 250.00 | 7.50 | 94.20 | 57.90 | 24.20 | 0.01 |
| WM2 | 0.79 | 8.60 | 2.67 | 820.00 | 281.00 | 229.00 | 7.13 | 86.20 | 53.80 | 23.20 | 0.01 |

## 7.3. Charge Balance

Charge balance data for all Fourmile Creek samples, tributary samples, and mine drainage samples.

| Sample | $F^-$ | $Cl^-$ | $NO_3^-$ | $SO_4^{2-}$ | $HCO_3^-$ | $Ca^{2+}$ | $K^+$ | $Mg^{2+}$ | $Na^+$ | $Sr^{2+}$ | Charge Balance |
|---|---|---|---|---|---|---|---|---|---|---|---|
| | meq/L | meq/L | meq/L | meq/L | meq/L | meq/L | meq/L | meq/L | meq/L | meq/L | |
| FCAAG1 | 0.01 | 0.23 | 0.01 | 1.10 | 0.92 | 1.14 | 0.05 | 0.72 | 0.25 | 0.00 | -2.75 |
| FCAAG2 | 0.02 | 0.25 | 0.00 | 1.14 | 1.09 | 1.25 | 0.05 | 0.79 | 0.27 | 0.01 | -2.76 |
| FCAEG1 | 0.01 | 0.04 | 0.00 | 0.11 | 0.48 | 0.30 | 0.02 | 0.21 | 0.10 | 0.00 | -1.27 |
| FCAEG2 | 0.01 | 0.06 | 0.00 | 0.14 | 0.57 | 0.36 | 0.02 | 0.25 | 0.12 | 0.00 | -1.94 |
| FCAMG1 | 0.01 | 0.07 | 0.00 | 0.33 | 0.62 | 0.51 | 0.02 | 0.35 | 0.13 | 0.00 | -0.75 |
| FCAMG2 | 0.01 | 0.08 | 0.00 | 0.35 | 0.73 | 0.56 | 0.03 | 0.39 | 0.16 | 0.00 | -1.74 |
| FCBC1 | 0.01 | 0.26 | 0.01 | 1.14 | 1.03 | 1.24 | 0.05 | 0.77 | 0.28 | 0.01 | -2.43 |
| FCBC2 | 0.02 | 0.27 | 0.00 | 1.13 | 1.17 | 1.31 | 0.06 | 0.82 | 0.31 | 0.01 | -2.04 |
| FCBRes1 | 0.01 | 0.24 | 0.01 | 1.11 | 0.97 | 1.20 | 0.05 | 0.75 | 0.26 | 0.01 | -1.56 |
| FCBRes2 | 0.02 | 0.27 | 0.00 | 1.14 | 1.14 | 1.28 | 0.05 | 0.80 | 0.29 | 0.01 | -2.90 |
| FCCR1 | 0.01 | 0.03 | 0.00 | 0.05 | 0.35 | 0.20 | 0.01 | 0.14 | 0.08 | 0.00 | -1.90 |
| FCCR2 | 0.01 | 0.05 | 0.00 | 0.07 | 0.42 | 0.24 | 0.02 | 0.17 | 0.10 | 0.00 | -2.62 |
| FCGR1 | 0.01 | 0.07 | 0.00 | 0.36 | 0.69 | 0.57 | 0.03 | 0.39 | 0.15 | 0.00 | -0.17 |
| FCGR2 | 0.01 | 0.09 | 0.00 | 0.41 | 0.82 | 0.65 | 0.03 | 0.44 | 0.16 | 0.00 | -2.32 |
| FCLG1 | 0.01 | 0.03 | 0.00 | 0.08 | 0.37 | 0.22 | 0.01 | 0.15 | 0.09 | 0.00 | -1.62 |
| FCLG2 | 0.01 | 0.05 | 0.00 | 0.10 | 0.44 | 0.27 | 0.02 | 0.19 | 0.11 | 0.00 | -2.01 |
| FCLM1 | 0.01 | 0.22 | 0.01 | 1.12 | 0.92 | 1.14 | 0.05 | 0.73 | 0.24 | 0.00 | -2.91 |
| FCLM2 | 0.02 | 0.24 | 0.00 | 1.15 | 1.07 | 1.29 | 0.05 | 0.81 | 0.28 | 0.01 | -0.82 |
| FCWM1 | 0.01 | 0.05 | 0.00 | 0.23 | 0.54 | 0.38 | 0.02 | 0.27 | 0.12 | 0.00 | -2.72 |
| FCWM2 | 0.01 | 0.07 | 0.00 | 0.22 | 0.63 | 0.44 | 0.02 | 0.31 | 0.14 | 0.00 | -1.11 |
| W-02 | 0.03 | 1.57 | 0.00 | 2.06 | 3.89 | 2.19 | 0.16 | 2.26 | 0.80 | 0.01 | -16.46 |
| W-04 | 0.06 | 2.23 | 0.02 | 6.71 | 4.17 | 3.50 | 0.15 | 6.72 | 0.64 | 0.04 | -8.85 |
| W-05 | 0.03 | 0.77 | 0.03 | 0.93 | 2.91 | 3.23 | 0.18 | 1.61 | 0.13 | 0.01 | 4.91 |
| W-06 | 0.03 | 0.84 | 0.05 | 4.54 | 1.51 | 3.65 | 0.14 | 2.26 | 0.61 | 0.01 | -2.17 |
| W-07 | 0.03 | 0.91 | 0.07 | 3.90 | 1.66 | 3.62 | 0.13 | 2.11 | 0.46 | 0.01 | -1.88 |
| W-08 | 0.03 | 0.10 | 0.01 | 3.21 | 0.09 | 2.19 | 0.09 | 1.33 | 0.07 | 0.00 | 3.47 |
| W-09 | 0.03 | 0.19 | 0.01 | 1.87 | 3.54 | 3.76 | 0.12 | 2.26 | 0.18 | 0.02 | 5.86 |
| W-10 | 0.03 | 0.27 | 0.01 | 1.44 | 4.62 | 3.42 | 0.15 | 2.00 | 0.57 | 0.01 | -1.73 |
| W-11 | 0.03 | 0.14 | 0.07 | 1.90 | 2.55 | 3.32 | 0.15 | 1.43 | 0.15 | 0.03 | 4.03 |
| W-12 | 0.02 | 0.06 | 0.02 | 0.97 | 2.47 | 2.24 | 0.10 | 1.49 | 0.11 | 0.02 | 5.65 |
| W-13 | 0.03 | 0.29 | 0.09 | 6.40 | 2.67 | 4.56 | 0.15 | 3.72 | 0.45 | 0.02 | -3.19 |
| W-14 | 0.01 | 0.18 | 0.06 | 3.17 | 1.77 | 2.56 | 0.10 | 1.91 | 0.37 | 0.01 | -2.39 |
| W-14 | 0.02 | 0.18 | 0.04 | 3.04 | 1.87 | 2.81 | 0.11 | 2.24 | 0.12 | 0.01 | 1.46 |
| W-14a | 0.01 | 0.20 | 0.06 | 2.65 | 1.56 | 2.62 | 0.10 | 1.97 | 0.12 | 0.00 | 3.49 |
| W-14b | 0.01 | 0.16 | 0.02 | 0.56 | 1.90 | 1.50 | 0.08 | 0.93 | 0.09 | 0.00 | -0.93 |
| W-15 | 0.01 | 0.11 | 0.00 | 0.66 | 1.72 | 1.28 | 0.10 | 0.75 | 0.22 | 0.00 | -3.19 |
| W-16 | 0.05 | 0.28 | 0.08 | 3.16 | 1.84 | 2.39 | 0.08 | 2.42 | 0.13 | 0.00 | -3.64 |
| W-17 | 0.01 | 0.03 | 0.00 | 0.30 | 2.09 | 1.45 | 0.04 | 1.01 | 0.06 | 0.01 | 2.76 |
| W-18 | 0.01 | 0.10 | 0.00 | 0.90 | 3.23 | 2.11 | 0.07 | 1.44 | 0.31 | 0.01 | -3.82 |
| W-19 | 0.01 | 0.01 | 0.00 | 0.60 | 1.29 | 1.16 | 0.02 | 0.57 | 0.07 | 0.00 | -2.25 |
| W2-02 | 0.03 | 1.59 | 0.00 | 2.14 | 3.84 | 2.19 | 0.16 | 2.29 | 0.81 | 0.01 | -16.39 |
| W2-05 | 0.02 | 0.62 | 0.03 | 0.95 | 3.06 | 3.21 | 0.17 | 1.58 | 0.13 | 0.01 | 4.42 |

| Sample | $F^-$ | $Cl^-$ | $NO_3^-$ | $SO_4^{2-}$ | $HCO_3^-$ | $Ca^{2+}$ | $K^+$ | $Mg^{2+}$ | $Na^+$ | $Sr^{2+}$ | Charge Balance |
|---|---|---|---|---|---|---|---|---|---|---|---|
| | meq/L | meq/L | meq/L | meq/L | meq/L | meq/L | meq/L | meq/L | meq/L | meq/L | |
| W2-06 | 0.03 | 0.87 | 0.02 | 4.56 | 1.66 | 3.81 | 0.13 | 2.41 | 0.67 | 0.01 | -0.81 |
| W2-07 | 0.04 | 1.09 | 0.03 | 4.23 | 1.75 | 3.95 | 0.13 | 2.26 | 0.53 | 0.01 | -1.87 |
| W2-08 | 0.03 | 0.11 | 0.01 | 3.67 | 0.08 | 2.29 | 0.08 | 1.39 | 0.08 | 0.00 | -0.66 |
| W-21 | 0.01 | 0.03 | 0.02 | 0.19 | 1.85 | 1.14 | 0.04 | 0.80 | 0.06 | 0.01 | -1.12 |
| W2-10 | 0.03 | 0.26 | 0.01 | 1.41 | 4.61 | 3.38 | 0.14 | 2.00 | 0.57 | 0.01 | -1.68 |
| W2-11 | 0.03 | 0.15 | 0.03 | 1.03 | 2.56 | 2.45 | 0.13 | 1.25 | 0.11 | 0.02 | 2.11 |
| W2-12 | 0.02 | 0.06 | 0.03 | 1.09 | 2.52 | 2.13 | 0.10 | 1.41 | 0.11 | 0.02 | 0.57 |
| W2-13 | 0.03 | 0.30 | 0.03 | 6.77 | 2.95 | 5.20 | 0.16 | 4.40 | 0.47 | 0.02 | 0.83 |
| W2-14 | 0.02 | 0.18 | 0.02 | 3.25 | 1.80 | 2.58 | 0.10 | 2.01 | 0.38 | 0.01 | -1.91 |
| W2-15 | 0.02 | 0.12 | 0.00 | 0.56 | 1.85 | 1.34 | 0.10 | 0.78 | 0.23 | 0.00 | -2.11 |
| W2-16 | 0.04 | 0.26 | 0.05 | 2.99 | 1.98 | 2.36 | 0.06 | 2.38 | 0.12 | 0.00 | -3.78 |
| W2-17 | 0.01 | 0.02 | 0.00 | 0.28 | 2.21 | 1.50 | 0.04 | 1.05 | 0.06 | 0.01 | 2.43 |
| W2-18 | 0.01 | 0.12 | 0.00 | 0.59 | 3.62 | 2.20 | 0.07 | 1.53 | 0.32 | 0.01 | -2.65 |
| W2-19 | 0.01 | 0.02 | 0.01 | 0.59 | 1.34 | 1.18 | 0.02 | 0.57 | 0.07 | 0.00 | -3.23 |
| W-22 | 0.01 | 0.56 | 0.01 | 0.22 | 1.50 | 1.69 | 0.04 | 0.84 | 0.09 | 0.03 | 8.10 |
| W2-21 | 0.01 | 0.02 | 0.01 | 0.19 | 1.92 | 1.17 | 0.04 | 0.83 | 0.06 | 0.01 | -1.01 |
| W2-22 | 0.01 | 0.56 | 0.01 | 0.16 | 1.66 | 1.53 | 0.03 | 0.75 | 0.08 | 0.03 | 0.34 |
| FH1 | 0.06 | 1.09 | 0.00 | 7.42 | 4.17 | 4.11 | 0.14 | 4.37 | 0.68 | 0.06 | -15.31 |
| FH2 | 0.10 | 1.08 | 0.01 | 6.83 | 4.27 | 4.00 | 0.13 | 4.44 | 0.62 | 0.06 | -14.11 |
| WM1 | 0.04 | 0.28 | 0.05 | 19.17 | 2.66 | 12.50 | 0.19 | 7.85 | 2.52 | 0.00 | 1.90 |
| WM2 | 0.04 | 0.25 | 0.04 | 17.08 | 4.61 | 11.45 | 0.18 | 7.18 | 2.34 | 0.00 | -2.00 |

## 7.4. Mass Flux Calculations

### *7.4.1. Fourmile Creek Intervals*

Data for intervals between adjacent sampling sites along Fourmile Creek, including the length downstream along Fourmile Creek between sampling sites, the names of tributaries that enter between sampling sites, and the total discharge from tributary input between sampling sites.

| Interval along Fourmile Creek | Length (km) | Tributaries Entering | Tributary Discharge Input (L/sec) | |
|---|---|---|---|---|
| | | | 7/25 | 8/03 |
| FCCR - FCLG | 1.84 | Bald | 0.73 | 0.42 |
| FCLG - FCAEG | 1.50 | Long, Sugarloaf, Emerson West | 3.58 | 1.83 |
| FCAEG - FCWM | 0.27 | Banana, Emerson | 2.67 | 0.92 |
| FCWM - FCAMG | 1.28 | Schoolhouse, Wall Street, Melvina West | 2.53 | 1.04 |
| FCAMG - FCGR | 1.70 | Melvina, Melvina East | 0.93 | 0.35 |
| FCGR - FCLM | 1.76 | Gold Run, Schoolhouse | 27.18 | 21.86 |
| FCLM - FCAAG | 1.30 | x | 0.00 | 0.00 |
| FCAAG - FCBRes | 1.89 | Sunbeam, Sand | 0.31 | 0.30 |
| FCBRes- FCBC | 1.46 | x | 0.00 | 0.00 |

### *7.4.2. Mass Flux from Tributaries*

The mass flux in mg/sec was calculated for each major solute in every tributary by multiplying the tributary's discharge by each solute's concentration. This table shows the sum mass flux for tributaries entering between adjacent Fourmile Creek sampling sites.

| Interval along Fourmile Creek | Incoming Mass Flux from Tributaries (mg/sec) | | | | | | | | | | |
|---|---|---|---|---|---|---|---|---|---|---|---|
| | $F^-$ | $Cl^-$ | $NO_3^-$ | $SO_4^{2-}$ | $HCO_3^-$ | $Ca^{2+}$ | $K^+$ | $Mg^{2+}$ | $Na^+$ | $SiO_2$ | $Sr^{2+}$ |
| FCCR1 - FCLG1 | 0.1 | 0.4 | 0.0 | 21.0 | 57.7 | 17.0 | 0.7 | 5.0 | 1.1 | 5.7 | 0.0 |
| FCLG1 - FCAEG1 | 1.3 | 16.1 | 3.8 | 212.7 | 637.2 | 151.3 | 9.7 | 68.7 | 21.4 | 63.2 | 1.3 |
| FCAEG1 - FCWM1 | 0.7 | 13.1 | 5.2 | 240.8 | 284.0 | 101.5 | 10.3 | 42.1 | 17.9 | 51.4 | 0.6 |
| FCWM1 - FCAMG1 | 1.5 | 19.8 | 12.3 | 544.4 | 403.4 | 202.2 | 13.4 | 86.6 | 19.7 | 44.7 | 2.8 |
| FCAMG1 - FCGR1 | 0.5 | 7.6 | 0.6 | 58.2 | 230.1 | 56.9 | 4.8 | 20.1 | 10.5 | 20.2 | 0.5 |
| FCGR1 - FCLM1 | 14.7 | 779.6 | 81.4 | 6140.6 | 2638.1 | 2036.4 | 147.2 | 772.8 | 383.2 | 550.6 | 13.8 |
| FCLM1 - FCAAG1 | 0.0 | 0.0 | 0.0 | 0.0 | 0.0 | 0.0 | 0.0 | 0.0 | 0.0 | 0.0 | 0.0 |
| FCAAG1 - FCBRes1 | 0.2 | 18.5 | 0.1 | 46.0 | 74.0 | 15.3 | 0.9 | 6.0 | 3.0 | 1.7 | 0.2 |
| FCBRes1 - FCBC1 | 0.0 | 0.0 | 0.0 | 0.0 | 0.0 | 0.0 | 0.0 | 0.0 | 0.0 | 0.0 | 0.0 |
| FCCR2 - FCLG2 | 0.0 | 0.3 | 0.3 | 11.9 | 34.1 | 9.8 | 0.4 | 2.9 | 0.7 | 3.2 | 0.0 |
| FCLG2 - FCAEG2 | 0.7 | 9.2 | 1.3 | 97.4 | 360.2 | 81.0 | 4.9 | 37.3 | 11.6 | 33.5 | 0.7 |
| FCAEG2 - FCWM2 | 0.3 | 4.3 | 0.5 | 56.1 | 103.3 | 30.6 | 3.5 | 12.2 | 5.7 | 17.0 | 0.2 |
| FCWM2 - FCAMG2 | 0.6 | 7.1 | 1.9 | 161.7 | 171.2 | 72.1 | 5.4 | 30.9 | 6.0 | 16.0 | 1.0 |
| FCAMG2 - FCGR2 | 0.2 | 3.1 | 0.2 | 25.0 | 96.2 | 24.3 | 1.9 | 8.7 | 4.3 | 8.2 | 0.2 |
| FCGR2 - FCLM2 | 13.4 | 661.2 | 23.8 | 4832.2 | 2240.6 | 1677.7 | 112.8 | 641.6 | 332.9 | 440.1 | 11.1 |
| FCLM2 - FCAAG2 | 0.0 | 0.0 | 0.0 | 0.0 | 0.0 | 0.0 | 0.0 | 0.0 | 0.0 | 0.0 | 0.0 |
| FCAAG2 - FCBRes2 | 0.1 | 17.0 | 0.1 | 31.3 | 71.2 | 13.3 | 0.8 | 4.9 | 2.8 | 1.8 | 0.1 |
| FCBRes2 - FCBC2 | 0.0 | 0.0 | 0.0 | 0.0 | 0.0 | 0.0 | 0.0 | 0.0 | 0.0 | 0.0 | 0.0 |

### *7.4.3. Fourmile Creek Concentration Changes*

Changes in concentration of Fourmile Creek samples downstream between adjacent sampling sites for each major solute.

| Interval along Fourmile Creek | Change in Concentration along Fourmile Creek (ppm) | | | | | | | | | | |
|---|---|---|---|---|---|---|---|---|---|---|---|
| | $F^-$ | $Cl^-$ | $NO_3^-$ | $SO_4^{2-}$ | $HCO_3^-$ | $Ca^{2+}$ | $K^+$ | $Mg^{2+}$ | $Na^+$ | $SiO_2$ | $Sr^{2+}$ |
| FCCR1 - FCLG1 | 0.01 | 0.09 | 0.08 | 1.10 | 1.30 | 0.48 | 0.04 | 0.17 | 0.23 | 0.39 | 0.01 |
| FCLG1 - FCAEG1 | 0.00 | 0.33 | -0.08 | 1.80 | 7.10 | 1.69 | 0.11 | 0.71 | 0.33 | 0.49 | 0.02 |
| FCAEG1 - FCWM1 | 0.01 | 0.19 | 0.14 | 5.70 | 3.40 | 1.55 | 0.12 | 0.70 | 0.36 | 0.41 | 0.01 |
| FCWM1 - FCAMG1 | 0.00 | 0.62 | 0.05 | 4.40 | 5.00 | 2.47 | 0.15 | 0.95 | 0.32 | 0.49 | 0.03 |
| FCAMG1 - FCGR1 | 0.01 | 0.23 | 0.00 | 1.90 | 4.30 | 1.30 | 0.15 | 0.55 | 0.31 | 0.20 | 0.02 |
| FCGR1 - FCLM1 | 0.06 | 5.15 | 0.40 | 36.10 | 13.90 | 11.30 | 0.79 | 3.99 | 2.12 | 1.70 | 0.07 |
| FCLM1 - FCAAG1 | 0.00 | 0.37 | -0.07 | -0.90 | 0.30 | 0.00 | 0.08 | -0.07 | 0.15 | 0.10 | 0.00 |
| FCAAG1 - FCBRes1 | 0.01 | 0.42 | 0.00 | 0.50 | 2.50 | 1.30 | 0.13 | 0.35 | 0.37 | 0.30 | 0.01 |
| FCBRes1 - FCBC1 | -0.01 | 0.57 | 0.03 | 1.70 | 4.00 | 0.70 | -0.01 | 0.27 | 0.35 | 0.10 | 0.01 |
| FCCR2 - FCLG2 | 0.01 | 0.06 | 0.00 | 1.50 | 1.30 | 0.58 | 0.04 | 0.21 | 0.26 | 0.73 | 0.01 |
| FCLG2 - FCAEG2 | 0.00 | 0.31 | 0.00 | 1.80 | 7.80 | 1.78 | 0.07 | 0.75 | 0.34 | 0.46 | 0.02 |
| FCAEG2 - FCWM2 | 0.01 | 0.17 | 0.08 | 3.80 | 3.60 | 1.59 | 0.10 | 0.69 | 0.33 | 0.40 | 0.02 |
| FCWM2 - FCAMG2 | 0.01 | 0.36 | -0.05 | 6.40 | 5.80 | 2.27 | 0.18 | 0.97 | 0.44 | 0.30 | 0.03 |
| FCAMG2 - FCGR2 | 0.01 | 0.50 | 0.07 | 2.90 | 5.80 | 1.80 | 0.08 | 0.61 | 0.17 | 0.20 | 0.02 |
| FCGR2 - FCLM2 | 0.06 | 5.20 | 0.07 | 35.30 | 15.10 | 12.90 | 0.94 | 4.47 | 2.59 | 1.80 | 0.09 |
| FCLM2 - FCAAG2 | -0.01 | 0.51 | 0.03 | -0.30 | 1.20 | -0.80 | -0.07 | -0.22 | -0.14 | -0.10 | -0.01 |
| FCAAG2 - FCBRes2 | 0.02 | 0.51 | 0.00 | -0.10 | 3.30 | 0.50 | 0.11 | 0.09 | 0.51 | -0.10 | 0.00 |
| FCBRes2 - FCBC2 | 0.00 | 0.10 | -0.06 | -0.40 | 1.70 | 0.60 | 0.19 | 0.16 | 0.33 | 0.40 | 0.00 |

## 7.5. Isotope Data

Oxygen and hydrogen isotope data for all Fourmile Creek samples, tributary samples, and mine drainage samples.

| Sample | $\delta^{18}O$ | $\delta^{2}H$ | | Sample | $\delta^{18}O$ | $\delta^{2}H$ |
|---|---|---|---|---|---|---|
| FCAAG1 | -16.16 | -138.10 | | W-13 | -14.20 | -117.37 |
| FCAAG2 | -14.25 | -129.03 | | W-14 | -14.62 | -118.15 |
| FCAEG1 | -17.46 | -141.64 | | W-14a | -13.77 | -117.31 |
| FCAEG2 | -16.56 | -135.12 | | W-14b | -14.61 | -120.65 |
| FCAMG1 | -16.48 | -139.06 | | W-15 | -14.34 | -117.85 |
| FCAMG2 | -16.93 | -135.77 | | W-16 | -14.62 | -118.16 |
| FCBC1 | -16.40 | -135.54 | | W-17 | -14.61 | -113.44 |
| FCBC2 | -16.01 | -131.59 | | W-18 | -13.94 | -118.45 |
| FCBRes1 | -16.27 | -133.45 | | W-19 | -14.89 | -120.63 |
| FCBRes2 | -14.71 | -142.72 | | W2-02 | -13.65 | -110.47 |
| FCCR1 | -17.31 | -141.91 | | W2-05 | -14.18 | -115.12 |
| FCCR2 | -16.87 | -137.18 | | W2-06 | -13.54 | -120.31 |
| FCGR1 | -16.77 | -137.73 | | W2-07 | -14.09 | -113.25 |
| FCGR2 | -16.54 | -136.08 | | W2-08 | -14.09 | -112.75 |
| FCLG1 | -17.47 | -141.49 | | W-21 | -14.13 | -116.57 |
| FCLG2 | -16.64 | -140.47 | | W2-10 | -13.30 | -126.26 |
| FCLM1 | -16.36 | -136.83 | | W2-11 | -14.58 | -117.89 |
| FCLM2 | -16.02 | -133.42 | | W2-12 | -14.90 | -122.13 |
| FCWM1 | -17.03 | -138.27 | | W2-13 | -14.16 | -117.73 |
| FCWM2 | -16.79 | -138.94 | | W2-14 | -13.85 | -118.25 |
| W-02 | -13.67 | -112.20 | | W2-15 | -14.54 | -119.14 |
| W-04 | -13.98 | -113.87 | | W2-16 | -14.93 | -119.00 |
| W-05 | -14.29 | -115.69 | | W2-17 | -14.28 | -113.08 |
| W-06 | -14.04 | -115.56 | | W2-18 | -14.46 | -120.97 |
| W-07 | -13.72 | -111.37 | | W2-19 | -14.87 | -120.38 |
| W-08 | -14.22 | -113.53 | | W-22 | -15.00 | -120.17 |
| W-09 | -14.58 | -116.86 | | W2-21 | -14.42 | -116.49 |
| W-10 | -13.29 | -122.63 | | W2-22 | -14.88 | -120.15 |
| W-11 | -14.45 | -116.84 | | FH1 | -14.81 | -120.24 |
| W-12 | -15.40 | -116.91 | | FH2 | -14.74 | -118.38 |

# 7.6. Trace Element Data

## *7.6.1. Amherst Samples*

Trace element data for all samples run at Amherst using ICP-MS, including many tributary samples and Firehouse mine drainage (b.d.l. = below detection limit). The detection limit was calculated by tripling the absolute value of the measured concentration of each element in the blank standard.

| Sample | Ag | Al | As | Ba | Be | Bi | Cd | Co | Cr |
|---|---|---|---|---|---|---|---|---|---|
| | ppb | ppb | ppb | ppb | ppb | ppb | ppb | ppb | ppb |
| FH1 | 0.071 | 4.998 | 18.680 | 24.760 | b.d.l. | b.d.l. | b.d.l. | 1.690 | 0.691 |
| FH2 | b.d.l. | 78.140 | 7.009 | 86.020 | b.d.l. | b.d.l. | b.d.l. | 0.197 | b.d.l. |
| W-02 | b.d.l. | 25.920 | 5.840 | 100.200 | b.d.l. | b.d.l. | b.d.l. | 0.222 | 0.497 |
| W-04 | 0.137 | 56.250 | 6.375 | 119.100 | b.d.l. | b.d.l. | 0.113 | 0.134 | 1.056 |
| W-05 | b.d.l. | 7.899 | 6.985 | 19.800 | b.d.l. | b.d.l. | 0.525 | 0.117 | 1.265 |
| W-07 | 0.078 | 40.710 | 14.410 | 35.230 | b.d.l. | b.d.l. | b.d.l. | 1.066 | b.d.l. |
| W-08 | 0.086 | 615.500 | 1.320 | 41.810 | b.d.l. | b.d.l. | 4.464 | 3.460 | 1.008 |
| W-09 | b.d.l. | 20.850 | 0.606 | 79.070 | b.d.l. | b.d.l. | b.d.l. | 0.351 | b.d.l. |
| W-11 | 0.216 | 43.450 | 3.376 | 142.200 | b.d.l. | b.d.l. | b.d.l. | 0.114 | b.d.l. |
| W-12 | 0.196 | 96.180 | 0.850 | 62.930 | b.d.l. | b.d.l. | b.d.l. | 0.162 | 0.492 |
| W-14 | 0.210 | 61.230 | 5.314 | 90.750 | b.d.l. | b.d.l. | b.d.l. | 0.277 | 0.423 |
| W-14a | b.d.l. | 32.410 | 4.637 | 96.980 | b.d.l. | b.d.l. | b.d.l. | 0.456 | b.d.l. |
| W-14b | 0.328 | 24.760 | 1.158 | 79.780 | b.d.l. | b.d.l. | b.d.l. | 0.288 | 0.538 |
| W-16 | 0.119 | 106.500 | 3.724 | 28.570 | b.d.l. | b.d.l. | b.d.l. | 0.177 | b.d.l. |
| W-17 | b.d.l. | 22.100 | b.d.l. | 145.100 | b.d.l. | b.d.l. | b.d.l. | 0.050 | b.d.l. |
| W-19 | b.d.l. | 55.270 | b.d.l. | 34.060 | b.d.l. | b.d.l. | b.d.l. | 0.374 | b.d.l. |
| W2-02 | b.d.l. | 39.950 | 7.875 | 89.000 | b.d.l. | b.d.l. | 0.172 | 0.215 | 0.623 |
| W2-05 | b.d.l. | 4.486 | 20.490 | 115.000 | b.d.l. | b.d.l. | b.d.l. | 0.314 | 0.798 |
| W2-08 | b.d.l. | 95.320 | 1.043 | 22.150 | 0.218 | b.d.l. | 3.495 | 3.568 | 1.130 |
| W-21 | b.d.l. | 21.170 | b.d.l. | 195.700 | b.d.l. | b.d.l. | b.d.l. | 0.088 | b.d.l. |
| W2-11 | b.d.l. | 7.443 | 2.358 | 94.100 | b.d.l. | b.d.l. | b.d.l. | 0.275 | b.d.l. |
| W2-12 | b.d.l. | 2.487 | 0.657 | 58.450 | b.d.l. | b.d.l. | b.d.l. | b.d.l. | b.d.l. |
| W2-16 | b.d.l. | 23.250 | 0.894 | 26.530 | b.d.l. | b.d.l. | 0.214 | 0.116 | b.d.l. |
| W2-17 | b.d.l. | 3.147 | b.d.l. | 150.500 | b.d.l. | b.d.l. | b.d.l. | 0.022 | b.d.l. |
| W2-19 | b.d.l. | 4.489 | b.d.l. | 34.120 | b.d.l. | b.d.l. | b.d.l. | 0.037 | b.d.l. |
| W-22 | b.d.l. | 128.000 | 0.623 | 181.700 | b.d.l. | b.d.l. | b.d.l. | 0.150 | 0.591 |
| W2-21 | b.d.l. | 3.355 | b.d.l. | 200.000 | b.d.l. | b.d.l. | b.d.l. | b.d.l. | b.d.l. |
| W2-22 | 0.152 | 113.600 | b.d.l. | 158.000 | b.d.l. | b.d.l. | b.d.l. | 0.228 | 0.359 |
| | | | | | | | | | |
| **Detection Limit (ppb)** | 0.063 | 0.941 | 0.493 | 0.146 | 0.196 | 0.332 | 0.088 | 0.020 | 0.280 |

| Sample | Cs | Cu | Fe | Ga | In | Li | Mn | Ni |
|---|---|---|---|---|---|---|---|---|
| | ppb | ppb | ppb | ppb | ppb | ppb | ppb | ppb |
| FH1 | b.d.l. | 10.33 | 53.87 | 9.68 | b.d.l. | 17.2 | 212.5 | 7.296 |
| FH2 | b.d.l. | 1.21 | 33.03 | 5.394 | b.d.l. | 16.04 | 257.5 | 6.976 |
| W-02 | b.d.l. | 11.31 | 35.63 | 19.7 | b.d.l. | 39.92 | 6.331 | 4.063 |
| W-04 | b.d.l. | 7.09 | 15.36 | 21.41 | b.d.l. | 13.3 | 92.39 | 1.08 |
| W-05 | b.d.l. | 17.91 | 122 | 27.8 | b.d.l. | 4.489 | 13.31 | 0.6998 |
| W-07 | b.d.l. | 2.271 | 4.297 | 4.611 | b.d.l. | 3.445 | 44.22 | 3.631 |
| W-08 | b.d.l. | 56.97 | 896.4 | 10.53 | b.d.l. | 5.399 | 1364 | 15.75 |
| W-09 | b.d.l. | 5.922 | 16.12 | 19.88 | b.d.l. | 4.821 | 18.27 | b.d.l. |
| W-11 | b.d.l. | 2.598 | 32.01 | 33.16 | b.d.l. | 3.801 | 0.8426 | 0.7276 |
| W-12 | b.d.l. | 15.32 | 98.94 | 15.27 | b.d.l. | 2.929 | 4.056 | b.d.l. |
| W-14 | b.d.l. | 30.45 | 144.9 | 21.6 | b.d.l. | 3.252 | 64.34 | 0.8108 |
| W-14a | b.d.l. | 19.73 | 81.75 | 22.52 | b.d.l. | 3.454 | 231.3 | 0.9015 |
| W-14b | b.d.l. | 40.62 | 189.5 | 18.61 | b.d.l. | 2.053 | 170.5 | 0.9181 |
| W-16 | b.d.l. | 25.8 | 310.3 | 6.631 | b.d.l. | 2.548 | 11.9 | 3.336 |
| W-17 | b.d.l. | 5.316 | 9.031 | 34.88 | b.d.l. | 1.258 | 2.218 | b.d.l. |
| W-19 | b.d.l. | 7.858 | 42.71 | 8.232 | b.d.l. | 0.5919 | 1.212 | b.d.l. |
| W2-02 | b.d.l. | 3.068 | 9.13 | 21 | b.d.l. | 52.52 | 13.82 | 4.319 |
| W2-05 | b.d.l. | 1.006 | 25.23 | 27.48 | b.d.l. | 4.558 | 76.19 | b.d.l. |
| W2-08 | b.d.l. | 14.62 | 12.41 | 5.332 | b.d.l. | 4.878 | 1369 | 14.17 |
| W-21 | b.d.l. | 10.35 | 26.93 | 48.52 | b.d.l. | 1.01 | 4.721 | b.d.l. |
| W2-11 | b.d.l. | 0.9366 | 11.24 | 22.36 | b.d.l. | 2.489 | 79.41 | b.d.l. |
| W2-12 | b.d.l. | 1.623 | 3.182 | 13.64 | b.d.l. | 2.58 | 1.597 | b.d.l. |
| W2-16 | b.d.l. | 0.9767 | 8.837 | 6.202 | b.d.l. | 2.931 | 147.1 | 9.372 |
| W2-17 | b.d.l. | 1.06 | 3.22 | 35.49 | b.d.l. | 1.241 | b.d.l. | b.d.l. |
| W2-19 | b.d.l. | 1.798 | 5.473 | 8.407 | b.d.l. | 0.5808 | b.d.l. | b.d.l. |
| W-22 | b.d.l. | 9.503 | 161.7 | 45.63 | b.d.l. | 1.911 | 3.422 | 0.8209 |
| W2-21 | b.d.l. | 1.808 | 5.25 | 49.7 | b.d.l. | 1.024 | b.d.l. | b.d.l. |
| W2-22 | b.d.l. | 28.58 | 159 | 40.58 | b.d.l. | 1.589 | 24.8 | b.d.l. |
| | | | | | | | | |
| **Detection Limit (ppb)** | 0.5217 | 0.8955 | 0.4563 | 0.25446 | 0.3549 | 0.023433 | 0.7071 | 0.6243 |

| Sample | Pb | Rb | Se | Sr | Tl | U | V | Zn |
|---|---|---|---|---|---|---|---|---|
| | ppb | ppb | ppb | ppb | ppb | ppb | ppb | ppb |
| FH1 | 1.619 | 12.18 | 0.553 | 4325 | b.d.l. | 16.98 | b.d.l. | 5.076 |
| FH2 | b.d.l. | 12.7 | 0.4428 | 4139 | b.d.l. | 17.2 | b.d.l. | 10.07 |
| W-02 | 0.574 | 6.023 | b.d.l. | 767.7 | b.d.l. | 14.4 | 0.5999 | 3.281 |
| W-04 | 2.126 | 5.165 | b.d.l. | 2523 | b.d.l. | 33.91 | 1.177 | 5.565 |
| W-05 | 0.54 | 2.83 | b.d.l. | 448.9 | b.d.l. | 8.365 | 1.053 | 11.54 |
| W-07 | b.d.l. | 5.703 | b.d.l. | 585.1 | b.d.l. | 2.02 | b.d.l. | 68.9 |
| W-08 | 1.702 | 3.523 | b.d.l. | 185.3 | b.d.l. | 0.9847 | 0.7813 | 1225 |
| W-09 | b.d.l. | 0.9777 | b.d.l. | 792.8 | b.d.l. | 4.113 | 1.649 | 1.643 |
| W-11 | b.d.l. | 1.18 | b.d.l. | 1186 | b.d.l. | 2.915 | 2.04 | 1.558 |
| W-12 | 0.5546 | 2.494 | b.d.l. | 833.4 | b.d.l. | 5.939 | 0.991 | 3.492 |
| W-14 | 1.964 | 1.765 | b.d.l. | 341.4 | b.d.l. | 1.304 | 0.4896 | 4.362 |
| W-14a | 0.6831 | 1.024 | b.d.l. | 302.6 | b.d.l. | 0.5563 | b.d.l. | 9.715 |
| W-14b | 0.7633 | 0.6927 | b.d.l. | 206.7 | b.d.l. | 0.2525 | b.d.l. | 7.768 |
| W-16 | 1.622 | 2.543 | b.d.l. | 264 | b.d.l. | 3.818 | b.d.l. | 9.397 |
| W-17 | b.d.l. | b.d.l. | b.d.l. | 337.3 | b.d.l. | 2.277 | b.d.l. | b.d.l. |
| W-19 | 0.4255 | b.d.l. | b.d.l. | 210.3 | b.d.l. | 0.1342 | b.d.l. | 1.515 |
| W2-02 | b.d.l. | 6.768 | b.d.l. | 790.3 | b.d.l. | 16.37 | 0.6576 | 10.56 |
| W2-05 | b.d.l. | 2.602 | b.d.l. | 440.5 | b.d.l. | 5.023 | 0.8619 | 9.832 |
| W2-08 | b.d.l. | 2.709 | b.d.l. | 186.7 | b.d.l. | 0.9389 | b.d.l. | 973.4 |
| W-21 | b.d.l. | b.d.l. | b.d.l. | 424.3 | b.d.l. | 1.222 | b.d.l. | 5.629 |
| W2-11 | b.d.l. | b.d.l. | b.d.l. | 676.9 | b.d.l. | 1.788 | 0.7098 | 4.86 |
| W2-12 | b.d.l. | 2.252 | b.d.l. | 783.1 | b.d.l. | 4.754 | 0.7428 | 8.678 |
| W2-16 | b.d.l. | 1.655 | b.d.l. | 262 | b.d.l. | 2.138 | b.d.l. | 34.78 |
| W2-17 | b.d.l. | b.d.l. | b.d.l. | 349.8 | b.d.l. | 2.221 | b.d.l. | 5.282 |
| W2-19 | b.d.l. | b.d.l. | b.d.l. | 211.2 | b.d.l. | 0.1394 | b.d.l. | 2.38 |
| W-22 | 0.83 | b.d.l. | b.d.l. | 947.7 | b.d.l. | 0.7943 | b.d.l. | 7.033 |
| W2-21 | b.d.l. | b.d.l. | b.d.l. | 429.4 | b.d.l. | 1.399 | b.d.l. | 3.888 |
| W2-22 | 5.14 | b.d.l. | b.d.l. | 913.4 | b.d.l. | 1.066 | b.d.l. | 9.826 |
| | | | | | | | | |
| **Detection Limit (ppb)** | 0.3663 | 0.6774 | 0.4221 | 0.07986 | 0.27798 | 0.08331 | 0.3657 | 1.248 |

### *7.6.2. USGS Samples*

Select trace element data for all samples run by the USGS in Boulder using ICP-AES, including all Fourmile samples, some tributary samples, and Wood Mine drainage.

| Sample | Al | B | Ba | Fe | Mn | Zn |
|---|---|---|---|---|---|---|
| | ppm | ppm | ppm | ppm | ppm | ppm |
| FCAAG1 | 0.009 | 0.013 | 0.032 | 0.014 | 0.072 | 0.007 |
| FCAAG2 | 0.007 | 0.014 | 0.037 | 0.027 | 0.093 | 0.008 |
| FCAEG1 | 0.010 | <0.007 | 0.021 | 0.021 | 0.009 | 0.002 |
| FCAEG2 | 0.007 | <0.007 | 0.025 | 0.020 | 0.010 | 0.002 |
| FCAMG1 | 0.004 | <0.007 | 0.027 | 0.017 | 0.031 | 0.003 |
| FCAMG2 | 0.004 | <0.007 | 0.032 | 0.031 | 0.045 | 0.002 |
| FCBC1 | 0.015 | 0.015 | 0.031 | 0.009 | 0.049 | 0.005 |
| FCBC2 | 0.012 | 0.018 | 0.034 | 0.012 | 0.027 | 0.004 |
| FCBRes1 | 0.010 | 0.014 | 0.031 | 0.008 | 0.058 | 0.006 |
| FCBRes2 | 0.009 | 0.013 | 0.036 | 0.017 | 0.072 | 0.006 |
| FCCR1 | 0.028 | <0.007 | 0.016 | 0.039 | 0.004 | 0.001 |
| FCCR2 | 0.012 | <0.007 | 0.020 | 0.029 | 0.005 | 0.002 |
| FCGR2 | 0.006 | <0.007 | 0.029 | 0.018 | 0.027 | 0.002 |
| FCGR2 | 0.004 | <0.007 | 0.034 | 0.034 | 0.036 | 0.002 |
| FCLG1 | 0.020 | <0.007 | 0.016 | 0.029 | 0.002 | <0.001 |
| FCLG2 | 0.012 | <0.007 | 0.020 | 0.022 | 0.001 | 0.002 |
| FCLM1 | 0.010 | 0.011 | 0.033 | 0.017 | 0.093 | 0.015 |
| FCLM2 | 0.007 | 0.014 | 0.039 | 0.032 | 0.117 | 0.012 |
| FCWM1 | 0.005 | <0.007 | 0.024 | 0.016 | 0.012 | 0.002 |
| FCWM2 | 0.007 | <0.007 | 0.028 | 0.017 | 0.011 | 0.002 |
| W-06 | 0.004 | 0.043 | 0.047 | 0.004 | 0.255 | 0.145 |
| W-07 | <0.003 | 0.040 | 0.034 | 0.003 | 0.033 | 0.040 |
| W-10 | <0.003 | 0.033 | 0.104 | 0.016 | 0.097 | 0.004 |
| W-13 | <0.003 | 0.025 | 0.051 | 0.003 | 0.076 | 0.008 |
| W-14 | <0.003 | 0.022 | 0.087 | 0.026 | 0.150 | 0.005 |
| W-15 | 0.003 | 0.018 | 0.085 | 0.006 | <0.001 | 0.003 |
| W-18 | <0.003 | 0.015 | 0.119 | 0.092 | 0.588 | 0.004 |
| W2-06 | 0.006 | 0.044 | 0.041 | 0.006 | 0.252 | 0.134 |
| W2-07 | <0.003 | 0.040 | 0.019 | 0.004 | 0.044 | 0.050 |
| W2-10 | 0.004 | 0.031 | 0.100 | 0.015 | 0.084 | 0.004 |
| W2-13 | <0.003 | 0.028 | 0.052 | 0.006 | 0.075 | 0.004 |
| W2-14 | 0.006 | 0.022 | 0.080 | 0.019 | 0.037 | 0.004 |
| W2-15 | 0.004 | 0.018 | 0.085 | 0.006 | 0.002 | 0.003 |
| W2-18 | <0.003 | 0.015 | 0.123 | 0.010 | 0.715 | 0.004 |
| WM1 | <0.003 | 0.031 | 0.012 | 0.003 | 0.013 | 0.006 |

# 7.7. Sediment Data

## *7.7.1. Sampling Sites*

Names, locations, and dates of collection for all sediment samples. Samples denoted HWS are flood deposit samples, and those denoted S are streambed sediment samples. See Figure 2.2b for a map of all sediment sample locations.

| Sample Name | Location | Date Collected |
|---|---|---|
| HWS-01 | Fourmile Creek downstream of Sweet Home (FCASH) | 8/01 |
| HWS-02 | Fourmile Creek below Resevoir (FCBRes) | 8/01 |
| HWS-03 | Fourmile Creek at mouth of Arkansas (FCAAG) | 8/01 |
| HWS-04 | Fourmile Creek at Logan Mill (FCLM) | 8/01 |
| HWS-05 | Gold Run | 8/01 |
| HWS-06 | Fourmile Creek upstream of Gold Run (FCAGR) | 8/01 |
| HWS-07 | Melvina Gulch | 8/01 |
| HWS-08 | Fourmile Creek upstream of Wood Mine (FCWM) | 8/01 |
| HWS-09 | Emerson Gulch | 8/01 |
| HWS-10 | Upper Emerson Gulch | 8/01 |
| HWS-11 | Long Gulch | 8/01 |
| S-01 | Dry Gulch | 8/01 |
| S-02 | Sand Gulch | 7/27 |
| S-03 | Arkansas Gulch | 8/01 |
| S-04 | Sunbeam Gulch | 7/27 |
| S-05 | Sweet Home Gulch | 7/27 |
| S-06 | Gold Run | 7/27 |
| S-08 | Black Hawk Gulch | 7/27 |
| S-09 | Melvina East Gulch | 7/27 |
| S-10 | Melvina Gulch | 7/27 |
| S-11 | Melvina West Gulch | 7/27 |
| S-12 | Wall Street | 7/27 |
| S-13 | Schoolhouse Gulch | 7/27 |
| S-14 | Emerson Gulch | 7/27 |
| S-15 | Banana Gulch | 7/27 |
| S-17 | Sugarloaf Gulch | 7/27 |
| S-18 | Long Gulch | 7/27 |
| S-19 | Bald Gulch | 7/27 |
| S-20 | Potato Gulch | 7/27 |
| S-21 | Bear Gulch | 7/27 |
| S-22 | Todd Gulch | 7/27 |

## *7.7.2. Major Oxides*

Percentages of major oxides in sediment samples, determined using XRF.

| Sample | $SiO_2$ | $TiO_2$ | $Al_2O_3$ | $Fe_2O_3$ | MnO | MgO | CaO | $Na_2O$ | $K_2O$ | $P_2O_5$ | Total % |
|---|---|---|---|---|---|---|---|---|---|---|---|
| | % | % | % | % | % | % | % | % | % | % | |
| HWS-01 | 65.54 | 0.91 | 15.30 | 6.19 | 0.11 | 2.19 | 2.64 | 2.49 | 3.90 | 0.46 | 99.72 |
| HWS-02 | 60.48 | 1.24 | 16.45 | 8.27 | 0.20 | 3.32 | 3.01 | 1.92 | 4.13 | 0.50 | 99.53 |
| HWS-03 | 60.34 | 1.23 | 16.69 | 8.29 | 0.18 | 3.33 | 2.99 | 2.18 | 4.27 | 0.53 | 100.02 |
| HWS-04 | 60.88 | 1.15 | 16.60 | 7.81 | 0.16 | 3.26 | 3.00 | 2.26 | 4.12 | 0.52 | 99.75 |
| HWS-05 | 65.59 | 0.88 | 15.52 | 5.81 | 0.10 | 2.04 | 3.08 | 2.74 | 3.51 | 0.47 | 99.76 |
| HWS-06 | 62.68 | 1.08 | 16.44 | 7.33 | 0.14 | 2.62 | 2.95 | 2.47 | 3.79 | 0.50 | 100.01 |
| HWS-07 | 68.34 | 0.48 | 16.41 | 3.81 | 0.05 | 1.29 | 2.76 | 3.58 | 3.11 | 0.21 | 100.04 |
| HWS-08 | 58.21 | 1.32 | 17.17 | 8.78 | 0.12 | 4.06 | 3.66 | 2.44 | 3.69 | 0.38 | 99.83 |
| HWS-09 | 56.34 | 1.27 | 20.71 | 9.71 | 0.29 | 2.69 | 2.40 | 1.15 | 4.74 | 0.40 | 99.70 |
| HWS-10 | 75.99 | 0.46 | 13.05 | 3.66 | 0.05 | 0.72 | 0.66 | 1.37 | 3.97 | 0.10 | 100.02 |
| HWS-11 | 69.29 | 0.75 | 15.78 | 5.43 | 0.06 | 1.39 | 1.40 | 1.73 | 4.03 | 0.17 | 100.02 |
| S-01 | 73.25 | 0.29 | 13.87 | 3.00 | 0.04 | 0.71 | 1.42 | 2.46 | 4.35 | 0.14 | 99.52 |
| S-02 | 67.79 | 0.62 | 14.65 | 5.67 | 0.11 | 1.85 | 2.55 | 2.49 | 3.53 | 0.28 | 99.54 |
| S-03 | 71.94 | 0.23 | 15.35 | 2.13 | 0.04 | 0.68 | 1.73 | 3.37 | 3.94 | 0.12 | 99.52 |
| S-04 | 73.95 | 0.40 | 12.96 | 3.49 | 0.06 | 1.15 | 2.26 | 2.71 | 3.48 | 0.18 | 100.63 |
| S-05 | 70.80 | 0.36 | 14.85 | 3.60 | 0.04 | 1.09 | 2.36 | 2.78 | 3.54 | 0.21 | 99.62 |
| S-06 | 67.77 | 0.62 | 15.84 | 4.37 | 0.08 | 1.59 | 2.69 | 2.89 | 3.71 | 0.29 | 99.85 |
| S-08 | 73.67 | 0.29 | 14.55 | 2.57 | 0.15 | 0.76 | 1.77 | 2.37 | 3.97 | 0.12 | 100.21 |
| S-09 | 68.10 | 0.41 | 16.07 | 4.18 | 0.06 | 1.37 | 2.85 | 3.34 | 3.49 | 0.22 | 100.08 |
| S-10 | 70.19 | 0.36 | 15.45 | 4.01 | 0.04 | 0.93 | 2.21 | 3.17 | 3.34 | 0.17 | 99.87 |
| S-11 | 68.77 | 0.51 | 16.20 | 3.71 | 0.06 | 1.33 | 2.96 | 3.22 | 3.18 | 0.24 | 100.16 |
| S-12 | 69.95 | 0.58 | 14.69 | 4.64 | 0.05 | 1.43 | 2.35 | 2.19 | 3.61 | 0.35 | 99.84 |
| S-13 | 70.58 | 0.43 | 15.17 | 3.02 | 0.06 | 1.06 | 2.80 | 2.75 | 2.86 | 0.24 | 98.97 |
| S-14 | 68.79 | 0.65 | 15.94 | 4.83 | 0.08 | 1.49 | 2.21 | 2.05 | 3.80 | 0.21 | 100.06 |
| S-15 | 67.26 | 0.53 | 16.32 | 4.29 | 0.06 | 1.91 | 3.66 | 3.41 | 2.40 | 0.17 | 100.02 |
| S-17 | 70.63 | 0.62 | 14.49 | 5.20 | 0.06 | 1.28 | 1.52 | 1.83 | 3.94 | 0.18 | 99.75 |
| S-18 | 75.33 | 0.46 | 13.50 | 3.68 | 0.04 | 0.81 | 0.87 | 1.54 | 4.46 | 0.11 | 100.80 |
| S-19 | 67.34 | 0.69 | 16.64 | 6.49 | 0.07 | 1.39 | 1.81 | 1.47 | 3.70 | 0.22 | 99.83 |
| S-20 | 72.27 | 0.56 | 14.83 | 4.89 | 0.05 | 0.85 | 0.55 | 1.90 | 4.14 | 0.12 | 100.15 |
| S-21 | 69.32 | 0.69 | 16.08 | 6.37 | 0.06 | 1.02 | 0.63 | 1.47 | 3.77 | 0.10 | 99.50 |
| S-22 | 76.65 | 0.34 | 13.39 | 2.64 | 0.05 | 0.25 | 0.46 | 2.62 | 3.70 | 0.09 | 100.19 |

### *7.7.3. Carbon, Nitrogen, and Mercury*

EA data for weight % carbon and weight % nitrogen were used to calculate C:N ratios. Mercury data from Hyrda-C mercury analysis and EA data for weight % carbon were used to calculate Hg:C ratios.

| Sample | LOI (%) | Wt % C | Wt % N | C : N | Hg (ppb) | Hg : C (ppb/wt %) |
|---|---|---|---|---|---|---|
| HWS-01 | 1.81 | 0.68 | 0.05 | 13.60 | 47 | 69.12 |
| HWS-02 | 9.72 | 5.83 | 0.24 | 24.29 | 154 | 26.42 |
| HWS-03 | 7.50 | 4.52 | 0.23 | 19.65 | 152 | 33.63 |
| HWS-04 | 4.91 | 2.74 | 0.13 | 21.08 | 85 | 31.02 |
| HWS-05 | 2.81 | 0.77 | 0.06 | 12.83 | 48 | 62.34 |
| HWS-06 | 3.36 | 1.94 | 0.11 | 17.64 | 90 | 46.39 |
| HWS-07 | 1.33 | 0.41 | 0.03 | 13.67 | 6 | 14.63 |
| HWS-08 | 3.95 | 1.07 | 0.09 | 11.89 | 33 | 30.84 |
| HWS-09 | 20.66 | 12.78 | 0.67 | 19.07 | 257 | 20.11 |
| HWS-10 | 1.63 | 0.81 | 0.06 | 13.50 | 10 | 12.35 |
| HWS-11 | 2.62 | 0.88 | 0.06 | 14.67 | 16 | 18.18 |
| S-01 | 1.84 | 0.57 | 0.02 | 28.50 | 11 | 19.30 |
| S-02 | 5.18 | 1.84 | 0.09 | 20.44 | 7 | 3.80 |
| S-03 | 1.41 | 0.71 | 0.02 | 35.50 | 9 | 12.68 |
| S-04 | 0.80 | 0.16 | 0.02 | 8.00 | 8 | 50.00 |
| S-05 | 1.12 | 0.44 | 0.03 | 14.67 | 16 | 36.36 |
| S-06 | 1.04 | 0.20 | 0.00 | x | 102 | 510.00 |
| S-08 | 2.84 | 0.43 | 0.00 | x | 72 | 167.44 |
| S-09 | 3.65 | 1.74 | 0.10 | 17.40 | 23 | 13.22 |
| S-10 | 0.78 | 0.29 | 0.01 | 29.00 | 11 | 37.93 |
| S-11 | 1.57 | 0.71 | 0.07 | 10.14 | 21 | 29.58 |
| S-12 | 3.29 | 1.25 | 0.05 | 25.00 | 63 | 50.40 |
| S-13 | 1.00 | 0.14 | 0.02 | 7.00 | 30 | 214.29 |
| S-14 | 5.67 | 1.31 | 0.11 | 11.91 | 141 | 107.63 |
| S-15 | 0.97 | 0.22 | 0.01 | 22.00 | 6 | 27.27 |
| S-17 | 8.50 | 5.92 | 0.30 | 19.73 | 41 | 6.93 |
| S-18 | 1.50 | 0.43 | 0.04 | 10.75 | 8 | 18.60 |
| S-19 | 16.12 | 8.47 | 0.54 | 15.69 | 191 | 22.55 |
| S-20 | 3.18 | 1.63 | 0.08 | 20.38 | 45 | 27.61 |
| S-21 | 7.75 | 5.44 | 0.26 | 20.92 | 43 | 7.90 |
| S-22 | 8.10 | 0.57 | 0.08 | 7.13 | 6 | 10.53 |